DOCTORAL THESIS

Peak-to-Average Power Ratio Reduction in Optical-OFDM Systems using Lexicographical Permutations

UNIVERSITY OF THE WITWATERSRAND, JOHANNESBURG

By

Roland NIWAREEBA

ORCID: 0000-0002-5908-6174

A thesis submitted to the Faculty of Engineering and Built Environment, University of the Witwatersrand, Johannesburg, in fulfilment of the requirements for the degree of Doctor of Philosophy in Electrical Engineering

May 2023

Declaration of Authorship

I, Roland Niwareeba, declare that this thesis titled, "Peak-to-Average Power Ratio Reduction in Optical-OFDM Systems using Lexicographical Permutations" and the work presented in it are my own. I confirm that:

- This work was done wholly while in candidature for a research degree at the University of the Witwatersrand, Johannesburg.
- Where any part of this thesis has previously been submitted for a degree or any other qualification at this University or any other institution, this has been clearly stated.
- Where I have consulted the published work of others, this is always clearly attributed.
- Where I have quoted from the work of others, the source is always given. With the exception of such quotations, this thesis is entirely my own work.
- I have acknowledged all main sources of help.
- Where the thesis is based on work done by myself jointly with others, I have made clear exactly what was done by others and what I have contributed myself.

Signed:

Date: 16th May 2023

This Thesis is dedicated to my wife, Sheilla Akatukunda and children, *Maria Shereen, Rothard Baraka* and *Shenice Kenyangi* *for their patience and endurance during during the years I was away pursuing my PhD.*

Abstract

The work presented in this thesis extends and contributes to the research in reducing the high Peak-to-Average Power Ratio (PAPR) in optical-Orthogonal Frequency Division Multiplexing (OFDM) systems using probabilistic-based and hybrid techniques. Whereas the high PAPR problem has been extensively studied and a number of solutions provided for the conventional Radio Frequency (RF)-OFDM systems, there are only a few solutions proposed specifically for PAPR reduction in optical-OFDM systems. Although the probabilistic-based techniques such as Conventional Selected Mapping (CSLM) and Data Position Permutation (DPP) result into significant PAPR reduction performance with negligible Bit Error Rate (BER) degradation, the resulting increase in both hardware and computational complexity as a result of a large number of Inverse Fast Fourier Transform (IFFT) operations that have to be performed to generate the candidate signals is still a major drawback.

In order to reduce the complexity, in this research, two techniques which are applied in optical-OFDM systems are proposed. The first technique is the hybrid method composed of a modified CSLM and μ-law companding techniques called Low Complexity Hybrid Selected Mapping (LCHSLM). The proposed method achieves almost 50% reduction in complexity compared to CSLM with less BER degradation. The second technique based on lexicographical permutations called Lexicographical Symbol Position Permutation (LSPP) works by dividing the optical-OFDM symbol into a number of sub-blocks and performing lexicographical permutations to obtain the candidate signals after the IFFT operations. In the proposed LSPP, all the candidate permutation sequences are not obtained at once unlike in the DPP where the number of candidate permutation sequences increases at a factorial rate of growth as the number of sub-blocks increases resulting in a more complex system.

Additionally, the research proposes an algorithm where a threshold PAPR value is introduced and the candidate signals are generated until a candidate with a PAPR value less or equal to the threshold is obtained. The results show that the complexity in terms of IFFT operations can be reduced substantially depending on the selected threshold and the number of candidate signals. Furthermore, the research introduces a new algorithm based on the global gain (net gain) to determine the most suitable number of permutation candidate sequences to achieve a reasonable PAPR reduction performance without increasing the time and hardware complexity to levels that the systems cannot tolerate.

Acknowledgements

It is my pleasure to reflect back and remember all those individuals who have supported me along this long and fascinating doctoral quest. Without their assistance and constant encouragement, I would never have been able to complete this thesis. It has indeed been a great honour to spend some time at the Wits Optical Communication Lab in the School of Electrical and Information Engineering, University of the Witwatersrand, Johannesburg.

First and foremost, I would like to express my heartfelt gratitude to my main supervisor Prof Ling Cheng and co-supervisor Dr Mitchell A. Cox for their continuous support, guidance, and encouragement over the last couple of years. From the very beginning, they introduced me to an interesting research area and allowed me the freedom to explore different directions. They were always available when I needed them and they always checked on me to find out how I was progressing in my PhD. They always supported my decisions and at the same time provided valuable feedback and more insights that helped to improve our work. They were not only mentors but also very good friends from whom I learned many useful techniques.

Doctoral students often talk about loneliness during their course of study, but thankfully, this is something that I never experienced even though I did most of the research work during the COVID 19 pandemic where physical interaction was limited. My heartfelt thanks go to my supportive colleagues at the Wits Optical Communication Lab, particularly Dr Femi Kolade, Dr Mulu Shimaponda-Nawa, Lehlohonolo Sekokotoana, Noah Katsiru, Dr Kayode Adetunji and Leloko Lepolesa. The online and physical engagements we always had kept me motivated and I would like to also appreciate all the technical assistance you provided me with whenever I approached you.

I would like to acknowledge the financial support provided to me by the National Research Foundation (NRF) of South Africa. To this end, my sincere thanks go to the Grant officer at the University of the Witwatersrand, Mr Ndhuvazi Kubayi for his timely disbursement of grant funds and assistance. I also acknowledge the financial assistance from the University of the Witwatersrand in form of Postgraduate Merit Award (PMA) that helped me to settle my financial needs and also develop my teaching and tutoring skills in a multicultural environment.

In a special way, I would like to acknowledge Kyambogo University, Kampala, Uganda my employer that has supported me through staff development initiatives.

Finally, but most importantly, I would like to extend my warmest thanks to my loving and caring family for their everlasting love, invaluable support, patience and understanding. I have been away for most of the time from my family for the last four years and they have always supported me.

Roland NIWAREEBA
May 2023

Contents

Declaration of Authorship **i**

Abstract **iii**

Acknowledgements **iv**

List of Figures **viii**

List of Tables **x**

Acronyms **xi**

List of Symbols **xv**

Resulting Publications **xvi**

1 Introduction **1**

1.1 Overview 1

1.1.1 Problem Statement 3

1.1.2 Thesis Contribution 4

1.2 Thesis Organization 5

2 Optical-OFDM for Visible Light Communication Systems **7**

2.1 Overview of Visible Light Communication 7

2.1.1 Brief History of VLC 9

2.1.2 A Brief Overview of LED Properties 11

2.1.3 Received Power of Line of Sight Path 12

2.1.4 Applications of VLC 14

2.1.5 VLC Standardization 17

2.2 Overview of Orthogonal Frequency Division Multiplexing 18

2.2.1 Brief History of OFDM 19

2.2.2 Conventional OFDM System Description 20

2.2.3 Cyclic Prefix in OFDM 22

2.3 Overview of Optical-OFDM 25

2.3.1 Optical-OFDM versus RF-OFDM 26

2.3.2 Direct Current biased Optical-OFDM 27

2.3.3 Asymmetrically Clipped Optical-OFDM 29

2.3.4 Pulse Amplitude Modulation Discrete Multi-tone 31
2.3.5 Hybrid Optical-OFDM Modulation Techniques 32
2.4 Factors for Optical-OFDM Technique Selection 34
2.4.1 Bandwidth Efficiency, η_{BW} 34
2.4.2 Power Efficiency, η_P 34
2.4.3 Transmission Reliability 35
2.4.4 Other Factors 35

3 Peak-to-Average Power Ratio Problem in OFDM Systems 36
3.1 Introduction to PAPR 36
3.2 The OFDM System Model 37
3.2.1 Definition of the Peak-to-Average Power Ratio Problem 37
3.2.2 The CCDF of the PAPR 38
3.2.3 Theoretical Bounds in PAPR 39
3.3 Factors for PAPR Reduction Technique Selection in OFDM Systems 41
3.4 PAPR Reduction Techniques 43
3.4.1 Signal Distortion Techniques 45
3.4.2 Signal Scrambling Techniques 48
3.4.3 Hybrid Techniques 53

4 Low Complexity Hybrid SLM for PAPR Mitigation for ACO-OFDM 55
4.1 Introduction 55
4.2 Proposed Scheme (LCHSLM) 56
4.2.1 Complexity Analysis 58
4.3 Results and Discussions 59
4.4 Conclusion 62

5 PAPR Reduction in Optical-OFDM using Lexicographical Permutations with Low Complexity 63
5.1 Introduction 63
5.2 Proposed System for PAPR Mitigation 66
5.2.1 Lexicographical Symbol Position Permutation 66
5.2.2 Complexity Reduction 68
5.2.3 Complexity Reduction Analysis 68
5.3 Results and Discussions 69
5.3.1 Complexity Reduction Analysis 72
5.4 Conclusion 74

6 Adaptive PAPR Reduction in Optical-OFDM Systems using Lexicographical Symbol Position Permutation 75
6.1 Introduction 76

6.2 Introduction 76
6.3 Background 77
6.3.1 Global Gain 77
6.4 Adjacent and Interleaved Lexicographical Permutation Sequences 78
6.4.1 Most Suitable Number of Candidate Permutation Sequences 78
6.5 Results and Discussions 79
6.5.1 Performance of Lexicographical Symbol Position Permutation Categories 80
6.5.2 Analyzing suitable permutation sequence candidates to minimize computational complexity 82
6.6 Conclusion 85

7 Conclusion **86**
7.1 Contributions 86
7.2 Recommendations for Future Work 87

References **89**

List of Figures

2.1 Global growth of mobile devices and connections 8
2.2 Visible light in the electromagnetic spectrum in the context of other communication technologies 8
2.3 The photophone invented by Alexander Graham Bell 9
2.4 LoS propagation model in an office a typical office environment 12
2.5 Optical power distribution of a LoS at the receiving plane given the parameters in Table 2.1 14
2.6 Illuminance distributions given the parameters in Table 2.1 14
2.7 Comparing the bandwidth utilization between single-carrier modulation, conventional FDM system and OFDM system 19
2.8 Block diagram of the transmitter and receiver in a conventional OFDM System . 20
2.9 OFDM Symbols with Cyclic Prefix 23
2.10 Block diagram of the DCO-OFDM system 27
2.11 Signal $x(n)$ after IFFT operation 28
2.12 Signal $x(t)$ after adding a suitable DC offset (7 dB) 29
2.13 Signal $x(t)$ after zero clipping 29
2.14 BER against SNR curves for DCO-OFDM communication system for 4-QAM, 16-QAM, 64-QAM and 256-QAM with a DC bias of 7 dB 30
2.15 BER against SNR curves for DCO-OFDM communication system for 4-QAM, 16-QAM, 64-QAM and 256-QAM with a DC bias of 13 dB 31
2.16 Block diagram of the ACO-OFDM system 31

3.1 PAPR performance of a DCO-OFDM system with $N = 32,\ 64,\ 128,\ 256,\ 512$ and 1024 subcarriers 41
3.2 Taxonomy of PAPR reduction techniques 45
3.3 Peak cancellation process 47
3.4 OFDM schematic employing μ-law companding for PAPR reduction 47
3.5 Conventional selective mapping for DCO-OFDM 48
3.6 PAPR reduction performance of the original OFDM system and CSLM with $V = 6, 16, 24$ and 32 50
3.7 PTS technique block diagram 51

4.1 Proposed Method-LCHSLM for ACO-OFDM 57
4.2 PAPR reduction performance of LCHSLM compared to CSLM and μ-law companding techniques 60

4.3 PAPR reduction performance of CSLM with μ-law companding and LCHSLM . 60
4.4 Comparison of BER of LCHSLM, CSLM and μ-law companding techniques. . . 61

5.1 Proposed Scheme for PAPR mitigation 66
5.2 PAPR performance comparison between the original DCO OFDM, LSPP and CSLM for $S = 8$ sub-blocks. 70
5.3 PAPR comparison for LSPP with $U = 16$ and 32 candidate signals for $S = 8$ and 16 sub-blocks. For the same number of candidate signals, increasing the number of sub-blocks improves the PAPR reduction performance. 71
5.4 Comparison of BER performance of the original OFDM system, the CSLM and LSPP for $U = 8$ and 16 candidate signals 72
5.5 IFFT operations for different γ and U 72
5.6 Complexity reduction performance for different γ and U 73

6.1 Algorithm for obtaining the most suitable number of candidate permutation sequences based on global gain. 79
6.2 Comparing the PAPR performance of DCO-OFDM versus the three types of lexicographical permutations: random, interleaved, and adjacent for $Q = 16$ sub-blocks and the number of candidate signals, $V = 8, 16$ and 32. 80
6.3 Comparing the BER performance of DCO-OFDM versus the three types of lexicographical permutations: random, interleaved, and adjacent for $Q = 16$ sub-blocks and the number of candidate signals, $V = 8, 16$ and 32 82
6.4 Z_1 and Z_2 for different candidate sequences 82
6.5 Global gain for different numbers of candidate sequences at different levels of importance attached to PAPR reduction performance (σ_1) and computational complexity (σ_2) 83
6.6 Global gain for different numbers of random lexicographical permutation sequences, V at a $CCDF = 10^{-3}$, number of subcarriers, $N = 256$. 84

List of Tables

2.1 System parameters for the VLC link in a typical office environment 13
2.2 Comparison of Optical-OFDM and RF-OFDM system characteristics 26

4.1 Simulation Parameters 59
4.2 PAPR reduction comparison for CSLM, μ-law companding, CSLM combined with μ-law companding and the proposed LCHSLM 60

5.1 Simulation Parameters 69
5.2 Complexity Reduction 73

6.1 Simulation Parameters 80
6.2 Global gain, Ω values for different numbers of random lexicographical permutation sequences at a $CCDF = 10^{-3}$ and number of subcarriers, $N = 256$ for three different cases i.e. Case 1 $(\sigma_1 = 0.8, \sigma_2 = 0.2)$, Case 2 $(\sigma_1 = 0.2, \sigma_2 = 0.8)$ and Case 3 $(\sigma_1 = \sigma_2 = 0.5)$ 83

Acronyms

4G	Fourth Generation
5G	Fifth Generation
6G	Sixth Generation
ACO-OFDM	Asymmetrically Clipped Optical-OFDM
ADC	Analog-to-Digital Converter
ADO-OFDM	Asymmetrically Clipped DC biased Optical-OFDM
AI	Artificial Intelligence
AU	Augmented Reality
AWGN	Additive White Gaussian Noise
BER	Bit Error Rate
BPSK	Binary Phase Shift Keying
CAP	Carrierless Amplitude and Phase
CBC	Complement Block Coding
CCDF	Complementary Cumulative Distribution Function
CCRR	Computational Complexity Reduction Ratio
CDF	cumulative distribution function
CIP	Channel Inversion Pre-coding
CSLM	Conventional Selected Mapping
DAC	Digital-to-Analog Converter
DC	Direct Current
DCO-OFDM	Direct Current biased Optical-OFDM
DFT	Discrete Fourier Transform
DMT	Discrete Multitone
DPP	Data Position Permutation
DSRC	Dedicated Short-Range Communication
DVB-S	Digital Video Broadcasting-Satellite
DVB-T	Digital Video Broadcasting-Terrestrial
FDM	Frequency Division Multiplexing
FEC	Forward Error Correction

FFT	Fast Fourier Transform
FHT	Fast Hartley Transform
HACO-OFDM	Hybrid Asymmetrically Clipped Optical-OFDM
i.i.d.	independent and identically distributed
ICI	Intercarrier Interference
IFFT	Inverse Fast Fourier Transform
IM/DD	Intensity Modulation with Direct Detection
IoT	Internet of Things
ISI	Inter-Symbol Interference
LACO-OFDM	Layered Asymmetrically Clipped Optical-OFDM
LCHSLM	Low Complexity Hybrid Selected Mapping
LED	Light Emitting Diode
Li-Fi	Light Fidelity
LoS	Line of Sight
LPF	Low Pass Filter
LSPP	Lexicographical Symbol Position Permutation
LT	Luby Transform
LTE	Long-Term Evolution
M-PSK	M-ary Phase Shift Keying
M-QAM	M-ary Quadrature Amplitude Modulation
MAC	Medium Access Control
MCM	Multi-carrier Modulation
MCR	Modified Code Repetition
MIMO	Multiple Input-Multiple Output
OFDM	Orthogonal Frequency Division Multiplexing
OOK	On-Off-Keying
PAM	Pulse Amplitude Modulated
PAPR	Peak-to-Average Power Ratio
PD	Photo Detector
PTS	Partial Transmit Sequence
QAM	Quadrature Amplitude Modulation
QPSK	Quadrature Phase Shift Keying

RF	Radio Frequency
RMS	Root Mean Square
SI	Side Information
SLM	Selected Mapping
SNR	Signal-to-Noise Ratio
SPP	Symbol Position Permutation
VLC	Visible Light Communication
VR	Virtual Reality
WiFi	Wireless Fidelity
WiMAX	Worldwide interoperability for Microwave Access
WNW	Wideband Network Waveform

List of Symbols

A	Normalization constant in μ-law companding operation
α	Related to the oversampling factor
BW_{sys}	System bandwidth
C	Signal threshold for clipping purposes
dB	Decibel
DC_{bias}	Direct current bias
E_b	Average energy per bit
E_{pulse}	Energy per pulse
$H(0)$	DC channel gain
I	luminous intensity
j	Imaginary operator equivalent to $\sqrt{-1}$
k	k^{th} time index
K_m	Maximum visibility
L	Number of layers in ACO-OFDM
max	Maximum
min	Minimum
$\mathcal{N}$	Normal distribution
N	Number of subcarriers
P_t	Transmit optical power
Q	Number of permutation sub-blocks
$\varnothing$	Angle of irradiance
$\mathrm{sgn}[x(n)]$	Signum function of $x(n)$
$T_s(\psi)$	Gain of the optical filter
U	Number of candidate signals (SLM)
$V(\lambda)$	Standard luminous curve

X^*	Complex conjugate of X
$X(k)$	Transmitted frequency domain signal
$\hat{X}(k)$	Estimate of frequency domain signal $X(k)$
$x(n)$	transmitted discrete time domain signal
$x(t)$	Transmitted continuous time domain signal
$Y(k)$	Received frequency domain signal
$y(n)$	Received discrete time domain signal
$y(t)$	Received continuous time domain signal
$\Phi_{1/2}$	Semi-angle of the LED
Ω	Global (net) gain
$V(\lambda)$	Standard luminous curve
σ^2	Variance of the OFDM subcarrier
γ	Threshold value of PAPR
$\langle\cdot\rangle$	Statistical expectation
%	Percentage
$\circledast_N$	Circular convolution of modulo N
π	Number pi
θ	Angle of $x(n)$ in clipping operation
η_{BW}	Bandwidth efficiency
η_P	Power efficiency
Φ	Luminous flux
$g(\psi)$	Gain of the optical concentrator
ψ_c	Width of field of view at the receiver
ψ	Angle of incidence with respect to the axis normal to the receiver surface

Note that this is not an exhaustive list of every symbol that has been used in this thesis. There are several symbols that are used only once, such as those in the literature overview Chapters, and some of them are not listed here. Whenever a symbol is used with a different definition in the text, that definition will take precedence over the definition given here.

Resulting Publications†

Journal Papers

1) R. Niwareeba, M. A. Cox and L. Cheng, "PAPR Reduction in Optical-OFDM Using Lexicographical Permutations With Low Complexity," in IEEE Access, vol. 10, pp. 1706-1713, 2022, doi: 10.1109/ACCESS.2021.3138193 (Chapter 5).

2) R. Niwareeba, M. A. Cox and L. Cheng, “Low complexity hybrid SLM for PAPR mitigation for ACO-OFDM”. In: ICT Express 8.1 (2022), pp. 72–76. (Chapter 4).

Under Review

1) R. Niwareeba, M. A. Cox and L. Cheng, “Adaptive PAPR Reduction in Optical-OFDM Systems using Lexicographical Symbol Position Permutation-Submitted”. In: (Submitted to MDPI Electronics-Under Review). (Chapter 6)

† The Chapters in which these publications have had a contribution have been indicated in brackets.

1 Introduction

1.1 Overview

Visible Light Communication (VLC) technology has recently attracted considerable attention from researchers in academia, industry and governments around the globe due to its numerous advantages such as interference-free communication, high levels of security, low cost due to the utilization of the license-free spectrum, availability of the Light Emitting Diode (LED) used for communication, low power consumption, ability to perform indoor localization among others [1–3]. In order to attain the higher data rates required nowadays, multi-carrier modulation techniques such as Orthogonal Frequency Division Multiplexing (OFDM) have been considered for practical implementation in VLC systems [4–6]. In addition to the higher data rates, OFDM also has high spectral efficiency, can combat Inter-Symbol Interference (ISI) in a diffuse optical channel without the need for complex equalization filters at the receiver and it is easy to be practically implemented using Inverse Fast Fourier Transform (IFFT) and Fast Fourier Transform (FFT) operations [7].

Most of the practical VLC systems currently deployed use Intensity Modulation with Direct Detection (IM/DD) and therefore the optical carrier used for modulating the light intensity must be real and unipolar. The real valued signal is usually obtained by constraining the signal to the Hermitian symmetry before the IFFT operation. To obtain a unipolar signal, a number of approaches have been considered resulting in different forms of optical-OFDM. A suitable Direct Current (DC) bias can be added resulting in Direct Current biased Optical-OFDM (DCO-OFDM) [8]. On the other hand, in Asymmetrically Clipped Optical-OFDM (ACO-OFDM) [9], no DC bias is added and the unipolar signal is obtained by clipping the signal at the zero level. However, the spectral efficiency is half of that of DCO-OFDM since half of the subcarriers are used. In Pulse Amplitude Modulated (PAM)-Discrete Multitone (DMT) modulation [10], only the imaginary parts of all the subcarriers are modulated using PAM symbol levels before the IFFT operation and the entire negative excursion of the resulting time domain signal is clipped just like in ACO-OFDM. Other variants of optical-OFDM include Asymmetrically Clipped DC biased Optical-OFDM (ADO-OFDM) [11] that simultaneously transmits ACO-OFDM and DCO-OFDM signals on the odd and even subcarriers respectively, Flip-OFDM [12] and Layered ACO-OFDM [13].

Regrettably, despite the advantages of OFDM, the multi-carrier nature of OFDM means that there will be constructive addition at certain instants of the subcarriers after the IFFT operation leading to a higher peak value. Consequently, this will result in a high Peak-to-Average Power Ratio (PAPR) [14].

It is important to keep the devices at the transmitter such as the LED, the Digital-to-Analog Converter (DAC) and the power amplifier in the linear region of operation for reliable transmission. However, this is difficult to achieve in practice due to the high PAPR and as a consequence, the high peaks are often clipped leading to signal distortion and an increase in Bit Error Rate (BER).

Therefore, a lot of attention has been put on PAPR reduction and several techniques have been proposed in the traditional OFDM for Radio Frequency (RF) communication systems. These techniques are summarised in literature [14–19]. However, since the transmitted signal in VLC must be real and positive due to the use of IM/DD as earlier pointed out, most of these techniques cannot be directly applied in VLC systems.

In this thesis, an extensive survey of PAPR reduction techniques for both RF and optical-OFDM systems available in literature is presented. In the proposed taxonomy, the techniques are categorised into three broad categories. The first category is the signal scrambling techniques such as coding-based including block codes [20, 21], convolutional codes [22, 23], fountain codes [24–28] and probabilistic-based such as Selected Mapping (SLM) [29–32] and Partial Transmit Sequence (PTS) [33]. The second category is the signal distortion techniques such as signal clipping [34, 35], peak windowing [36, 37] and companding techniques [38–41]. The third category which is introduced in this thesis is the hybrid techniques [42] which combines two or more techniques in order to benefit from the advantages of either technique.

The Conventional Selected Mapping (CSLM) is a popular method because of its significant PAPR reduction performance with negligible BER degradation. In CSLM, multiple candidate signals are generated by multiplying the OFDM symbol in the frequency domain with random phase sequences. The candidate signal after the IFFT operation with the least PAPR is selected for transmission and the Side Information (SI) associated with this candidate signal is transmitted for efficient recovery at the receiver. However, the large number of IFFT operations that are required to generate the candidate signals makes this approach complex. Moreover, the higher the number of candidate signals, the better the performance in terms of PAPR reduction, making this CSLM method more complex in practical implementation. In order to solve the complexity problem associated with the CSLM method, this thesis proposes a novel hybrid technique based on the modified CSLM and μ-law companding techniques called Low Complexity Hybrid Selected Mapping (LCHSLM) scheme. The aim is to reduce the complexity of the CSLM and achieve a reasonable PAPR reduction performance with minimal BER degradation. It is demonstrated through computer simulations that the proposed technique significantly reduces the PAPR compared to using CSLM or μ-law companding alone in addition to achieving almost 50% reduction in complexity.

Related to the CSLM technique, symbol or bit interleaving [43] and the Data Position Permutation (DPP) [44] techniques also involve the generation of multiple candidate signals and the one with the least PAPR is selected for transmission. Specifically, in the DPP technique, the OFDM symbol is divided into S sub-blocks which are then permutated to generate the candidate permutation sequences. However, in the DPP technique, the number of candidate permutation sequences that can be generated is limited since it is given by $S!$ and therefore as the number of sub-blocks increases, the number of permutation sequences increases at a factorial rate of growth leading to a more complex transmitter system as a result of the large number of IFFT operations that have to be performed. In order to solve the complexity problem associated with the DPP method, in this thesis, a novel technique based on lexicographical permutations called Lexicographical Symbol Position Permutation (LSPP) is introduced. To this end, the three different ways of selecting the U permutation candidate sequences, that is, adjacent, interleaved, and random are compared in terms of PAPR reduction performance by computer simulation using Complementary Cumulative Distribution Function (CCDF) diagrams. Simulation results show that random lexicographical permutation sequences give a slightly better PAPR reduction performance compared to adjacent and interleaved lexicographical permutations. Furthermore, the thesis introduces an algorithm for complexity reduction using LSPP by setting a threshold PAPR value and generating the permutation candidate sequences one by one until a candidate sequence with PAPR below the threshold is reached. In this way, if the m-th, $(m \leq U)$ permutation sequence satisfies the threshold condition, then $U-m$ candidate sequences are not generated and consequently, $U-m$ IFFT operations are not performed. This new method does not only reduce the PAPR but also results in a significant reduction in computational complexity.

Finally, since different application environments require different PAPR values and complexity, this thesis introduces a new algorithm based on the global gain (net gain) to determine the most suitable number of permutation candidate sequences to achieve a reasonable PAPR reduction performance without increasing the time and hardware complexity to levels that the systems cannot tolerate.

1.1.1 Problem Statement

The high PAPR problem has been extensively studied and there are several techniques that have been proposed for the conventional RF-OFDM systems. These techniques cannot be applied directly in optical-OFDM for VLC systems since the practical VLC systems currently deployed use IM/DD and therefore the optical carrier used for modulating the light intensity must be real and unipolar. There are only a few solutions that have been proposed explicitly for use in optical-OFDM systems. All the proposed solutions have advantages and disadvantages over one another when they are implemented, i.e., each technique must sacrifice one or more performance parameters for PAPR reduction. It has been suggested [16, 45], that the following factors must be considered when selecting a particular technique for PAPR reduction: PAPR reduction capability, computational complexity, spectral spillage, BER degradation and loss in throughput due to the SI. For example, clipping techniques are simple to implement and result in significant PAPR reduction but introduce in-band distortion and out-of-band radiation leading to high BER performance degradation. On the other hand, probabilistic-based techniques such as CSLM and DPP are distortion-less techniques that achieve significant PAPR reduction performance at the expense of increased computational complexity. The complexity in CSLM is caused by two main factors: firstly, due to the generation and multiplication of the random phase sequences with the OFDM symbol and secondly as a result of the many IFFT operations that must be performed to generate the candidate signals. Although there is no generation and multiplication of the random phase sequences with the OFDM symbol in the DPP technique, the complexity is escalated by the fact that the number of candidate sequences increases at a factorial rate of growth as the number of sub-blocks increases. These challenges led to the research questions of this thesis given below:

1. *How can significant PAPR reduction performance be achieved with minimal side effects of the techniques used such as increase in complexity and BER degradation?*

   This question is answered by introducing a new hybrid technique for PAPR reduction composed of a modified CSLM and μ-law companding techniques. The new technique is less complex in terms of the number of IFFT operations compared to the CSLM and achieves a significant PAPR reduction performance with minimal BER degradation. The details of this research are given in Chapter 4 and have been published [42].

2. *Which category of lexicographical permutation sequences among random, adjacent, and interleaved gives better PAPR reduction performance and how can the complexity be reduced?*

   This question is answered firstly, by developing algorithms to generate the three categories of lexicographical permutations and compare the PAPR reduction performance by simulation using CCDF diagrams and secondly by developing an algorithm for complexity reduction using LSPP by setting a threshold PAPR value and generating the permutation candidate sequences one by one until a candidate sequence with PAPR below the threshold is reached. To this end, we compare both the simulation and mathematical formulation to establish the effectiveness of the proposed algorithm. The results from this research are given in Chapters 5 and 6, partly published [46] and submitted for publication [47].

3. *How can the PAPR reduction performance and computational complexity be optimized for different application scenarios that require different levels of PAPR values and computational complexities?*

   This question is answered by introducing a new algorithm based on the global gain (net gain) to determine the most suitable number of permutation candidate sequences to achieve a reasonable PAPR reduction performance without increasing the time and hardware complexity to levels that the systems cannot tolerate. The results of this research are given in Chapter 6 and have been submitted for publication [47].

1.1.2 Thesis Contribution

This thesis makes original contributions to the body of knowledge in the field of VLC technology, specifically focusing on the high PAPR which is a major drawback affecting the implementation of

OFDM as a modulation technique in VLC systems. The main contributions of this thesis are as follows:

(i) In the first contribution, an extensive survey of PAPR reduction techniques available in literature is presented. In the taxonomy presented, the available PAPR reduction techniques are categorised into three broad categories, namely, signal scrambling techniques such as coding, PTS and SLM techniques; signal distortion techniques such as signal clipping, peak windowing and companding transforms such as μ-law and A-law transforms. The third category which is introduced are the hybrid techniques which combines two or more techniques in order to benefit from the advantages of either technique.

(ii) In the second contribution, a new hybrid technique for PAPR reduction for ACO-OFDM communication systems is presented. This technique is composed of a modified CSLM together with μ-law companding techniques. The results show that this technique is able to achieve a considerable PAPR reduction performance with low complexity and negligible BER degradation.

(iii) In the third contribution, a new PAPR reduction technique based on lexicographical permutations of the OFDM symbols in frequency domain for DCO-OFDM systems is presented. Furthermore, a new way of reducing the complexity based on a threshold PAPR value is introduced. This is based on the fact that different applications and scenarios require different PAPR reduction performance. The results show that the complexity in terms of IFFT operations can be reduced substantially depending on the selected threshold and the number of candidate signals used.

(iv) In the final contribution, a comparison of the different categories of lexicographical permutations, namely, random, interleaved and adjacent in terms of PAPR reduction performance is presented. The results show that random lexicographical permutations achieve a better PAPR reduction performance compared to interleaved and adjacent lexicographical permutations. However, the random lexicographical permutations require a large number of sub-blocks to avoid the possibility of generating repeated candidate sequences. Therefore, interleaved and adjacent lexicographical permutation sequences can be preferred in situations where the number of OFDM subcarriers is small. Furthermore, a new method of obtaining the most suitable number of candidate permutation sequences based on global (net) gain to achieve a reasonable PAPR reduction performance without increasing the computational complexity beyond system requirements is introduced.

1.2 Thesis Organization

This chapter provides a brief introduction together with the problem statement and the original contributions of this thesis. The rest of the thesis is organized as follows:

Chapter 2 presents a review of VLC as well as a general description of the OFDM system while emphasizing the main aspects that need to be modified in order for the conventional OFDM used in RF systems to be used in VLC systems. This is followed by a review of the current optical-OFDM techniques proposed in literature as well as the factors to be considered when selecting a particular optical-OFDM technique.

Chapter 3 presents the PAPR problem in OFDM systems. In Chapter 2, the high PAPR problem is identified as the main challenge in the practical implementation of OFDM systems. Additionally, in this chapter, a detailed survey and classification of the PAPR reduction techniques available in literature is presented. Furthermore, the chapter includes a discussion of the factors that can be used to determine the trade-offs between the PAPR reduction capability of a technique and other design factors such as complexity, BER and bandwidth requirements.

Chapter 4 presents the new hybrid technique proposed for ACO-OFDM systems. In Chapter 3, it is pointed out that no single technique can achieve a high PAPR reduction without compromising other performance parameters in the system such as complexity, BER and bandwidth. Therefore, the best strategy is to employ hybrid techniques that combine two or more PAPR reduction techniques. The technique presented in this chapter incorporates a modified CSLM and companding techniques to achieve a considerable PAPR reduction performance with low complexity when compared to CSLM or companding technique used individually.

Chapter 5 presents a new PAPR reduction technique based on lexicographical permutations called LSPP for PAPR reduction in DCO-OFDM systems. Furthermore, a new way of reducing the complexity is introduced based on a threshold PAPR value. It is demonstrated that the complexity in terms of IFFT operations can be reduced substantially depending on the selected threshold and the number of candidate signals.

Chapter 6 presents a comparison of PAPR reduction of the different categories of lexicographical permutations, namely, random which was presented in Chapter 5, interleaved and adjacent which are introduced in this chapter. Furthermore, this chapter presents a new method of obtaining the most suitable number of candidate permutation sequences to achieve a reasonable PAPR reduction performance without increasing the computational complexity beyond system requirements.

Chapter 7 concludes by highlighting the most important results in this thesis and future research directions are presented.

2 Optical-OFDM for Visible Light Communication Systems

This chapter presents the main concepts in Orthogonal Frequency Division Multiplexing (OFDM) while emphasizing the specific aspects that need to be modified in order for the conventional OFDM used in Radio Frequency (RF) applications to be applied in Visible Light Communication (VLC) systems. In Section 2.1, an overview of VLC is presented in which the main concepts, applications and standardization efforts in VLC are discussed. Section 2.2 presents the fundamental concepts in OFDM modulation scheme used in RF communication systems. This section introduces the OFDM system architecture and explains the building blocks in the OFDM system. A fundamental concept of the cyclic prefix is discussed and it is shown mathematically that this cyclic prefix has the potential to combat Inter-Symbol Interference (ISI) which is a key advantage of OFDM systems over single-carrier systems. In Section 2.3, an overview of optical-OFDM is presented. The key differences between optical-OFDM and RF-OFDM are discussed in this section, which is followed by a discussion of the various optical-OFDM techniques presented in literature. Finally, the chapter concludes with a discussion on the factors to be considered when selecting a particular optical-OFDM technique in Section 2.4.

2.1 Overview of Visible Light Communication

The current and future high speed wireless demands such as Virtual Reality (VR), Augmented Reality (AU), Internet of Things (IoT), driverless cars, telemedicine, Artificial Intelligence (AI), etc. will be unable to be met by current RF communication systems. It was predicted that the demand for RF spectrum will exceed the supply by 2035 [48] and that more than 70 percent of the global population will have mobile connectivity by 2023 [49]. It was further predicted by Cisco that by 2023, the global mobile devices will grow to 13.1 billion up from 8.8 billion in 2018 shown in Figure 2.1 representing almost a 50% increase [49].

Therefore, there has been a growing interest from academia, governments, industry and standardization bodies to solve this impending spectrum crunch and alternative solutions such as use of millimeter-wave [50] and VLC [51] have been proposed. However, use of millimeter-wave has its own challenges such as lack of security, requirement for much smaller cells implying high costs in deployment, absorption by gases and moisture which reduces the range and signal strength.

VLC refers to a type of communication system that uses the Light Emitting Diode (LED) or the laser as an optical source to emit light in the visible light spectrum (380nm-780nm) shown in

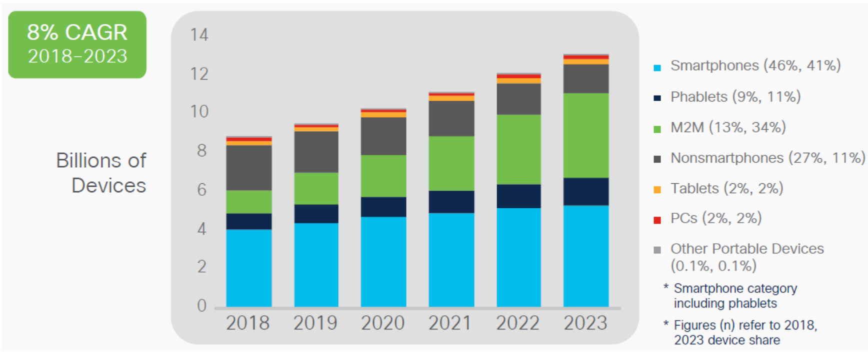

Figure 2.1: Global growth of mobile devices and connections (Source: [49])

Figure 2.2 for both illumination and data communication [7].

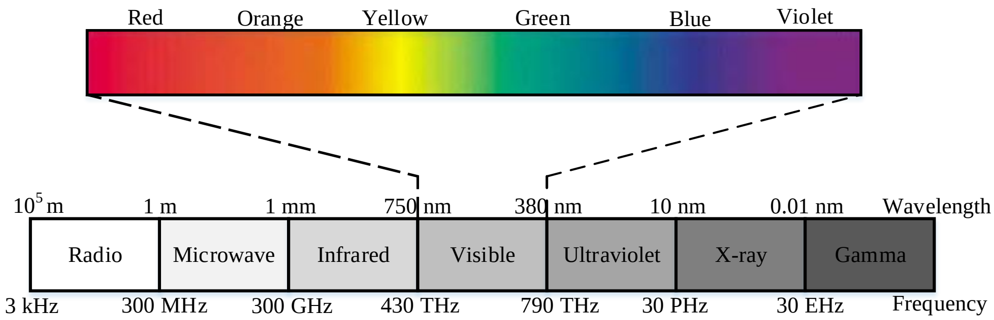

Figure 2.2: Visible light in the electromagnetic spectrum in the context of other communication technologies

It is expected that VLC will be an integral part of the Fifth Generation (5G), Sixth Generation (6G) mobile communication standards and beyond [1]. VLC is currently used as a complementary technology in situations where the RF technology is of limited use, for example in underwater [52] and mining tunnels [53]. Therefore, VLC will remain in use as a complementary technology to RF technology to support high data rate communication anywhere and anytime because of its unique features which include: Firstly, the visible light spectrum is unlicensed and this means there are no utilization tariffs. Secondly, VLC is a highly secure technology since light does not penetrate through walls and other objects. Thirdly, VLC is immune to electromagnetic interference and therefore, it can be used in places such as hospitals and air crafts. Lastly but most importantly, VLC uses LED lights which are ubiquitous implying that the already existing lighting infrastructure can be used for both illumination and data communication.

The increasing popularity and usage of solid-state lighting that is slowly replacing the old incandescent light bulbs with LED bulbs has been one of the main drivers towards VLC technology. The LED is preferred over an incandescent light bulb due to its long life expectancy, high power efficiency, high reliability, high tolerance to humidity and minimal heat generation [51]. The solid-state lighting is expected to gain more popularity after the recent implementation of phased banning of incandescent light bulbs in countries such as the European Union, United States, Brazil, Canada, Australia and many other countries around the world [54].

2.1.1 Brief History of VLC

The transmission of information using optical radiation from one point to another through air dates back to antiquity times when it is interpreted in a broad sense. For instance, in about 800 BC, Romans and Greeks used fire beacons for signaling and by around 150 BC, smoke signals were being used by native Americans for the same purpose of signaling. Claude Chappe developed the Semaphore in France in 1794. The semaphore was a method of signaling by means of flags or lights and messages were read by telescopic sightings. This semaphore was used by the French sea navigators [7].

The major development in the area of VLC was by Alexander Graham Bell (1847-1992) who was best known for his invention of the telephone but also had several other inventions attributed to his name. In the early 1880, Bell successfully demonstrated the transmission of an audio signal using a mirror vibrated by a person's voice. This experimental demonstration of VLC using sunlight as the source was called the photophone shown in Figure 2.3 [2]. Bell and his assistant Charles Summer Tainter demonstrated this wireless transmission over a distance of 213 m. Bell's experiment did not go very far because of the crudity of instruments used and the nature of intermittent radiation of sunlight. However, the idea of the photophone led to the birth of fiber-optic communications that achieved popular worldwide usage starting in the 1980s. VLC is a version of optical communication that uses unguided media as opposed to fiber optic communication that uses a fiber optic cable for transmission of light signals.

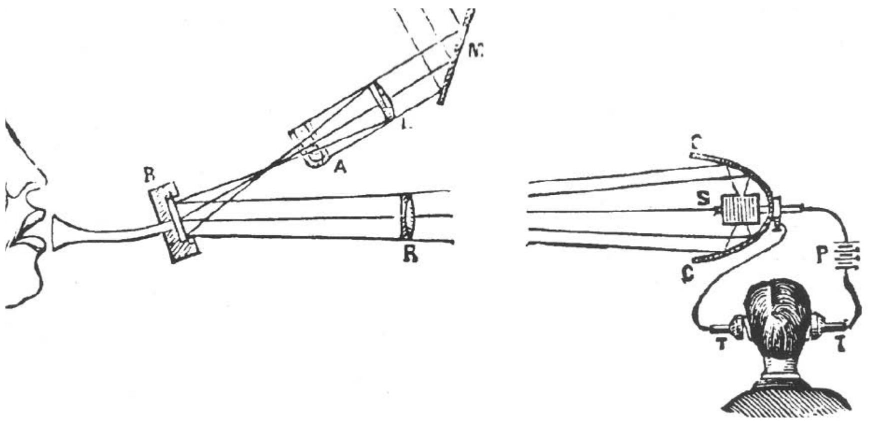

Figure 2.3: The photophone invented by Alexander Graham Bell (Source: [2])

The major turning point in the history of VLC was the discovery of the phenomenon of electroluminescence in 1907 by H.J. Round. Round showed that light was generated at the cathode by passing an electrical current through a crystal of silicon carbide (SiC) [55]. In 1936, George Destriau also observed that electroluminescence was produced when an electric field was applied to Zinc Sulphide (ZnS) powder suspended in an insulator [56].

In 1955 Rubin Braunstein reported infrared emissions from several semiconductors including Gallium Arsenide (GaAs) , Silicon-Germanium (SiGe), Gallium Antimonide (GaSb) and Indium Phosphide (InP) [57]. Braunstein further reported in 1957 that rudimentary devices could be used for non-radio communications over a short distance. He had set up an optical communications link [58].

The next major milestone came with the demonstration of visible-spectrum (red) LED by Allen and Cherry in 1961 [59]. The very first blue-violet LED was discovered in 1972 by Herb Maruska and Wally Rhines using magnesium-doped gallium nitride at Stanford University [60]. These developments started a new era in the area of optical communication and from then a number of researchers have been participating on a global scale in the area of LED-based and optical communication in general.

The initial commercial developments of fiber-optic communication systems started around 1975 when a system was developed that was capable of operating at a bit rate of 45 Mbps [61].

The term VLC was coined by Nakagawa and his team at Keio University in Japan towards the end of the 1990s [1, 51]. They demonstrated the first VLC system using white LED for data transmission.

In 2011, Hass et al. at the University of Edinburgh, UK proposed a high speed wireless communication system based on optical radiation transmitted over a line of sight called Light Fidelity (Li-Fi) [62].

In [63] Yeh et al. demonstrated a VLC system at a data rate of 37 Mbps for a distance of up to 1.5 m using white-light phosphor-LED. The authors note that the bandwidth of phosphor-LED can be increased from 1 MHz up to about 12 MHz using the analogue pre-distortion technique without using the blue filter.

In [64], Xicong et al. experimentally demonstrated a VLC system that can transmit up to 40 Mbps for a distance of 200 cm using a large off-the-shelf LED panel with dimensions of 60×60 cm^2. Using a low complexity multi-band Carrierless Amplitude and Phase (CAP) modulation scheme, the authors were able to increase the transmission distance up to 2 m with the same data rate [65].

Recently, in [66], Rui et al. demonstrated the transmission at 15.73 Gbps in a VLC system over a distance of 1.6 m by applying Forward Error Correction (FEC) and wavelength division multiplexing to efficiently modulate four wavelengths in the visible light spectrum using the commercially available components. In order to achieve the high data, the authors utilize OFDM modulation technique with adaptive bit loading.

These practical demonstrations show the potential of using the already existing lighting infrastructure for both illumination and data communication.

The increasing research activities in the area of VLC communication in academia, industry and standardization bodies has mainly been driven by the increasing popularity and developments in solid-state lighting technology. The solid state light bulbs have a longer life and are highly energy efficient compared to the original incandescent light bulbs. These lighting sources will remain dominant in the near future. Therefore, VLC technology will remain popular due to its low research, development and installation costs because the same lighting fixtures can be used for both illumination and data communications simultaneously and has several other applications including indoor positioning, underwater communication, providing RF safe communication in hospitals, home/office networking.

2.1.2 A Brief Overview of LED Properties

LED lights have two most important basic properties, i.e. luminous intensity and the transmit optical power. The luminous intensity, measured in candela (cd) is defined as the measure of the wavelength-weighted power emitted by a light source in a particular direction per unit solid angle and it is related to illumination at an illuminated surface. The luminous intensity, I is given by

$$I = \frac{d\Phi}{d\Omega} \tag{2.1}$$

where Ω is the spatial angle and Φ is the luminous flux, which can be obtained from the energy flux, Φ_e as given by [51]

$$\Phi = K_m \int_{380}^{780} V(\lambda)\Phi_e(\lambda)d\lambda \tag{2.2}$$

where $V(\lambda)$ is the standard luminous curve, and K_m is the maximum visibility which is about 683 lm/W when the wavelength $\lambda = 555\,\text{nm}$. The transmit optical power, P_t represents the total radiated energy from all directions from the LED and is given by

$$P_t = \int_{\Lambda_{\min}}^{\Lambda_{\max}} \int_{0}^{2\pi} \Phi_e d\theta d\lambda \tag{2.3}$$

where $\Lambda_{\min}$ and $\Lambda_{\max}$ are determined from the responsivity curve of the photo diode.

Figure 2.4 shows a scenario of an office environment using LED-based lighting panels for both illumination and wireless data connection to the users.

In this case, the dominant transmission mode is the Line of Sight (LoS). Assuming a Lambertian radiation pattern by the LEDs, the radiation intensity at the desk surface is given [7]

$$I(\varnothing) = I(0)\frac{m_l + 1}{2\pi}\cos^{m_l}(\varnothing) \tag{2.4}$$

where $\varnothing$ is the angle of irradiance with respect to the axis normal to the transmitter surface, $I(0)$ is

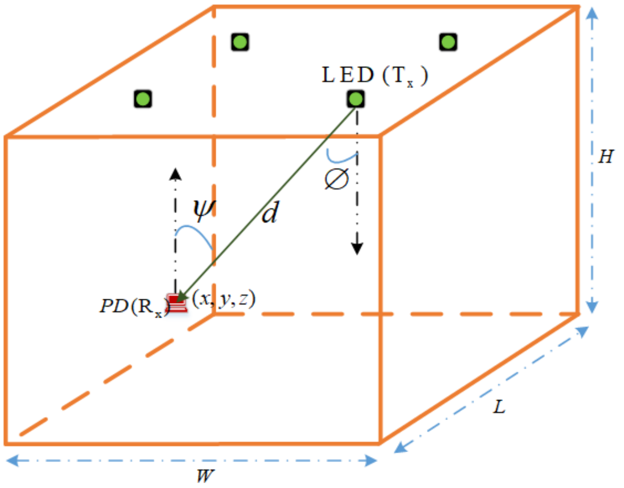

Figure 2.4: LoS propagation model in an office a typical office environment

the center luminous intensity and m_l is the measure of the directivity of the light beam also called the order of Lambertian emission given by

$$m_l = \frac{\ln(2)}{\ln(\cos\Phi_{1/2})} \tag{2.5}$$

where $\Phi_{1/2}$ is the semi-angle of the LED which is the angle measured with respect to the LED's light emission center line at which the radiant intensity falls to 50% of its maximum value.

2.1.3 Received Power of Line of Sight Path

For the LoS path, the horizontal luminous intensity at a point (x, y, z) is given by

$$I_{hor} = I(0)\cos^{m_l}(\varnothing)/d^2\cos(\psi) \tag{2.6}$$

where ψ is the angle of incidence with respect to the axis normal to the receiver surface and d is the distance from the LED to the detector's surface.

The received optical power is given by

$$P_r = H(0)P_t \tag{2.7}$$

where $H(0)$ is the Direct Current (DC) channel gain given by [51]

$$H(0) = \begin{cases} \frac{(m+1)A_d}{2\pi d^2}\cos^{m_l}(\varnothing)T_s(\psi)g(\psi)\cos(\psi), & 0 \le \psi \le \psi_c \\ 0, & \psi > \psi_c \end{cases} \tag{2.8}$$

where A_d is the area of the photo detector, $T_s(\psi)$ is the gain of the optical filter, ψ_c is the width of field of view at the receiver, $g(\psi)$ is the gain of the optical concentrator given by

$$g(\psi) = \begin{cases} \dfrac{n^2}{\sin^2\psi_c}, & 0 \leq \psi \leq \psi_c \\ 0, & 0 \geq \psi_c \end{cases} \tag{2.9}$$

where n denotes the refractive index.

Table 2.1: System parameters for the VLC link in a typical office environment

Parameter	**Value**
Room size $(L \times W \times H)$	5 m $\times$ 5 m $\times$ 3 m
Location (4 LEDs)	(1.25,1.25,3), (1.25,3.75,3), (3.75,1.25,3), (2.5,2.5,3)
Semi-angle at half power	15° and 75°
Transmit power per LED	20 mW
Number of LEDs per array	$60 \times 60(3600)$
Center luminous intensity	300-910 lx
Receive plane above the floor	0.85 m
Active area (A)	1 cm^2
Half-angle FOV	60°
Elevation	90°
Azimuth	0°
Optical filter gain	1.0
Refractive index of the lens at PD	1.5

One of the possible application areas of VLC is in an office environment. Consider a typical office environment of size 5 m $\times$ 5 m $\times$ 3 m (Length $\times$ Width $\times$ Height) as shown in Figure 2.4 with four LEDs and a Photo Detector (PD) as the receiver with parameters given in Table 2.1.

For the non-LoS or diffuse path, the light must first hit a reflective surface (for example, another wall or other objects in the room) and then arrive at the PD and all the reflections must be considered. However, the impulse response is mainly dominated by the first reflection [51].

Figures 2.5a and 2.5b show the distribution of optical power at a PD considering LEDs with semi-angle at half power of 15° and 75° respectively. It can be observed that there is an almost uniform power distribution at the center of the room with maximum and minimum power levels of 14.5 dB and -14.5 dB respectively depending on the half angle of the LED.

Figures 2.6a and 2.6b show the distribution of horizontal illuminance at a PD with the LED lights with specifications as listed in Table 2.1. From these figures, it can be observed that maximum values of illuminance of 568.10 lx and 911.69 lx are obtained at the center of the room for one LED and four LEDs respectively. The sufficient illuminance required by International Organisation for Standardisation (ISO) of 300 to 1500 lx [51] is obtained at all the places in the room. Therefore,

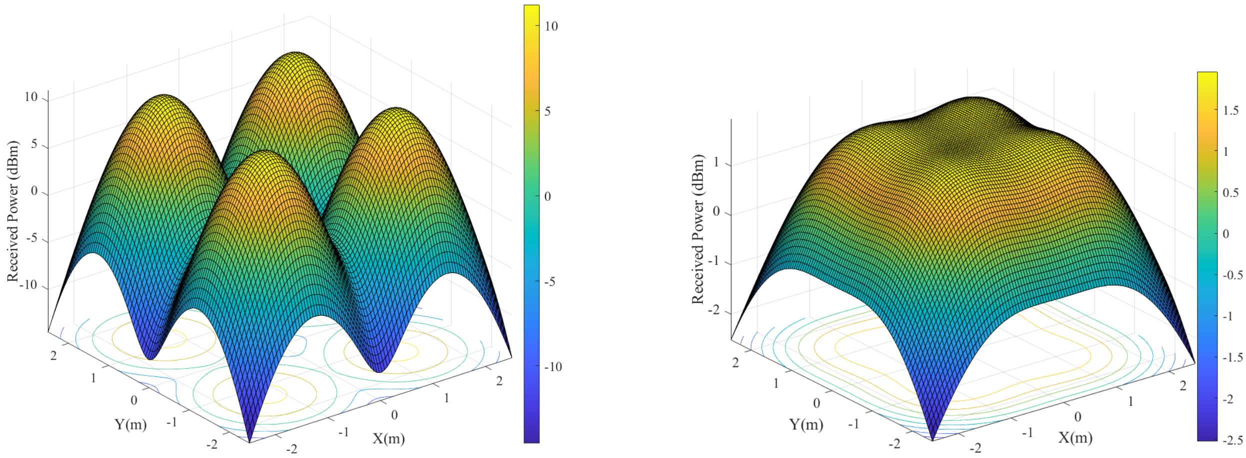

(a) FWHM =15^0 **(b)** FWHM =75^0

Figure 2.5: Optical power distribution of a LoS at the receiving plane given the parameters in Table 2.1

LED lighting has the potential to provide sufficient illumination as well as data communication simultaneously.

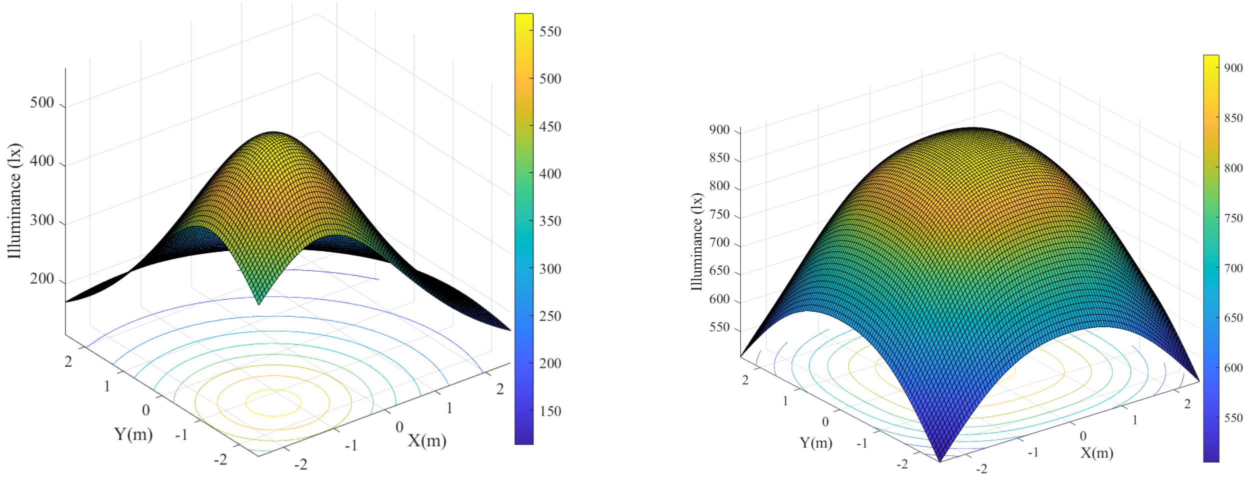

(a) Single LED **(b)** Four LEDs

Figure 2.6: Illuminance distributions given the parameters in Table 2.1

2.1.4 Applications of VLC

The inherent features of VLC such as license free spectrum, immunity to electromagnetic interference, high security, low cost and high data rates make it an attractive candidate in a number of applications requiring wireless communication technology. Some of the current and potential future applications of VLC are discussed next.

Intelligent Transportation Systems

Intelligent Transportation Systems (ITS) refers to the use of advanced information and communication technologies in the transportation sector to help improve road traffic management, reduce accidents, reduce congestion and ultimately provide a more intelligent use of transport networks. Recently, there has been increasing interest in the use of VLC in ITS to replace or complement the existing RF systems [67–69]. VLC-based systems can be deployed in ITS systems by utilizing the existing infrastructure such as the LED-based traffic lights, billboards and the LED-based car head lights to minimize road traffic accidents by providing information regarding road terrains, driving speeds, pedestrian crossing warning signs, etc. Although this information is currently being provided by RF technology in the form of Dedicated Short-Range Communication (DSRC), VLC can provide the unique features which are needed such as low latency, high reliability and high security [68].

Hospital Environments

Hospitals around the world are increasingly adopting E-health which is a broad group of activities that use electronic means to deliver health-related information, resources and services. E-health has widely been supported by the medical devices such as blood pressure monitors, infusion pumps, patient monitors that are increasingly becoming wireless. E-health services result in large amounts of data and thus reliable communication systems with sufficient capacity in hospitals are urgently needed to distribute and exchange these large data amounts. In order to allow for flexibility and re-modification of the health facilities, the use of communication cables should be avoided. This means that wireless technologies have to be greatly used. The main current wireless technologies in an indoor hospital environment are Z-wave, Bluetooth, ZigBee, Wireless Fidelity (WiFi) and Low-power wide area networks which are all based on the highly congested and costly radio frequency spectrum [70]. In addition, considering the safety of the patients, medical personnel and precision instruments, electromagnetic radiation of the communication systems in hospitals should be kept as low as possible. These strict requirements have led to the abandonment of RF technologies in some departments such as casualty ward and theatre and limiting the power radiated by the communication equipment. Medical devices such as infusion pumps and patient monitors require more stringent set of security protocols and require constant connectivity. In addition medical data is critical and should be protected against intruders.

Therefore, VLC has emerged as a promising solution in hospital environments and various solutions have been proposed by researchers [71]. In [71], a VLC system is proposed for transmission of medical data in hospitals. The researchers use Channel Inversion Pre-coding (CIP) to reduce the interference and the results show improved performance compared to the conventional VLC systems. In [72], an indoor hospital transportation robot known as HOSPI is developed. In HOSPI, the installed lighting in the building is combined with the navigational sensors of the robot to improve the control system.

Underwater Communication

The increasing dependence of human life on the water and its associated activities has meant that activities such as underwater exploration, sports activities such as diving have increased. Consequently, there is a need to find a reliable communication system for data transmission in underwater environments [73–75]. The underwater environment is a challenging one due to factors like multi-path propagation, strong signal attenuation especially over long ranges and time variations of the channel. Several researchers have demonstrated using VLC for transmission of data in underwater environments [52].

Underground Mines

VLC is a promising technique in underground mines in order to realize both communication and illumination at the same time. Reliable communication and monitoring systems are needed in underground mines due to the presence of toxic gases, falling debris, etc. in order to guarantee the safety of the miners and improve productivity in underground mines. Because of the complexity in underground mines, traditional wire-line communication systems such as coaxial cable, twisted pair and fiber optics are not easily realizable. Besides a sharp increase in the attenuation makes the traditional wireless communication systems based on RF technology unreliable. Consequently technologies such as Bluetooth, ZigBee, infrared and ultra-wide-band have been applied in underground mines to some extent. However, VLC is superior to these technologies specially for short range communications due to its numerous advantages outlined earlier. Consequently, many researchers have studied the possibility of VLC application in underground mines [53].

The working face and the mining roadway in underground mines are considered in [53] and the characterization of the optical channel path-loss and shadowing effects are performed. Results show that the path-loss exponent is linear in the log domain and the value of the path-loss exponent of non-LoS is larger than that of LoS. Additionally, the Root Mean Square (RMS) delay spread is inversely proportional to the distance between the transmitter and the receiver.

Aircraft Wireless Communication

The provision of an in-flight data communication system for passengers is becoming a trend in the current modern aircrafts. Some of the service providers provide WiFi solutions and aircraft-to-earth data communication links [76]. These solutions are however not economical to implement since they result into a low baud rate providing less user experience to passengers who are used to the high data connectivity on ground. Moreover, using the RF spectrum may interfere with the existing flight navigation systems [77]. VLC would be an alternative to these systems since the existing infrastructure like LED lights can be used for both illumination, reading and data communication.

Manufacturing Environments

The current wireless technologies such as Wireless Local Area Network (WLAN), Bluetooth and ZigBee have limited bandwidth rendering them ineffective in manufacturing environments. Nevertheless, numerous components such as sensors, robotic arms, conveyor belts, monitoring systems, mobile devices, machines and equipment need to be connected together to communicate and exchange data without using communication cables that would be problematic since these components can be very many in a manufacturing environment. This makes the use of VLC attractive since the existing lighting infrastructure in a factory can be used for data communication, sensing, indoor positioning and lighting at the same time [78]. In addition to high bandwidth, VLC also ensures security of the data since light does not penetrate walls and therefore there is no possibility of eavesdropping compared to using RF technology.

2.1.5 VLC Standardization

The potential applications of VLC have grown in the recent years and the VLC industry as a whole requires standards in order to facilitate product development by allowing products from diverse suppliers to be interconnected and by facilitating innovation to create a large market for common products. Therefore, there has been a number of efforts aimed at creating standards in VLC. The first efforts resulted into the creation of the Visible Light Communication Consortium (VLCC) in Japan in 2003. The members of VLCC created two standards in 2006 that were accepted by the Japan Electronics and Information Technology Industries Association (JEITA) in 2007. These standards include the JEITA CP-1221, which covers the basics of VLC communication system and the JEITA CP-1222 which is a standard for Visible Light ID System [2]. Both of these standards have small data rates of up to 4.8 Kbps. Furthermore, in 2013, the JEITA CP-1223 visible light beacon system standard was approved as an improved version of the JEITA CP-1222 [79].

IEEE 802.15.7

Due to the potential of VLC technology and the increasing interest of researchers in both academia and industry in this technology, IEEE introduced IEEE 802.15.7 which was approved in 2011 [80]. This standard defines the physical and Medium Access Control (MAC) sublayer in an optically transparent media using light wavelengths and promises data rates sufficient to support audio and video multimedia services [80]. This standard also involves the mobility of the optical link and considers the compatibility issues in various lighting infrastructures, problems due to interference from natural day light sources, artificial illumination sources such as incandescent lamps and noise. The standard adheres to the approved eye safety standards and also accommodates the optical camera communication technology.

This standard was required to solve the unique challenges in VLC usage that render the existing 802.11 and IrDA standards insufficient [81]. The standard covers issues such as network topologies, collision avoidance, dimming control support, visibility support, coloured status indication, colour stabilisation, performance quality parameters and acknowledgment.

This standard proposes On-Off-Keying (OOK), colour shift keying (CSK) and Variable Pulse Position (VPP) modulation techniques for both indoor and outdoor VLC systems. In this standard, multiple diverse network topologies such as peer-to-peer and star configurations are supported with the highest achievable data rate for indoor communication up to 96 Mbps. However, the data rate could be improved significantly by employing a Multiple Input-Multiple Output (MIMO) system and other advanced modulation formats [6, 82].

ITU-T G.9991 Standard

The International Telecommunication Union (ITU) released the ITU-T G.9991 Standard in March 2019. This standard defines the VLC system architecture and gives the specifications for the physical layer, data link layer and the management layer for high speed indoor optical wireless communication transceiver system using visible light and infrared communications [79, 83].

2.2 Overview of Orthogonal Frequency Division Multiplexing

OFDM is a digital Multi-carrier Modulation (MCM) scheme that extends the concepts of single-subcarrier modulation by using multiple subcarriers within the same channel.

When compared to the conventional Frequency Division Multiplexing (FDM) system, where a guard band is necessary between the subcarriers resulting in an inefficient spectrum usage, in an OFDM system, instead of transmitting a high-rate data stream with a single-subcarrier, closely spaced subcarriers that are orthogonal to each other are transmitted in parallel. Each of these subcarriers is modulated at a low symbol rate using the conventional digital modulation schemes such as M-ary Quadrature Amplitude Modulation (M-QAM), for example, 16-Quadrature Amplitude Modulation (QAM), 64-QAM, 256-QAM, etc or M-ary Phase Shift Keying (M-PSK), for example, Quadrature Phase Shift Keying (QPSK) or Binary Phase Shift Keying (BPSK). The combination of several subcarriers enables data rates similar to the conventional single-carrier modulation schemes within the same bandwidth. As shown in Figure 2.7, OFDM is more spectrally efficient compared to FDM and single-carrier modulation systems [84].

As will be described in Section 2.2.2, OFDM uses the Inverse Fast Fourier Transform (IFFT) operation for modulation and multiplexing operation. This results in a sinc-shaped spectrum of the individual subcarriers. Therefore, each OFDM subcarrier has significant side lobes over the frequency range that includes many other subcarriers [85]. This is one of the disadvantages of OFDM, i.e. it is quite sensitive to frequency offset and phase noise. However, the resulting interference will be insignificant as long as the subcarriers are orthogonal to each other and the transceivers are well synchronized with each other.

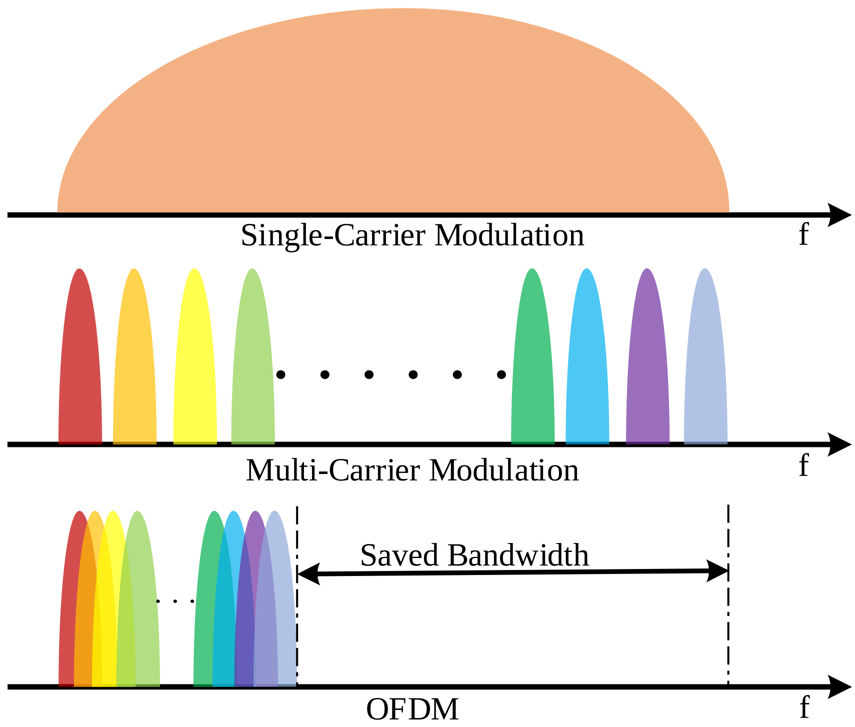

Figure 2.7: Comparing the bandwidth utilization between single-carrier modulation, conventional FDM system and OFDM system

OFDM has recently become a popular modulation scheme for wideband digital communication systems and is used in applications such as audio broadcasting, digital television broadcasting, digital subscriber line, internet access, power line networks, Fourth Generation (4G), 5G mobile communication systems and VLC systems [9, 10, 86–89].

The main advantage of OFDM compared to single-subcarrier modulation is its ability to cope with severe channel conditions, for example attenuation, selective fading due to multipath channel, etc without the need for complex equalization filters at the receiver. The low symbol rate makes the use of a guard interval in form of a cyclic prefix practical, making it possible to combat ISI in a dispersive channel.

2.2.1 Brief History of OFDM

The history of FDM which is a precursor of OFDM can be traced in the 1870s when researchers such as Alexander Graham Bell, Elisha Gray and Thomas Edison started researching on ways of transmitting several non-interfering telegraph channels aimed at increasing the capacity of the telegraph transmission lines [90]. FDM had two main challenges. Firstly, there was wastage of scarce wireless frequency spectrum in form of guard bands between the subchannels which was introduced to solve the problem of Intercarrier Interference (ICI). Secondly, each subchannel in FDM required a separate set of modulators and demodulators leading to very complex systems. The first challenge was solved by a proposal by Robert W. Chang of Bell Labs in 1966 who proposed to use subchannel signals with overlapping but non-interfering frequencies for transmission [91].

Chang's proposal marked the beginning of the introduction of OFDM.

The next key milestone in the development of OFDM came in 1971 with the proposal by Weinstein and Ebert who introduced the idea of using the Fast Fourier Transform (FFT) to generate orthogonal signals [92]. The FFT is an efficient and fast implementation of the Discrete Fourier Transform (DFT). The use of the cyclic prefix to eliminate ISI was proposed by Peled and Ruiz in 1980 [93].

The actual practical realizations of OFDM started in the mid-1980s when OFDM was used in wireless communications [94] and wired communications [95]. OFDM has also been used in long distance optical communication networks where it can help to reduce chromatic dispersion [96] and Passive Optical Networks (PONs) [97]. OFDM also forms the basis for the 4G wireless communication systems and is used in 4G wireless cellular standards such as Long-Term Evolution (LTE) and Worldwide interoperability for Microwave Access (WiMAX) [98]. Also, the wireless Local Area Network (LAN) standards such as 802.11 a/g/n are based on OFDM [99]. It is a key wireless access standard in the 5G networks and beyond [86, 87]. OFDM has also been widely investigated for use in VLC [9, 10, 88, 89] with data rates in excess of 40 Mbps realised [64].

2.2.2 Conventional OFDM System Description

In this section, the conventional OFDM system used in RF wireless communication is presented. Figure 2.8 shows the block diagram of the conventional OFDM system including both the transmitter and receiver sections. The different sections in the block diagram are described in the next paragraphs.

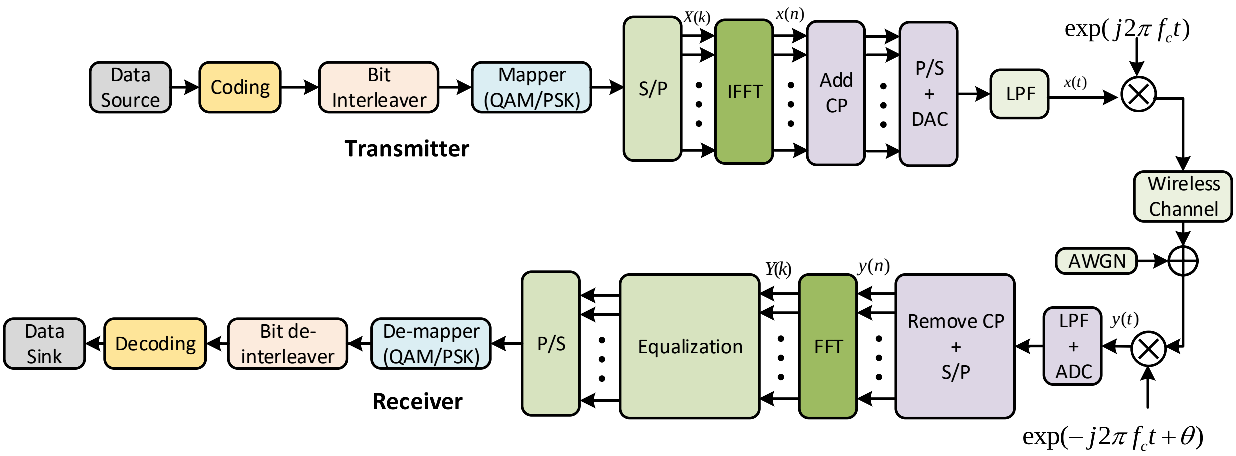

Figure 2.8: Block diagram of the transmitter and receiver in a conventional OFDM System. S/P: serial-to-parallel converter, P/S: parallel-to-serial converter, CP: cyclic prefix, DAC: digital-to-analog converter, ADC: analog-to-digital converter, LPF: low pass filter

At the OFDM transmitter, the input data stream is first coded using the FEC techniques such as convolutional codes, block codes, etc. This is followed by the bit interleaver. The input bits are then grouped and mapped onto source data symbols using a digital modulation scheme such as M-QAM or M-PSK. This mapping is usually performed based on Gray coded constellation mapping. The stream of data symbols is then converted from serial-to-parallel resulting in $\mathbf{X}$, where

$$\mathbf{X} = [X(0), X(1), \cdots, X(N-1)], \tag{2.10}$$

where N is the total number of subcarriers.

$\mathbf{X}$ is then passed through the IFFT module in order to generate the N time domain samples. The n-th time domain sample loaded onto the k-th subcarrier is given by

$$x(n) = \frac{1}{\sqrt{N}} \sum_{k=0}^{N-1} X(k) \exp(j\frac{2\pi kn}{N}) \tag{2.11}$$

It can be shown that for large values of N, using the central limit theorem that $x(n)$ follows a Gaussian distribution for both its real and imaginary components. This is due to the addition of a large number of independent and identically distributed (i.i.d.) random variables. This is true for any practical number of subcarriers, typically for $N \geq 16$ [100].

A cyclic prefix is then added to the time domain signal $x(n)$ and then converted from parallel-to-serial before being converted to analog by the Digital-to-Analog Converter (DAC). The resulting baseband analog signal is passed through a Low Pass Filter (LPF) resulting in a continuous time analog signal $x(t)$ which is then up-converted by a carrier frequency f_c and then transmitted across a wireless channel.

When an OFDM signal is transmitted through a wireless channel, noise will be added to it. In this thesis, this noise is modelled as Additive White Gaussian Noise (AWGN) with zero mean and variance σ_N^2. At the receiver, the signal is first down converted by mixing it with the signal

$$s(t) = \exp(-j2\pi f_c t + \theta), \tag{2.12}$$

where θ is the phase offset between the phase of the receiver Local oscillator (LO) and the carrier phase at the start of the received OFDM symbol. The resulting signal, $y(t)$ is then passed through LPF and converted from analog-to-digital to obtain the baseband discrete time signal.

The cyclic prefix is then removed and the resulting signal converted from serial-to-parallel to generate the time domain signal given by

$$\mathbf{y} = [y(0), y(1), \cdots, y(N-1)] \tag{2.13}$$

The signal **y** is then fed to the FFT module to produce the frequency domain signal

$$\mathbf{Y} = [Y(0), Y(1), \cdots, Y(N-1)] \tag{2.14}$$

The k-th frequency domain symbol is given by

$$Y(k) = \frac{1}{\sqrt{N}} \sum_{n=0}^{N-1} y(n) \exp(-j\frac{2\pi kn}{N}) \tag{2.15}$$

Equalization is then performed to obtain the estimates of the transmitted symbols. This is followed by parallel-to-serial conversion before demodulation. Finally, if interleaving and coding processes were done at the transmitter, the reverse processes of de-interleaving and decoding are performed to obtain the estimate of the transmitted data stream.

2.2.3 Cyclic Prefix in OFDM

The cyclic prefix is an important component in an OFDM system used to combat ISI. Consider a frequency selective channel modeled with L channel taps,

$$\mathbf{h}(l) = h(0),\ h(1), \cdots, h(L-1) \tag{2.16}$$

The received symbol y at a time instant n can be given by [101]

$$y(n) = h(0)x(n) + \underbrace{h(1)x(n-1) + \cdots + h(L-1)x(n-L+1)}_{\text{ISI component}} + w(n), \tag{2.17}$$

where $w(n)$ represents the AWGN component at time instant, n. From Equation (2.17), it can be observed that the received symbol $y(n)$ at the time instant n experiences ISI from the previous $L-1$ transmitted symbols.

Considering two OFDM symbols, $x(n) = x(0),\ x(1), \cdots, x(N-1)$ and $\tilde{x}(n) = \tilde{x}(0),\ \tilde{x}(1), \cdots, \tilde{x}(N-1)$ where $x(n)$ and $\tilde{x}(n)$ are the IFFT samples of the modulated samples $X(n)$ and $\tilde{X}(n)$ respectively.

The two OFDM blocks of symbols transmitted sequentially can be given as follows

$$\hat{x}(n) = \underbrace{\tilde{x}(0),\ \tilde{x}(1), \cdots, \tilde{x}(N-1)}_{\text{Previous OFDM symbol block}},\ \underbrace{x(0),\ x(1), \cdots, x(N-1)}_{\text{Current OFDM symbol block}} + \hat{w}(n) \tag{2.18}$$

The received symbols $y(0)$ and $y(1)$ corresponding to the transmitted symbol $x(0)$ and $x(1)$ respectively from the current OFDM symbol block can be given as follows

$$y(0) = h(0)x(0) + \underbrace{h(1)\tilde{x}(N-1) + \cdots + h(L-1)\tilde{x}(n-L+1)}_{\text{ISI component from the previous OFDM symbol block}} + w(0) \tag{2.19}$$

and

$$y(1) = h(0)x(1) + h(1)x(0) + \underbrace{h(2)\tilde{x}(N-1) + \cdots + h(L-1)\tilde{x}(n-L+2)}_{\text{ISI component from the previous OFDM symbol block}} + w(1) \tag{2.20}$$

It is clear from Equations (2.19) and (2.20) that $y(0)$ and $y(1)$ experience ISI from $\tilde{x}(N-1)$, $\tilde{x}(N-2),\cdots,\tilde{x}(n-L+1)$ and $\tilde{x}(N-1)$, $\tilde{x}(N-2),\cdots,\tilde{x}(n-L+2)$ symbols respectively from the previous OFDM symbol block.

The addition of the cyclic prefix combats ISI as follows: Consider a modified transmission scheme where the last L_{CP} samples from the OFDM symbol block are added to the beginning of the symbol as shown in Figure 2.9.

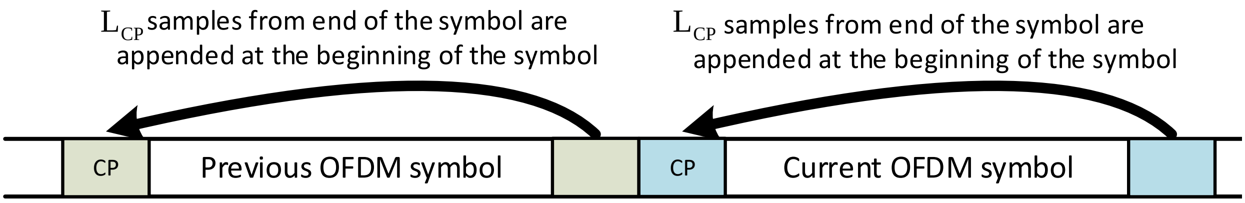

Figure 2.9: OFDM Symbols with Cyclic Prefix (CP)

The resulting transmitted bit stream can be expressed as follows

$$\begin{aligned} y(n) = &\underbrace{\tilde{x}(0),\ \tilde{x}(1),\cdots,\tilde{x}(N-1)}_{\text{Previous OFDM symbol block}},\ \underbrace{x(N-L_{\text{CP}}),\ x(N-L_{\text{CP}}+1),\cdots,x(N-1)}_{\text{CP}}, \\ &\underbrace{x(0),\ x(1),\cdots,x(N-1)}_{\text{Current OFDM symbol}} + w(n) \end{aligned} \tag{2.21}$$

For this transmission scheme, $y(0)$ is given by

$$y(0) = h(0)x(0) + \underbrace{h(1)x(N-1) + \cdots + h(L-1)x(N-L+1)}_{\text{ISI from the same OFDM symbol}} + w(0) \tag{2.22}$$

Therefore if $L_{\text{CP}} \geq L-1$, inter-OFDM symbol can be avoided and the ISI is restricted to samples from the same OFDM symbol. The samples, $y(n)$ are given by [102]

$$\begin{aligned}
&y(0) = h(0)x(0) + h(1)x(N-1) + \cdots + h(L-1)x(N-L+1) + w(0)\\
&y(1) = h(0)x(1) + h(1)x(0) + \cdots + h(L-1)x(N-L+2) + w(1)\\
&\vdots\\
&y(N-1) = h(0)x(N-1) + h(1)x(N-2) + \cdots + h(L-1)x(N-L) + w(N-1)
\end{aligned} \tag{2.23}$$

It can be observed from Equation (2.23) that the output $y(n)$ is a circular convolution between the channel filter $h(n)$ and the input $x(n)$ expressed as

$$\begin{aligned}
[y(0),\ y(1),\cdots,y(N-1)] &= [h(0),\ h(1),\cdots,h(L-1),\ 0,\cdots,0]\\
&\circledast_N [x(0),\ X(1),\cdots,x(N-1)] + [w(0),\ w(1),\cdots,w(N-1)],
\end{aligned} \tag{2.24}$$

where the operator $\circledast_N$ denotes the circular convolution of modulo N. Therefore, the output $\mathbf{y}$ can be written as

$$\mathbf{y} = \mathbf{h} \circledast_N \mathbf{x} + \mathbf{w}. \tag{2.25}$$

Since circular convolution can be represented by multiplication in the frequency domain, taking the IFFT of $y(n)$ will result into [101]

$$Y(k) = H(k)X(k) + W(k),\, 0 \leq k \leq N-1 \tag{2.26}$$

In vector notation, Equation (2.26) can be represented as follows

$$\begin{bmatrix} Y(0)\\ Y(1)\\ \vdots\\ Y(N-1) \end{bmatrix} = \begin{bmatrix} H(0) & 0 & \dots & 0\\ 0 & H(1) & \dots & 0\\ \vdots & \ddots & \vdots & \\ 0 & 0 & \dots & H(N-1) \end{bmatrix} \begin{bmatrix} X(0)\\ X(1)\\ \vdots\\ X(N-1) \end{bmatrix} + \begin{bmatrix} W(0)\\ W(1)\\ \vdots\\ W(N-1) \end{bmatrix} \tag{2.27}$$

which can be written as

$$\mathbf{Y}^T = [\mathbf{H}]\,\mathbf{X}^T + \mathbf{W}^T \tag{2.28}$$

where $\mathbf{Y}^T$ is the transpose of $\mathbf{Y}$, $\mathbf{X}^T$ is the transpose of $\mathbf{X}$, $\mathbf{W}^T$ is the transpose of the noise vector, $\mathbf{W}$ and the diagonal matrix $[\mathbf{H}]$ represents the channel matrix with channel coefficients $H(k), 0 \leq k \leq N-1$.

Impact of the Cyclic Prefix on the Data Rate

As explained above, the minimum length of the cyclic prefix required to combat ISI is $L-1$, where L is the number of channel taps/channel coefficients in the wireless channel. This $L-1$ is also the delay spread of the wireless channel [103].

However, since the samples $x(N-L_{\text{CP}})$, $x(N-L_{\text{CP}}+1), \cdots, x(N-1)$ are simply repeated at the beginning, they do not carry any additional information. Therefore, the effect of addition of a long cyclic prefix is loss in throughput of the system which can be computed as follows

$$\text{Loss in throughput} = \frac{L_{\text{CP}}-1}{N+L_{\text{CP}}-1}, \tag{2.29}$$

where N is the total number of subcarriers and L is the total number of channel coefficients. As N becomes very large, then

$$\lim_{N\to\infty} \frac{L_{\text{CP}}-1}{N+L_{\text{CP}}-1} \to 0 \tag{2.30}$$

Therefore, for a large N, the loss in throughput can be considered to be negligible. However, as N increases, the decoding delay at the receiver also increases since the system has to wait for the arrival of the entire block of N samples in order to begin the demodulation process. Therefore, there is a trade-off for increasing N versus the decoding delay.

2.3 Overview of Optical-OFDM

In practical VLC systems, the modulation and demodulation of the optical carrier are usually obtained through Intensity Modulation with Direct Detection (IM/DD) [7]. In IM/DD, the information is modulated onto the instantaneous power of the optical carrier and the detector will generate a current that is proportional to the instantaneous optical power. Therefore, only the intensity of the optical signal is detected, and there is no frequency or phase information.

The RF-OFDM discussed in Section 2.2 has been considered for practical implementation in VLC systems due to its numerous advantages including its ability to combat multi-path induced ISI in a dispersive optical channel without the need for complex equalization filters at the receiver. Also, the possibility of combining OFDM with any other multiple access schemes makes OFDM

Table 2.2: Comparison of Optical-OFDM and RF-OFDM system characteristics

Description	Optical-OFDM	RF-OFDM
Transmitter signal	Real and unipolar	Complex and bipolar
Modulation	Intensity modulation	Both intensity and phase
Detection	Direct detection	Coherent (mainly)
Media	Lightwave	RF electromagnetic waves

highly attractive in VLC systems where multiple LEDs are used for both illumination and data communication.

In spite of the advantages of OFDM used in RF communication systems, it cannot be applied in a straightforward manner to VLC systems without significant changes due to the reasons given in Section 2.3.1.

2.3.1 Optical-OFDM versus RF-OFDM

In VLC systems, the information is carried by fluctuations in light intensity which is detected by the front end optical devices and decoded at the receiver. This incoherent or direct transmission technique is referred to as IM/DD [2]. Whereas the RF signal is complex and bipolar, the optical power of the LED is intrinsically limited to be real and positive valued. As a result, the information bearing signal in optical-OFDM systems is also limited by the same fundamental constraints. Furthermore, eye safety and linearity considerations as well as the dynamic range of the front-end opto-electronic elements bring additional limitations to the transmitted signal [7]. Table 2.2 gives a summary of the comparison between the typical system characteristics in Optical-OFDM and RF-OFDM.

The real OFDM signal is generally obtained by constraining the frequency domain input to the IFFT to have Hermitian symmetry. The resulting bipolar output has to be made unipolar. To this end, two main approaches have been proposed. The first approach is to add a suitable DC component to the bipolar signal resulting in what is called Direct Current biased Optical-OFDM (DCO-OFDM) [8]. The DCO-OFDM technique uses both the even and odd subcarriers but results in an increase in optical power which is undesirable in VLC systems. To that end, the second approach was proposed where the unipolar signal is generated by clipping the entire negative excursion resulting in what is called the Asymmetrically Clipped Optical-OFDM (ACO-OFDM) [9]. With ACO-OFDM, by limiting the modulated symbols to only the odd subcarriers, the resulting clipping noise will be orthogonal to the transmitted information. Hence, the integrity of the transmitted information will be preserved. The Pulse Amplitude Modulated (PAM) Discrete Multitone (DMT) [10] also utilizes a similar principle like ACO-OFDM and in this technique only the imaginary parts of all the subcarriers are modulated using PAM symbol levels.

Due to the fact that the ACO-OFDM uses only half of the subcarriers and the PAM-DMT does not modulate information on real parts of the subcarriers, these two schemes are less spectrally efficient compared to DCO-OFDM. However, the DCO-OFDM technique is less power efficient compared to both ACO-OFDM and PAM-DMT due to the addition of the DC offset. It is because of this that hybrid techniques were proposed to strike a balance between power efficiency and spectrum efficiency. In the next Sections, the different Optical-OFDM techniques are discussed.

2.3.2 Direct Current biased Optical-OFDM

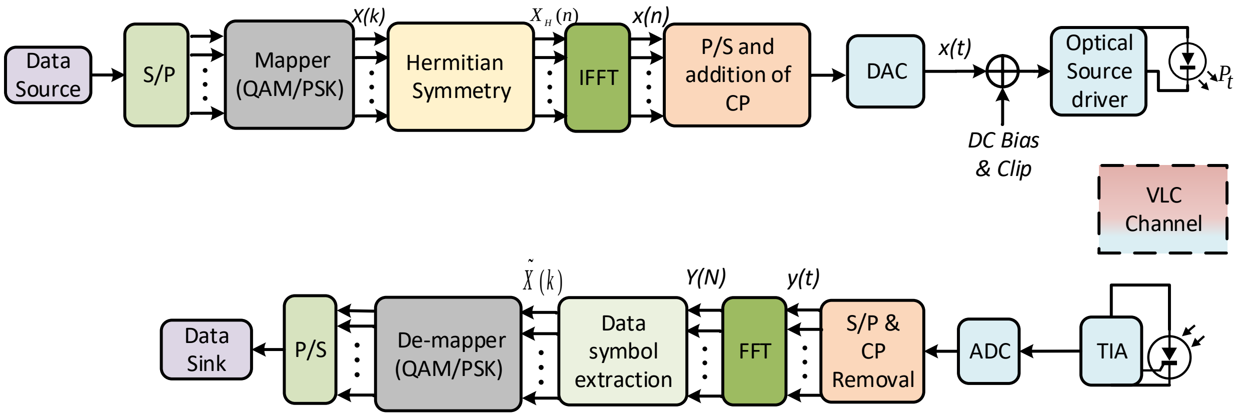

Figure 2.10: Block diagram of the DCO-OFDM system

Figure 2.10 shows the schematic diagram of the DCO-OFDM communication system including both the transmitter and the receiver. In this system, the real signal is obtained by imposing the Hermitian symmetry prior to the IFFT operation and a suitable DC offset is added to the signal to make it positive. The remaining negative peaks are clipped resulting in a real and unipolar signal suitable for transmission in an optical channel. At the DCO-OFDM transmitter, the transmitted bit stream is converted from serial-to-parallel and then mapped onto source data symbols using a digital modulation scheme such as M-QAM or M-PSK to obtain X given as

$$\mathbf{X} = [X(0), X(1), \cdots, X(N/2-1)] \tag{2.31}$$

In this system both the even and odd subcarriers are used to carry information and therefore the input to the IFFT module constrained to Hermitian symmetry is given by

$$\mathbf{X}_H = [0, X(0), X(1), \cdots, X(N/2-1), 0, X^*(N/2-1), \cdots, X^*(0)], \tag{2.32}$$

where X^* denotes the complex conjugate of X.

The n-th time domain real sample of the signal is now obtained by taking the N-point IFFT of Equation (2.32) as follows

$$x(n) = \frac{1}{\sqrt{N}} \sum_{k=0}^{N-1} X_H(k) \exp\left(j\frac{2\pi kn}{N}\right) \tag{2.33}$$

where N is the total number of subcarriers and $X_H(k)$ is the k-th subcarrier of the signal $\mathbf{X}_H$. Due to the use of Hermitian symmetry, and $X(0) = X(N/2) = 0$, the total number of unique data carrying subcarriers in the DCO-OFDM system is $N/2-1$. The signal $x(n)$ is then converted from parallel to serial and a cyclic prefix is appended in order to combat ISI. The continuous time domain signal, $x(t)$ is then obtained by converting $x(n)$ from digital to analog using the DAC. A DC offset, $\mathrm{DC_{bias}}$ is added to $x(t)$ to ensure that the transmitted signal is unipolar. It should be noted that a large DC bias will lead to an increase in optical power and therefore a suitable DC offset relative to the RMS value of the signal $x(t)$ is added [89] and hence

$$\mathrm{DC_{bias}} = \eta\sqrt{\langle|x(t)|^2\rangle}, \tag{2.34}$$

where η is a constant and the DC bias is defined as the bias of $10\log(\eta^2+1)$ dB [89].

The remaining negative peaks will then be clipped resulting in a real and unipolar signal that is subsequently fed to the LED for transmission in the VLC channel. Figures 2.11, 2.12 and 2.13 illustrate respectively the time domain signal after the IFFT operation, after adding a suitable DC offset (7 dB) and after zero clipping to obtain a real and unipolar signal suitable for transmission in a VLC optical channel.

At the receiver, the PD converts the received optical signal to an electrical signal which is then amplified by an amplifier, typically, a transimpedance amplifier. The signal $y(t)$ is then converted from analog to digital by the Analog-to-Digital Converter (ADC) and a serial-to-parallel conversion is performed before it is fed to the FFT module to obtain the frequency domain signal $Y(k)$. Data symbol extraction is then performed to obtain $\hat{X}(k)$ which is an estimate of $X(k)$. QAM or QPSK de-mapping is then performed on $\hat{X}(k)$ and a parallel-to-serial conversion is then performed to obtain the received data bits.

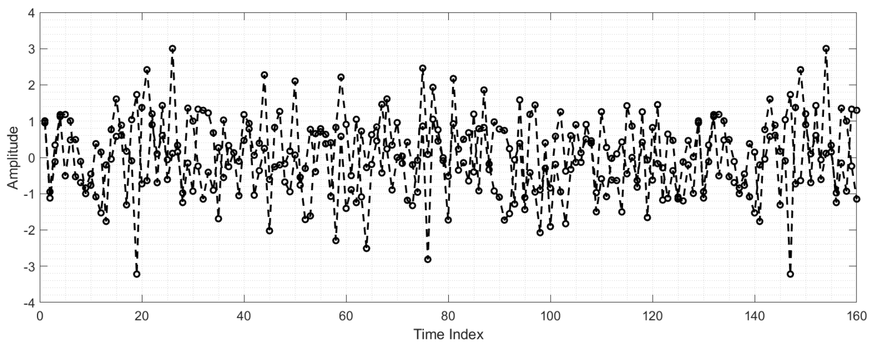

Figure 2.11: Signal $x(n)$ after IFFT operation

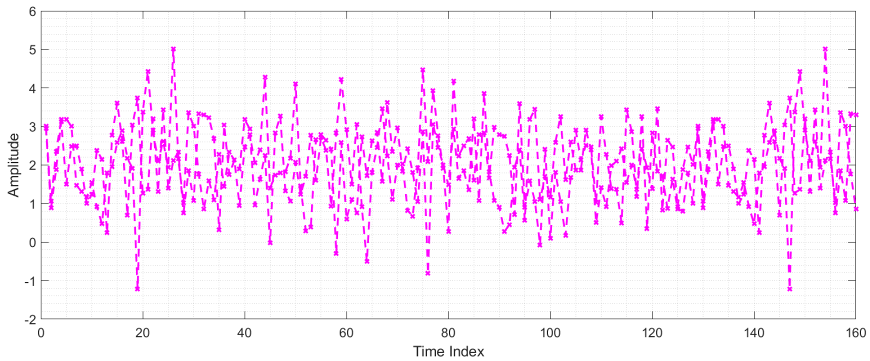

Figure 2.12: Signal $x(t)$ after adding a suitable DC offset (7 dB)

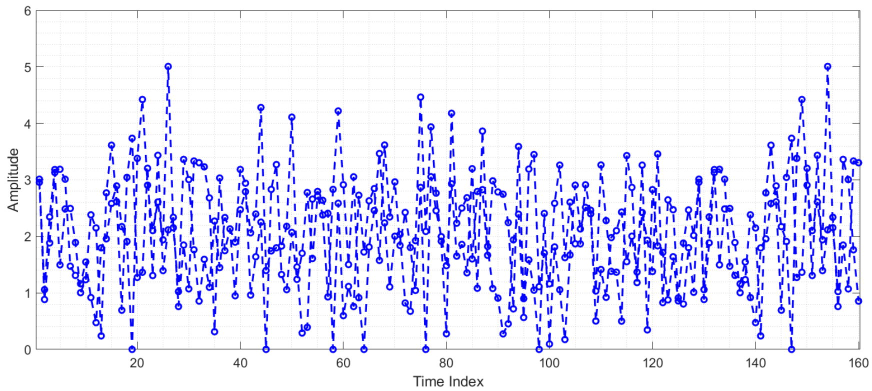

Figure 2.13: Signal $x(t)$ after zero clipping

Effect of DC Bias on the output signal

For smaller constellations such as 4-QAM and 16-QAM, a smaller DC bias such as 7 dB results in better Signal-to-Noise Ratio (SNR) performance as shown in Figure 2.14. If a large DC bias such as 13 dB is used, the bit errors due to the clipping noise reduce for large constellations such as 64-QAM and 256-QAM and this can be seen in Figure 2.15.

2.3.3 Asymmetrically Clipped Optical-OFDM

Figure 2.16 shows the block diagram of an ACO-OFDM [9] system including both the transmitter and the receiver sections showing the main components. At the ACO-OFDM transmitter, the transmitted bit stream is converted from serial-to-parallel and then mapped onto source data symbols using a digital modulation scheme such as M-QAM or M-PSK to obtain $\mathbf{X}$ given by Equation (2.31).

In an ACO-OFDM system, only the odd subcarriers are used to carry data symbols while the even subcarriers are used to form a bias signal that ensures the transmitted OFDM signal is positive. Further, the input to the IFFT is constrained to Hermitian symmetry to ensure that the IFFT output is real. Therefore, the input to the IFFT is given by

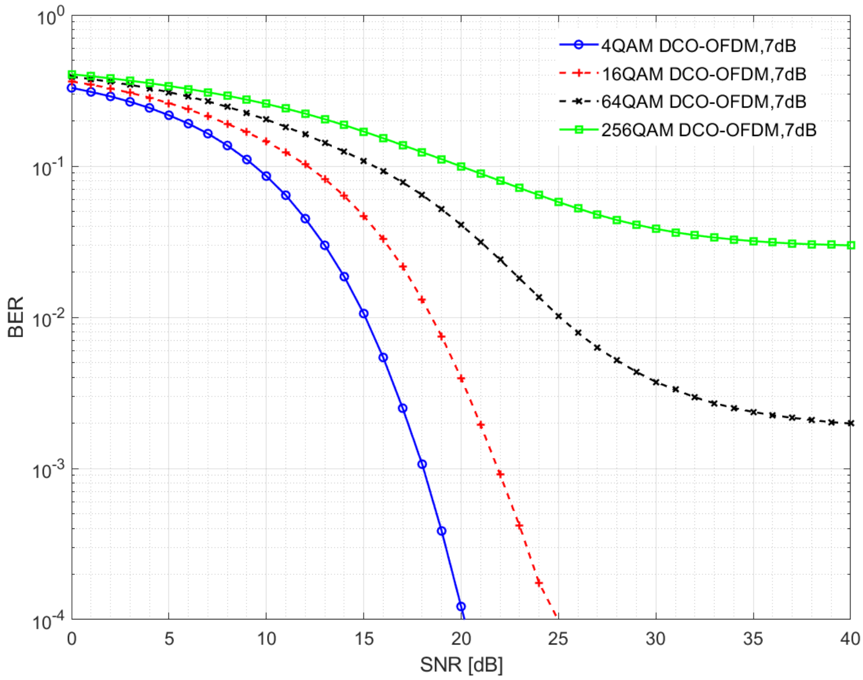

Figure 2.14: BER against SNR curves for DCO-OFDM communication system for 4-QAM, 16-QAM, 64-QAM and 256-QAM with a DC bias of 7 dB

$$X_H = [0, X(1), 0, X(3), \cdots, X(N/2-1), 0, X^*(N/2-1), \cdots, X^*(1)] \tag{2.35}$$

The IFFT transform of Equation (2.35) is taken using Equation (2.33) resulting in a real time domain signal that follows half-wave symmetry

$$x(n) = -x(n+N/2), 0 \leq n \leq (N/2-1) \tag{2.36}$$

Therefore, the negative signal excursion can be clipped without any loss of information.

The next step is to convert $x(n)$ from parallel-to-serial and addition of the cyclic prefix to combat ISI. The time domain signal is then converted from digital to analog to obtain the continuous time domain signal $x(t)$.

At the receiver, the received optical signal is detected by PD and converted from optical to electrical signal. The analog electrical signal is converted to a digital signal and the cyclic prefix is removed before the FFT operation. It was shown in [9] that the clipping distortion only affects the even subcarriers when transformed to the frequency domain and the data carrying subcarriers are not impaired at all. Since the data is transmitted only on the odd subcarriers, the transmitted data can be recovered by a simple FFT operation before appropriate de-mapping and converting from parallel to serial to recover the transmitted bit stream.

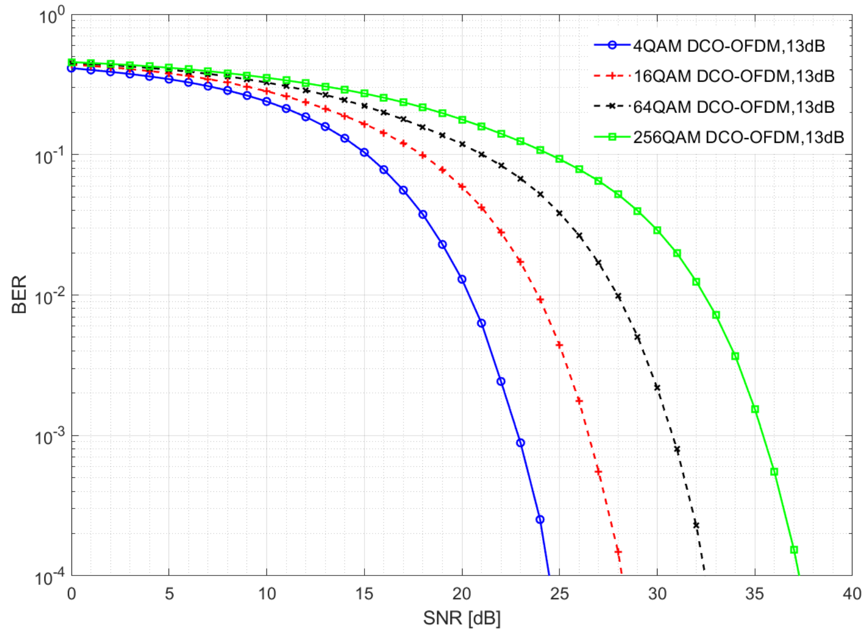

Figure 2.15: BER against SNR curves for DCO-OFDM communication system for 4-QAM, 16-QAM, 64-QAM and 256-QAM with a DC bias of 13 dB

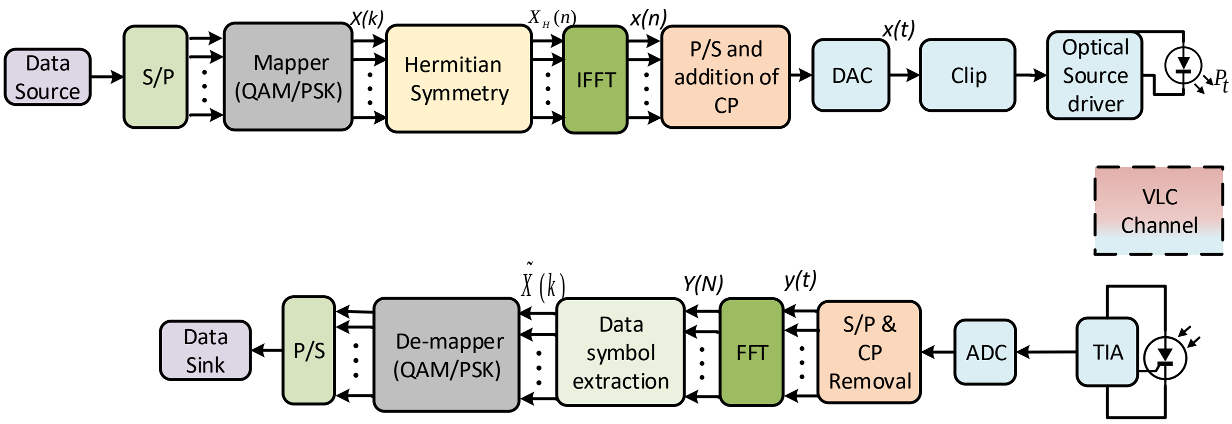

Figure 2.16: Block diagram of the ACO-OFDM system

2.3.4 Pulse Amplitude Modulation Discrete Multi-tone

In PAM-DMT [10], only the imaginary parts of the subcarriers are modulated using PAM symbol levels and all the subcarriers are used except the 0-th and $N/2$-th subcarriers. Therefore, the input to the IFFT module can be represented as

$$X = [0, X(1), X(2), \cdots, X(N/2-1), 0, X^*(N/2-1), \cdots, X^*(1)], \tag{2.37}$$

where, $X(k) = ib(k), k = 1, 2, \cdots, N/2-1$ is a real-valued PAM signal and X^* is the complex conjugate of X.

As shown in [104], the time-domain signal $x(n)$ after the IFFT operation follows symmetry as

$$x(n) = -x(N-n), \; (0 \leq n \leq N/2) \tag{2.38}$$

Therefore, the PAM-DMT signal, $x_{PAM}(n)$ can be clipped at zero without any loss of information as

$$x_{\mathrm{PAM}}(n) = \begin{cases} x(n), & x(n) \geq 0, \\ 0, & x(n) < 0 \end{cases} \tag{2.39}$$

The clipping noise is orthogonal to the desired information and therefore the data can be easily demodulated from the imaginary part of the subcarriers at the receiver. Unlike in ACO-OFDM, all the subcarriers are used to carry the data symbols resulting in a higher spectral efficiency.

2.3.5 Hybrid Optical-OFDM Modulation Techniques

The three basic Optical-OFDM techniques discussed above i.e. DCO-OFDM, ACO-OFDM and PAM-DMT have some limitations when it comes to practical implementation systems. For example, the DCO-OFDM system requires the addition of a DC offset in order to obtain a unipolar signal. This makes it less power efficient. Moreover, the increase in optical power is undesirable in VLC systems where it is required that the transmitted power be kept as low as possible due to stringent eye-safety regulations especially for indoor VLC systems. On the other hand, the ACO-OFDM system uses only half of the subcarriers with the even subcarriers not used for data transmission. Consequently, this results in a reduction in spectral efficiency. In a similar way, the PAM-DMT technique is also less spectrally efficient compared to the DCO-OFDM technique since the transmitted data is only modulated on the imaginary parts of the subcarriers.

Therefore, in order to strike a balance between spectral efficiency and power efficiency, several hybrid Optical-OFDM techniques [11, 13, 104] have been recently proposed for more realistic practical implementations. These techniques are referred to as hybrid techniques because they involve the three basic Optical-OFDM techniques i.e. DCO-OFDM, ACO-OFDM and PAM-DMT in their structures. These techniques are discussed in the next Sections.

Asymmetrically Clipped Direct Current biased Optical-OFDM

The Asymmetrically Clipped DC biased Optical-OFDM (ADO-OFDM) was proposed by Dissanayake et al. [11]. This technique is a hybrid combination of both ACO-OFDM and DCO-OFDM and it works by modulating information on both the odd and the even subcarriers but these two sets are treated differently. The resulting time domain signal from the odd subcarriers is clipped after the IFFT operation to generate x_{ACO} and due to the orthogonality property, the clipping noise only affects the even subcarriers. An appropriate DC bias is added to the unipolar time domain signal from the even subcarriers after the IFFT operation to generate x_{DCO}. Both x_{ACO} and x_{DCO} are appropriately added together to generate the time domain signal that undergoes further processing at the transmitter including addition of the cyclic prefix to combat multipath induced ISI. At the receiver side, the information that was transmitted on odd and even subcarriers is recovered separately and combined to obtain the transmitted information. The ADO-OFDM is spectrally more efficient compared to the ACO-OFDM since both the odd and even subcarriers are modulated with information unlike in ACO-OFDM where it is only the odd subcarriers that are modulated. It is more power efficient since the DC bias is added to only the even subcarriers compared to DCO-OFDM where the bias is added to both the odd and even subcarriers.

Hybrid Asymmetrically Clipped Optical-OFDM

Utilizing a similar approach that was used for the ADO-OFDM technique, Bilal and Mohsen [104] proposed the Hybrid Asymmetrically Clipped Optical-OFDM (HACO-OFDM) technique which is a combination of both ACO-OFDM and PAM-DMT techniques. In this hybrid scheme, the ACO-OFDM is used to modulate the odd subcarriers and PAM-DMT is used to modulate the imaginary parts of the even subcarriers drawn from a real one-dimensional (1D) constellation such as M-PAM. The clipping noise can be estimated and canceled at the receiver. The technique is less complex and is more power efficient since it does not require addition of the DC bias. It is also spectrally more efficient since all the subcarriers are used unlike the ACO-OFDM technique where only the odd subcarriers are used.

Layered Asymmetrically Clipped Optical-OFDM

Wang et al. [13] proposed the Layered Asymmetrically Clipped Optical-OFDM (LACO-OFDM) technique which consists of multiple layers of ACO-OFDM signals. Let L-layer LACO-OFDM refer to a layered ACO-OFDM with L layers, and layer l ACO-OFDM denote the l-th layer in LACO-OFDM.

In the n-th ACO-OFDM layer, only the $2^{l-1}(2k+1)$-th, $(k = 0, 1, \cdots, N/2^l - 1)$ subcarriers are modulated, denoted as $X^{(l)}_{\mathrm{ACO},k}$. After the IFFT operation, the negative signal excursion of the time domain signal can be clipped without loss of information resulting in $x^{(l)}_{\mathrm{ACO},n}$. In LACO-OFDM, different layers of ACO-OFDM are combined together in the time domain and transmitted simultaneously. The time domain LACO-OFDM signal with L layers can be written as

$$x_{L-\mathrm{ACO},n} = \sum_{i=1}^{L} \left\lfloor x^{(l)}_{\mathrm{ACO},n} \right\rfloor_c, \; n = 0, 1, \cdots N-1 \tag{2.40}$$

In LACO-OFDM, for a maximum number of layers $L = \log_2(N-1)$, the spectral efficiency is $(2 - 4/N)$ times that of conventional ACO-OFDM which converges to 2 for large values of N.

2.4 Factors for Optical-OFDM Technique Selection

There are several Optical-OFDM modulation techniques as discussed in the previous Sections. In order to select an appropriate technique, a number of factors should be considered including the following:

2.4.1 Bandwidth Efficiency, η_{BW}

Although the VLC spectrum can be considered to theoretically have an infinite bandwidth, other considerations limit the amount of the available bandwidth for distortion free communication. These factors include the LED modulation bandwidth [105], photodetector area and channel configurations, e.g. LoS, non-LoS and diffuse configurations. The bandwidth efficiency is defined by [106]

$$\eta_{\mathrm{BW}} = \frac{R_b}{\mathrm{BW}_{\mathrm{sys}}} \tag{2.41}$$

where $\mathrm{BW}_{\mathrm{sys}}$ is the system bandwidth and R_b is bitrate of the system.

Techniques that utilize both the odd and even subcarriers such as DCO-OFDM are preferred because they are more bandwidth efficient compared to those that do not use all the subcarriers such as ACO-OFDM.

2.4.2 Power Efficiency, η_P

In VLC systems, the transmitted power is usually limited by eye safety regulations especially for indoor VLC systems [7]. In addition, due to the use of portable battery powered equipment, it is desirable to ensure a longer battery life and this also puts a limit on the amount of power that is transmitted. The modulation techniques are usually compared in terms of the average optical power required to achieve a desired Bit Error Rate (BER) performance or the SNR over a given transmission link distance.

The power efficiency of a modulation technique is defined by [106]

$$\eta_P = \frac{\mathrm{E}_{\mathrm{pulse}}}{\mathrm{E}_{\mathrm{b}}} \tag{2.42}$$

where $\mathrm{E}_{\mathrm{pulse}}$ is the energy per pulse and E_{b} is the average energy per bit.

The DCO-OFDM technique involves the addition of a DC bias which increases the average transmitted power making it less power efficient compared to the ACO-OFDM technique.

2.4.3 Transmission Reliability

It is desirable to have a communication system with as few errors as possible. However, errors in a communication system are inevitable due to induced noise, signal distortion and ISI induced during the transmission process. There are a number of ways to improve the transmission reliability including coding, modulation and using diversity schemes. The ISI is eliminated in Optical-OFDM systems due to the addition of an appropriate cyclic prefix.

2.4.4 Other Factors

There are a number of other factors that affect the choice of a modulation scheme. The modulation scheme should be simple to implement and should be cost effective. Achieving a high power efficiency and/or high bandwidth efficiency will be of no use if the modulation technique is deemed too costly and expensive since VLC systems are intended to be produced in large quantities in order to meet the high demand [7].

3 Peak-to-Average Power Ratio Problem in OFDM Systems

This chapter presents the theoretical concepts of the Peak-to-Average Power Ratio (PAPR) problem which is considered as a serious drawback affecting the practical implementation of both Radio Frequency (RF) and optical-Orthogonal Frequency Division Multiplexing (OFDM) communication systems. Section 3.1 introduces the PAPR problem and discusses some of the implications of the high PAPR in Visible Light Communication (VLC) systems. Section 3.2 discusses the definition of the PAPR problem and the theoretical bounds of PAPR in both single-carrier and multicarrier OFDM systems. Section 3.3 discusses the factors that can be used to determine the trade-offs between PAPR reduction capability of a technique and other design considerations. Section 3.4 discusses the PAPR reduction techniques proposed in literature. Finally, in this chapter, we propose that the best strategy for PAPR reduction is to use hybrid techniques that take advantage of one or more techniques for PAPR reduction without sacrificing other performance parameters.

3.1 Introduction to PAPR

The current and future high speed wireless demands such as Virtual Reality (VR), Augmented Reality (AU), Internet of Things (IoT), driverless cars, telemedicine, Artificial Intelligence (AI), etc. require transmission technologies that can deliver high data rates. One of these technologies is OFDM, which in addition to higher data rates also has the ability to cope with severe channel conditions, for example attenuation and selective fading due to multipath channel without the need for complex equalization filters at the receiver. Moreover, the low symbol rate in OFDM makes the use of a guard interval in the form of a cyclic prefix practical, making it possible to combat Inter-Symbol Interference (ISI) in a dispersive channel.

Therefore, OFDM has been considered for high data rate applications as a key wireless access standard in the Fifth Generation (5G) networks and beyond [86, 87]. OFDM has also been widely investigated for use in VLC systems [9, 10, 88, 89] with data rates in excess of 40 Mbps realized [64, 65].

However, since the composite OFDM signal is a result of different subcarriers that are modulated independently, some of the subcarriers can add constructively leading to large signal envelope variations in the time domain when the input sequence to the Inverse Fast Fourier Transform (IFFT) is highly correlated. This is usually characterized by a high PAPR. The high PAPR is a serious problem in both RF-OFDM and Optical-OFDM that remains unresolved. The following are some of the implications of the high PAPR in OFDM systems:

1. Firstly, with a high PAPR it is impossible to contain the entire signal in the linear range of the transmitter devices like the power amplifier and the Digital-to-Analog Converter (DAC) without lower and/or upper clipping. Clipping of the signal will lead to distortion and an increase in Bit Error Rate (BER) leading to unreliable transmission.
2. Secondly, operating the transmitter devices beyond their linear ranges into the saturation region in order to accommodate all the large signal swings will lead to spectral growth in form of inter-modulation among the subcarriers and this will consequently lead to BER degradation.
3. Thirdly, it would be possible to design the transmitter devices with a large dynamic range. However, these will be more complex and will lead to an increase of the component devices at the transmitter which will subsequently lead to an increase in the overall cost of the transmitter.
4. Lastly, in VLC systems, the optical sources in particular, the Light Emitting Diode (LED) experience a significant drop in efficiency when they are operated outside their linear dynamic range due to the droop effect [7].

Considering the importance of OFDM and the seriousness of the high PAPR, a number of techniques have been proposed in the literature that could be employed to deal with this problem of the high PAPR. These techniques are described in Section 3.4.

3.2 The OFDM System Model

Figures 2.8, 2.10 and 2.16 illustrate the general schematic diagrams for the OFDM system in both RF-OFDM (Figure 2.8) and Optical-OFDM (Figures 2.10 and 2.16). For details regarding the operation of the RF-OFDM and Optical-OFDM systems, refer to Chapter 2. Because the composite OFDM signal is a summation of several subcarriers modulated independently, a high PAPR can result if these subcarriers are added constructively after the IFFT operation as illustrated in Figure 2.11. In this case, the received signal $y(t)$ will possess a significant amount of distortion. The PAPR of the OFDM signal can be reduced by modification of the signal characteristics in both time domain and frequency domain as will be explained later in Section 3.4.

3.2.1 Definition of the Peak-to-Average Power Ratio Problem

The PAPR is a measure of the power fluctuation in the composite OFDM signal and a high PAPR can appear in the OFDM signal when the N independent subcarriers are added to the same phase. The high PAPR leads to major inefficiencies in the performance of devices with limited dynamic range at the transmitter such as the LED, power amplifier and the DAC.

In a general sense, the electrical PAPR can be defined as the ratio of the peak power to average power of the analog transmitted signal and is given by

$$\text{PAPR}\{x(n)\} = \frac{\max\left\{|x(n)|^2\right\}}{\left\langle |x(n)|^2 \right\rangle}, \tag{3.1}$$

where $x(n)$ represents the time domain signal after the IFFT operation and $\langle \cdot \rangle$ denotes the statistical expectation. Additionally, the PAPR in dB can be written as

$$\text{PAPR}(\text{dB}) = 10\log_{10}(\text{PAPR}) \tag{3.2}$$

3.2.2 The CCDF of the PAPR

The cumulative distribution function (CDF) of the PAPR is widely a widely used performance metric for evaluating PAPR reduction techniques in multi-carrier communication systems. In the literature, the Complementary Cumulative Distribution Function (CCDF) of the PAPR is commonly used instead of the CDF itself, as it provides a more intuitive representation of PAPR exceeding a given threshold value, PAPR_0.

In [107], an approximate expression for the CCDF of the PAPR of a multi-carrier signal with Nyquist sampling rate is derived using the central limit theorem. Specifically, it is shown that for a large number of subcarriers, the real and imaginary parts of the time domain signal samples follow Gaussian distributions, each with a mean of zero and variance of 0.5. Consequently, the amplitude of a multi-carrier signal has a Rayleigh distribution, while the power distribution becomes a central chi-square distribution with two degrees of freedom.

The CDF of the amplitude of a signal sample is given by

$$F(\text{PAPR}_0) = 1 - e^{-\text{PAPR}_0} \tag{3.3}$$

and the CCDF of a data block is derived as follows [108]

$$\begin{aligned} \text{CCDF} = Pr\{\text{PAPR} > \text{PAPR}_0\} = 1 - Pr\{\text{PAPR} \leq \text{PAPR}_0\} &= 1 - F(\text{PAPR}_0)^N \\ &= 1 - \left(1 - e^{-\text{PAPR}_0}\right)^N \end{aligned} \tag{3.4}$$

where N is the number of subcarriers.

The frequency domain signal is usually oversampled L times in order to obtain an accurate approximation of the PAPR of the time domain signal. This oversampling is normally obtained through padding the frequency domain OFDM symbol with $N(L-1)$ zeros. Consequently, Equation (3.4) can be written as follows

$$\text{CCDF} = 1 - \left(1 - e^{-PAPR_0}\right)^{\alpha N}, \tag{3.5}$$

where α is the oversampling factor. It was shown in [109] that the discrete time domain signal can have about the same amplitude as the continuous time domain signal when an oversampling factor of $L = 4$ is used and this corresponds to an oversampling factor of $\alpha = 2.8$ [109].

3.2.3 Theoretical Bounds in PAPR

While analyzing the PAPR reduction requirements of an OFDM signal for a particular system, it is necessary to know the theoretical maximum values of the PAPR that can arise in the system. The high PAPR is a serious issue in OFDM systems compared to single-carrier systems. In the next Sections, the PAPR bounds of both single-carrier systems and OFDM systems are derived.

PAPR in a single-carrier system

Consider a single-carrier system with Binary Phase Shift Keying (BPSK) modulated symbols. Let the symbol stream in this system $x(0), x(1), \ldots$ be given as $+a, -a, +a, \ldots$ and so on. The power in each symbol is a^2. Also, in this system, the power in each symbol is peak power at any given time instant. Therefore

$$\text{Peak Power} = \text{Average Power} = \left\langle |x(n)|^2 \right\rangle = a^2 \tag{3.6}$$

In this case, the PAPR will be given as

$$\text{PAPR}\{x(n)\} = \frac{\max\left\{|x(n)|^2\right\}}{\left\langle |x(n)|^2 \right\rangle} = \frac{a^2}{a^2} = 1 = 0 \text{ dB}. \tag{3.7}$$

The relationship in Equation (3.7) above clearly shows that the PAPR in single-carrier systems is 0 dB, i.e. there is no deviation of the instantaneous power from the mean power.

PAPR in OFDM systems

Considering an M-ary Phase Shift Keying (M-PSK) modulated OFDM system, the signal constellation has the same amplitude level, thus the power across all the subcarriers is constant, i.e.

$|X(k)| = a$.

The n-th IFFT sample, $x(n)$ is given by the IFFT operation

$$x(n) = \frac{1}{N}\sum_{k=0}^{N-1} X(k)\exp\left(j\frac{2\pi kn}{N}\right) \tag{3.8}$$

The average power in the symbols is given by

$$\begin{aligned}\text{Average Power} = \left\langle |x(n)|^2 \right\rangle &= \frac{1}{N^2}\sum_{k=0}^{N-1}\left\langle |X(k)|^2\right\rangle \left\langle \left|\exp\left(j\frac{2\pi kn}{N}\right)\right|^2 \right\rangle \\ &= \frac{1}{N^2}\sum_{k=0}^{N-1}\left\langle |X(k)|^2\right\rangle = \frac{1}{N^2}\sum_{k=0}^{N-1} a^2 = \frac{a^2}{N}\end{aligned} \tag{3.9}$$

The peak power of the OFDM signal is given by [45]

$$\max_{0\le n\le N} |x(n)|^2 = \max_{0\le n\le N}\left|\frac{1}{N}\sum_{k=0}^{N-1} X(k)\exp\left(-j\frac{2\pi kn}{N}\right)\right|^2 \tag{3.10}$$

Recognizing that the maximum peak power will occur when all the subcarriers coherently added, the peak power of the OFDM signal will always be less than or equal to the highest peak, i.e

$$\max_{0\le n\le N} |x(n)|^2 \le \left(\frac{1}{N}\sum_{k=0}^{N-1}\max|X(k)|^2\right) = \left(\frac{aN}{N}\right)^2 = a^2 \tag{3.11}$$

The PAPR of the OFDM signal is obtained from Equation (3.1) as follows

$$\text{PAPR}\{x(n)\} = \frac{\max\left\{|x(n)|^2\right\}}{\left\langle |x(n)|^2\right\rangle} \le \frac{a^2}{a^2/N} \le N \tag{3.12}$$

Therefore, the PAPR of an M-PSK modulated signal is always less than N, where N is the total number of subcarriers.

Figure 3.1 shows the CCDF curves for a Direct Current biased Optical-OFDM (DCO-OFDM) system with $N = 32, 64, 128, 256, 512$ and 1024 subcarriers. In order to obtain the CCDF curves, an oversampling factor of $L = 4$ was used for a 16-Quadrature Amplitude Modulation (QAM) DCO-OFDM communication system with 10^6 data blocks generated. As can be observed from the CCDF curves, as the number of subcarriers increases, the PAPR of the DCO-OFDM system increases. This confirms the theoretical derivation above and also the CCDF in Equation (3.4).

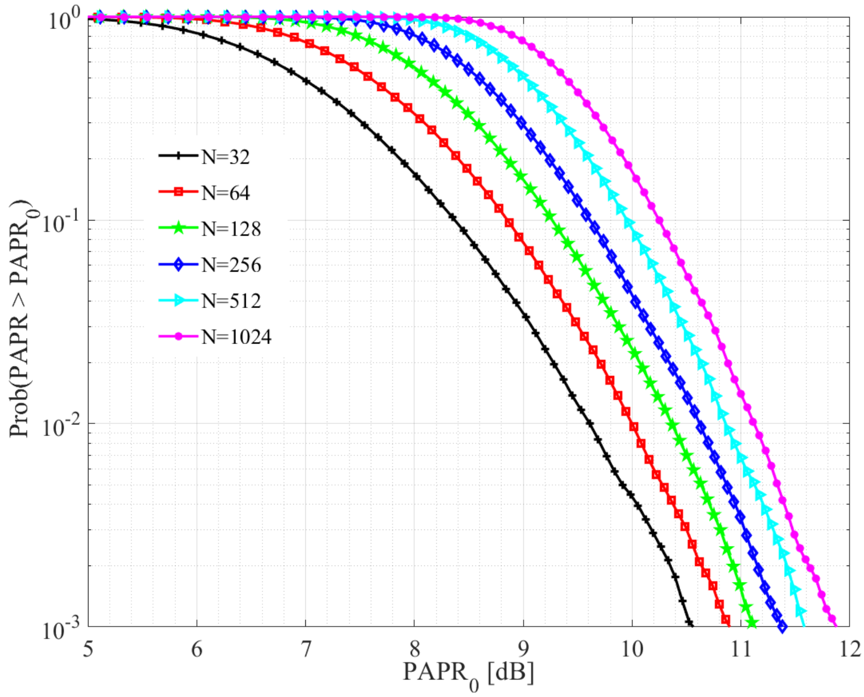

Figure 3.1: PAPR performance of a DCO-OFDM system with $N = 32, 64, 128, 256, 512$ and 1024 subcarriers

3.3 Factors for PAPR Reduction Technique Selection in OFDM Systems

As discussed in the previous Sections, most of the existing PAPR reduction techniques in literature have some drawbacks. Therefore, it is not only the PAPR reduction capability that should be considered when selecting an appropriate PAPR reduction technique, but also other design factors such as bandwidth and complexity should be considered. The key idea is to select a technique with as high PAPR reduction capability as possible while putting other design factors into consideration. The following factors can be used to determine the trade-offs between the PAPR reduction capability and other design factors [16, 45].

1. *High PAPR reduction capability:* The PAPR reduction technique should have a high PAPR reduction capability with as few undesirable side effects as possible.
2. *Low implementation complexity:* The complexity both in terms of hardware complexity and time complexity introduced as a result of the PAPR reduction technique should be as low as possible. In techniques such as Selected Mapping (SLM) and Partial Transmit Sequence (PTS), the complexity increases with the number of candidate signals but also the PAPR reduction performance improves with an increase in the number of candidate signals.

Therefore, there exists a trade-off between PAPR reduction capability and computational complexity in such techniques.

3. *No increase in bandwidth:* Bandwidth is a scare resource, and therefore the increase in bandwidth due to the use of the PAPR reduction technique should be kept minimum. The increase in bandwidth normally occurs in techniques such as coding and multiple signal representation techniques that require transmission of the Side Information (SI). There exists a trade-off between increase in bandwidth and distortion of the signal. Non-blind techniques suffer from increase in bandwidth without distorting the signal whereas blind techniques suffer from increased signal distortion without increasing the bandwidth. This signal distortion eventually results in BER performance degradation and it should be kept as low as possible. Even though the bandwidth in VLC systems can be considered as infinite, the actual bandwidth is limited by the modulation bandwidth of the LED. Therefore, the increase in bandwidth due to the use of the PAPR reduction technique should be carefully considered in both Optical-OFDM and RF-OFDM.
4. *No BER performance degradation:* The main aim of PAPR reduction technique is to make systems better including having a better BER performance. Therefore techniques that lead to an increase in BER performance degradation should be carefully considered. Furthermore, those techniques that involve the transmission of the SI can result into worse BER performance if the SI is not received correctly. Therefore, in such techniques the SI should be coded in order to minimize the possibility of errors.
5. *No spectral spillage:* The PAPR reduction technique can destroy the OFDM main features such as the ability to combat ISI. The spectral spillage should be kept as low as possible and therefore, techniques such as clipping are not desirable even though they can result into high PAPR reduction performance.
6. *No power increase in transmit signals:* For RF communication systems, the power in the transmit signals should be kept constant. In VLC systems, the transmit optical power is limited by several design factors and also the stringent eye safety regulation standards. Therefore techniques that lead to an increase in transmit power such as active constellation extension may not be suitable for RF and VLC communication systems.
7. *High efficiency and cost savings:* The efficiency of the PAPR reduction technique and the cost saving in terms of additional hardware that is introduced and the saving realized as a result of using devices such as the power amplifier, DACs with reduced dynamic ranges should be considered when choosing an appropriate PAPR reduction technique. The most efficient PAPR does not need to be the least achievable PAPR.

From the available PAPR reduction techniques proposed in literature, it is not enough to achieve a high PAPR reduction performance alone, other design factors as discussed above should be considered. However, it is not possible to satisfy all the design requirements such as no increase in complexity, no spectral spillage, no bandwidth increase and no increase in the overall cost.

Therefore there should be a compromise between the required PAPR reduction performance and other design factors.

The PAPR reduction performance can be achieved in the frequency domain and time domain by modifying the frequency and/or time characteristics of the signal. These modifications are transmitted to the receiver in form of SI. This SI should be correctly received otherwise there will be BER performance degradation. In order to ensure that the SI is received correctly, some form of coding needs to be performed on this information. Some systems such as voice communication are more error tolerant and in other systems are less error tolerant. Therefore, since the coding introduces additional complexity and increase in bandwidth, the coding scheme used should correspond with how tolerant the system can be to errors. On the other hand, blind techniques that not require the transfer of SI can be used in systems that are more tolerant to errors. Non-blind techniques are typically more complex and can require a higher bandwidth, but they often provide better performance in terms of BER. However, the performance of these techniques can still be impacted by errors in the transmission of the SI. While coding the SI can reduce the probability of errors occurring, it is not possible to guarantee error-free transmission through coding alone.

It is also important to note that when the PAPR is reduced, there may be some form of cost savings at the transmitter since linear systems such as the power amplifiers and DACs with reduced dynamic ranges could be used. However, the additional cost in form of filters and other components at the receiver should also be taken care of to determine the overall cost savings.

3.4 PAPR Reduction Techniques

The high PAPR is a serious drawback that affects the practical implementation of both RF-OFDM and Optical-OFDM systems mainly due to the use of devices and components with limited dynamic range at the transmitter such as DACs, power amplifiers and LEDs in case of VLC systems. This high PAPR leads to amplitude clipping when the signal goes outside the linear range leading to severe distortion and an increase in BER degradation. It would be possible to deal with this problem of high PAPR by using devices with a large dynamic range but this would increase the overall cost of the systems and its undesirable especially in VLC systems where the costs should be kept as low as possible in order to cater for the high demand that is currently present and expected to increase in the near future. Moreover, the high PAPR may lead to an increase in the transmitted optical power which is unacceptable in VLC systems where there is a strict requirement in terms of transmitted power due to stringent eye safety regulation standards.

Therefore, in order to solve the problem of high PAPR, many researchers have proposed several techniques to deal with this challenge in RF-OFDM systems and most recently in Optical-OFDM systems. Several review papers in literature propose different classifications of these techniques [15, 37, 45, 108, 110].

Vijayarangan et al. [110] propose two broad types of the PAPR reduction techniques, i.e signal scrambling techniques and signal distortion techniques. The signal scrambling techniques may further be divided into two categories: those without explicit SI such as Hadamard transform and dummy sequence insertion techniques and those with explicit SI which are further divided into two subcategories, i.e. coding based schemes such as block codes and probabilistic schemes such as SLM, PTS, interleaving and active constellation extension. The second broad category is the signal distortion techniques such as signal clipping, peak windowing and companding transforms such as μ-law and A-law transforms. The signal scrambling techniques are all variations on how to scramble the codes to decrease the PAPR while the signal distortion techniques reduce the high PAPR directly by distorting the signal before amplification [110].

Relatedly, Rahmatallah et al. [37] propose a classification of the PAPR reduction techniques into three broad categories: signal distortion techniques such as clipping and filtering, peak windowing, companding transforms and peak cancellation, multiple signaling and probabilistic techniques such as SLM, PTS, interleaving, tone reservation, and coding techniques such as the use of linear block codes, Golay complementary sequences and Turbo coding. The classification proposed by Sandoval et al. [15] adds another category of hybrid techniques to the taxonomy presented in [37].

Rajbanshi [45] classified the PAPR reduction techniques into two categories, i.e. deterministic and probabilistic approaches. The deterministic approaches reduce the PAPR by guaranteeing that the PAPR of the OFDM signal does not exceed a predetermined threshold while the probabilistic approaches minimize the probability that the PAPR of the signal does not exceed a predefined limit.

Yong et al. [108] argue that the PAPR reduction techniques can be classified into five approaches, i.e. clipping technique, coding technique, probabilistic (scrambling) technique, adaptive predistortion technique, and Discrete Fourier Transform (DFT)-spreading technique.

Finally, in the classification proposed by Geetha and Mahadevaswamy [111] , the PAPR reduction techniques are classified into two categories. The first category is the signal distortion techniques such as clipping and filtering, peak windowing, companding transforms. The second category is the signal non-distortion techniques such as SLM and PTS.

In this thesis, we use the classification proposed in [110] but add another category of hybrid techniques. Hybrid techniques combine two or more techniques in order to benefit from the advantages of either technique. Hybrid techniques have recently gained much attention because they can achieve better overall performance in terms of PAPR reduction performance and other design considerations such as complexity, BER degradation and the overall cost of the system. Figure 3.2 provides the proposed taxonomy of the PAPR reduction techniques with three categories i.e. signal scrambling techniques, signal distortion techniques and hybrid techniques with examples and subcategories of the techniques under each category. In the next Sections, some of these techniques are discussed.

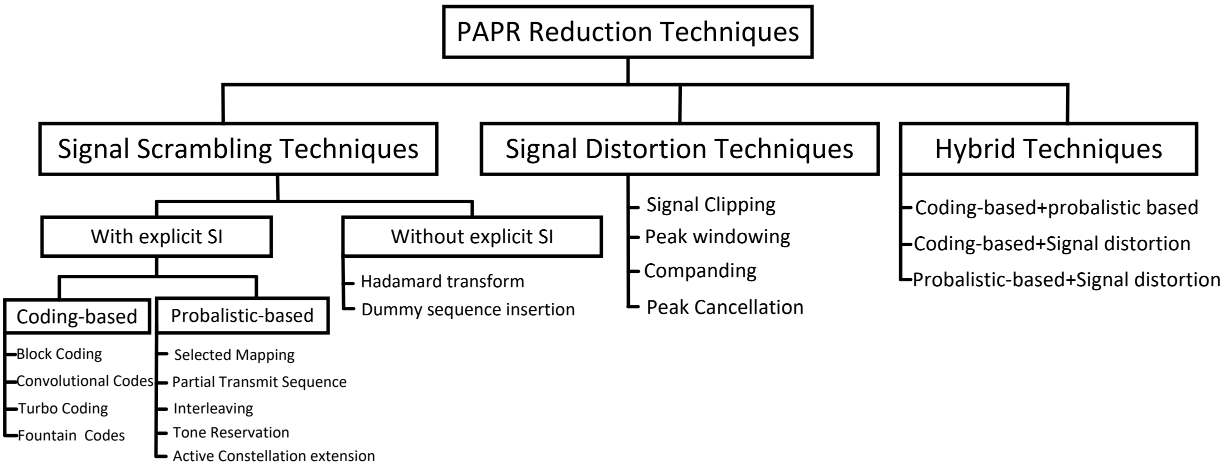

Figure 3.2: Taxonomy of PAPR reduction techniques

3.4.1 Signal Distortion Techniques

The signal distortion techniques include among others, signal clipping, peak windowing and use of companding transforms such as μ-law and A-law transforms. These techniques reduce the high PAPR by directly distorting the OFDM signal before amplification. These techniques are quite simple to implement and do not require the transmission of extra SI. However, a major disadvantage of these techniques is that they result into in-band distortion and out-of-band radiation and may result into severe BER degradation especially if the parameters such as companding and clipping parameters are not selected appropriately.

Clipping

Clipping is the simplest signal distortion PAPR reduction technique that achieves the PAPR reduction simply by clipping the signal peaks that exceed a predetermined threshold before the signal is passed through the power amplifier. This method uses a clipper that limits the signal envelope to a predefined clipping level, C if the signal exceeds that level and allow the signal to pass through if it is below that level. The output signal of a soft threshold can be given as [112, 113]

$$A[x(N)] = \begin{cases} x(n) & \text{for } |x(n)| < C \\ Ce^{j\theta} & \text{for } |x(n)| \geq C, \end{cases} \tag{3.13}$$

where $x(n)$ represents the OFDM signal in the time domain and θ is the angle of $x(n)$.

Clipping is generally a non-linear process performed at the transmitter. However, the receiver needs to know the location of the clip and the clipping level in order to be able to reconstruct the signal. Because it is difficult to obtain such information, the clipping technique normally results in in-band distortion and out-of-band radiation which severely affects the BER performance of the system. Filtering can reduce out-of-band radiation even though it can reduce in-band radiation. However filtering can also lead to peak regrowth which can be partially solved by repeated clipping and filtering [34]. Repeated clipping and filtering will also lead to an increase in computational complexity to the system [35].

Peak windowing

In peak windowing, unlike in the clipping technique the out-of-band radiation is minimized by using narrowband correcting functions such as Gaussian window, Kaiser, Hamming or cosine window which are multiplied with the OFDM signal to minimize the out-of-band radiation [36].

In order to reduce the PAPR, the window function must be aligned with the OFDM signal samples in such a way that its valley is multiplied by the higher signal peaks while the higher amplitudes of the window are multiplied by the lower signal peaks. This action attenuates the signal peaks in a much smoother way resulting in reduced signal distortion [37].

In peak windowing, the OFDM signal is multiplied with several windows and therefore the resulting spectrum is a convolution of the two spectrums, i.e. the spectrum of the original OFDM signal and the spectrum of the window being used. Therefore, the window should be as narrowband as possible but not too long in the time domain since this may lead to many signal samples being affected resulting in an increase in the BER [36].

Irrespective of the number of subcarriers used, in peak windowing, PAPR reduction up to 4 dB can be achieved making peak windowing an effective technique in PAPR reduction [36].

Peak cancellation

In the peak cancellation technique, a cancellation waveform generator is used to generate the peak cancellation waveform that is scaled, shifted and subtracted from the OFDM signal at those instances where the OFDM signal exhibits high peaks [114, 115]. The peak cancellation waveform is bandlimited to certain tones so that it has sharp and unique peaks in counter phase to the largest peaks of the OFDM signal. The peak cancellation process can be performed after the IFFT block as shown in Figure 3.3 by subtracting the peak cancellation waveform from the OFDM signal at those instances where a peak higher than the threshold is detected.

Compared to peak windowing, the peak cancellation technique does not generate out-of-band radiation. However, it has higher computational complexity compared to the peak windowing technique [116].

Companding

Due to the similarity of the OFDM signal and the speech signal in a sense that large signals only occur infrequently, Wang et al. [38] introduced the μ-law companding technique that had

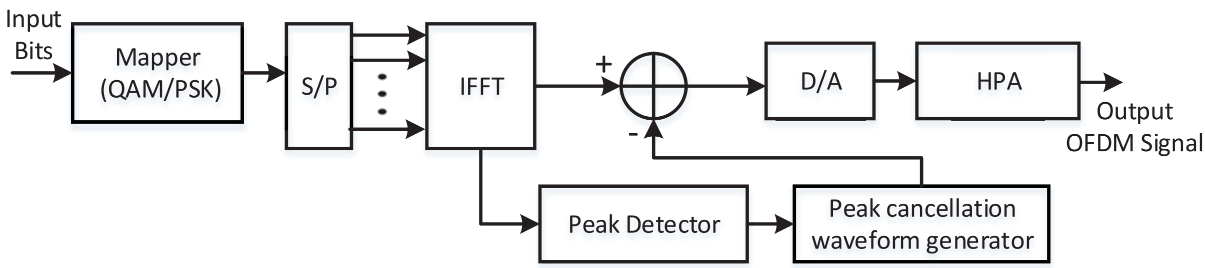

Figure 3.3: Peak cancellation process. S/P: serial-to-parallel converter, D/A: digital-to-analog converter, HPA: high power amplifier

earlier on been used to improve speech processing algorithms but this time for PAPR reduction in OFDM signals. The μ-law companding technique is a compression technique that achieves PAPR reduction through compressing large amplitudes and expanding the smaller amplitudes. As shown in Figure 3.4, the time domain signal after the IFFT operation, $x(n)$ is compressed before it is converted to analog form by

$$x_c(n) = \frac{A \ln\left[1 + \mu^{\frac{|x(n)|}{A}}\right]}{\ln[1+\mu]} \operatorname{sgn}[x(n)] \tag{3.14}$$

where $\operatorname{sgn}[x(n)]$ is the signum function of $x(n)$, A is the normalization constant such that $0 \leq |x(n)|/A \leq 1$. At the receiver side, a reverse process (expansion of the signal) is performed before the IFFT operation using the inverse of Equation (3.14) given by

$$y_c(n) = \frac{A}{\mu}\left[\exp\left(\frac{|y(n)|\ln(1+\mu)}{A}\right) - 1\right] \operatorname{sgn}[y(n)] \tag{3.15}$$

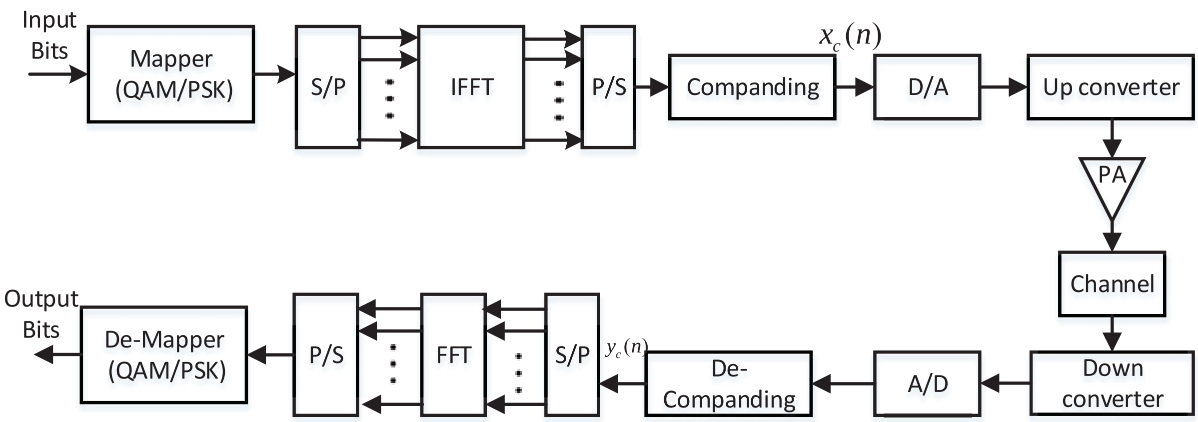

Figure 3.4: OFDM schematic employing μ-law companding for PAPR reduction. S/P: serial-to-parallel converter, P/S: parallel-to-serial converter, D/A: digital-to-analog converter, A/D: analog-to-digital converter, PA: power amplifier

Apart from the μ-law companding transform, there is a number of other companding transforms that have been proposed in literature including hyperbolic tangent companding transform [39],

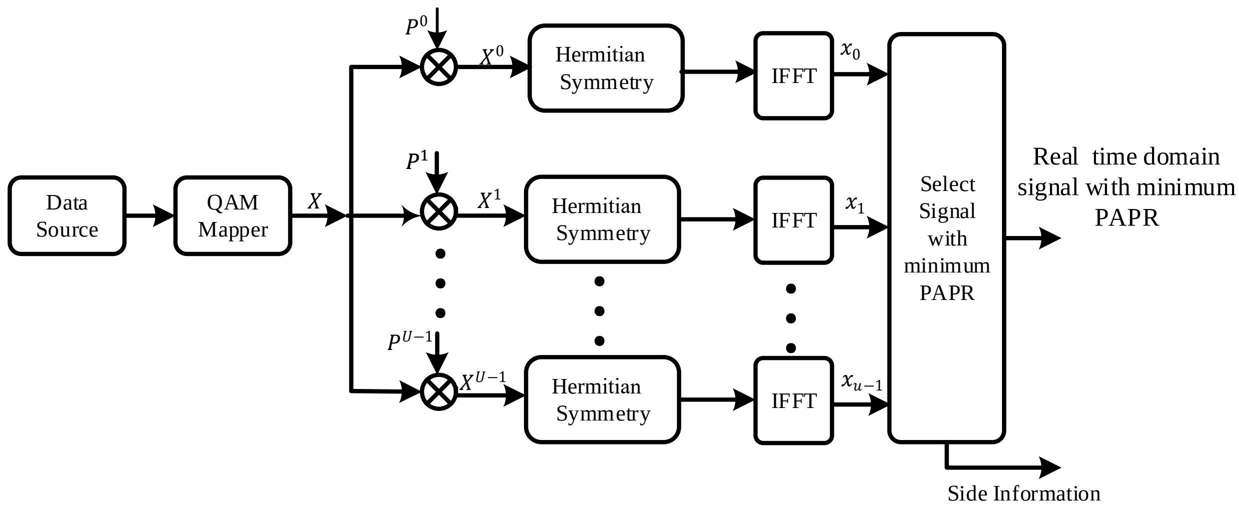

Figure 3.5: Conventional selective mapping for DCO-OFDM (Source: [46])

linear symmetric transforms [40], linear asymmetric transforms [117] and exponential companding transform [41].

The non-linear companding transform techniques can be considered as a special form of the clipping technique. However, unlike the clipping technique, non-linear companding transforms enlarge the small signal amplitudes increasing their resilience to channel noise while compressing the large amplitudes, while the clipping technique does not change the small signal amplitudes. Also, non-linear companding transforms compand the signal at the transmitter using a strict monotone function and therefore the original signal can be easily recovered at the receiver using a reverse function whereas the clipping technique deliberately clips the signal at those instances where the amplitude exceeds a certain threshold and therefore it is hard for the original signal to be recovered at the receiver leading to an increase in BER degradation.

The companding techniques have the advantage of providing good performance in terms of both BER and PAPR reduction performance. They also do not lead to throughput loss since there is no transmission of SI and they can be implemented with low complexity.

3.4.2 Signal Scrambling Techniques

Conventional Selected Mapping for DCO-OFDM

Figure 3.5 illustrates the block diagram of a DCO-OFDM transmitter system using the Conventional Selected Mapping (CSLM) for PAPR mitigation. Let $X = X(k)_{k=0}^{N/2-1}$ denote the input data symbol in the frequency domain, where $X(k) \sim \mathcal{N}(0,\sigma^2)$ denotes the M-ary Quadrature Amplitude Modulation (M-QAM) symbol mapped on the k-th subcarrier with zero mean and variance σ^2.

In CSLM, a set of U pseudo-random phase sequences, $P_{\text{CSLM}}^{(u)} = Ae^{j\theta_k^{(u)}}$ where $\theta_k^{(u)} \in [0,2\pi], 0 \leq u \leq U-1$ are multiplied component wise with the input data symbol to generate U different candidate sequences. In a DCO-OFDM communication system, both the odd and even subcarriers are used and to ensure a real time domain signal, the input to the IFFT is constrained to Hermitian symmetry. Therefore, the input to the IFFT will be given as

$$X^{(u)}_{\mathrm{CSLM}}(k) = X^{*(u)}_{\mathrm{CSLM}}(N-k) \text{ for } 0 < k < \frac{N}{2}, \tag{3.16}$$

where $X^{(u)}_{\mathrm{CSLM}}(0) = X^{(u)}_{\mathrm{CSLM}}(N/2) = 0$ and X^* is the complex conjugate of X. The U time domain candidate signals are generated by taking the N-point IFFT of the input frequency domain signals as follows:

$$x^{(u)}_{\mathrm{CSLM}}(n) = \frac{1}{\sqrt{N}} \sum_{k=0}^{N-1} X^{(u)}_{\mathrm{CSLM}}(k) \exp\left(j\frac{2\pi kn}{N}\right), \tag{3.17}$$

where $0 \leq n \leq N-1$.

The PAPR of the U time domain candidate signals is calculated according to Equation (3.1) and the candidate signal with the least PAPR is converted from parallel-to-serial, an appropriate cyclic prefix is often appended to combat ISI and Intercarrier Interference (ICI) that could be an issue in a dispersive optical wireless communication channel. The continuous time domain signal $x(t)$ is obtained by feeding the discrete time domain signal $x(n)$ to the DAC. A Direct Current (DC) offset, $\mathrm{DC}_{\mathrm{bias}}$ is added to $x(t)$ to ensure that the transmitted signal is unipolar. However, a large DC bias will lead to an increase in optical power and a small DC bias will lead to an increase in clipping noise leading to poor BER performance. Therefore, a suitable DC offset relative to the Root Mean Square (RMS) value of the signal $x(t)$ is added [89] and is given by

$$\mathrm{DC}_{\mathrm{bias}} = \eta \sqrt{\langle |x(t)|^2 \rangle}, \tag{3.18}$$

where η is a constant and the $\mathrm{DC}_{\mathrm{bias}}$ is defined as a bias of $10 \log\left(\eta^2 + 1\right)$ dB. Next, the remaining negative peaks are clipped resulting in a real and unipolar signal that is subsequently fed to the LED for transmission in the VLC channel.

Figure 3.6 presents the PAPR performance for CSLM. As shown in the figure the higher the number of candidate signals, V, the better the PAPR performance. As earlier indicated, these candidate sequences are generated through multiplication of random phase sequences with the input data symbol. This increases the complexity of the transmitter system. In addition, in CSLM, the SI is transmitted using a separate channel and this will require that some form of coding is used to ensure that the SI is received correctly leading to more complexity and bandwidth inefficiency.

Partial Transmit Sequence

In the PTS technique [33] for PAPR reduction in OFDM systems shown in Figure 3.7, the input sequence, X of N symbols given by $X = [X(0), X(1), ..., X(N-1)]$ is partitioned into U disjoint sub-sequences of equal length, $X^{(u)}$, $u \in \{0, 1, ..., U-1\}$ such that

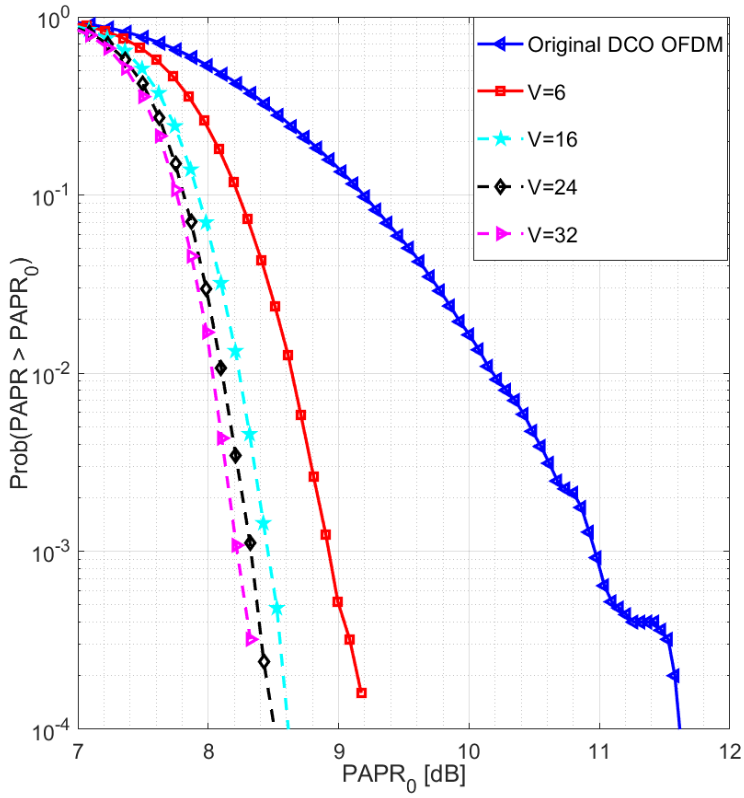

Figure 3.6: PAPR reduction performance of the original OFDM system and CSLM with $V = 6, 16, 24$ and 32

$$X = \sum_{u=0}^{U-1} X^{(u)} \tag{3.19}$$

For PTS, the partitioning sub-sequences can be divided into three categories, i.e. adjacent, interleaved and pseudo-random sub-sequences. Using the pseudo-random sub-sequences has been shown to provide better PAPR reduction performance [118]. Next, the sub-sequences are independently transformed into time domain by taking the IFFT operation to obtain $x^u,\ u \in \{0, 1, ..., U-1\}$ time domain sub-sequences which are then multiplied by the phase rotation factors, $b^u = e^{j\phi_u}$, where $\phi_u = [0, 2\pi), 0 \leq u \leq (U-1)$. The PAPR of each resulting sub-sequence is computed and the phase factors are selected in such a way so as to minimize the PAPR of the overall signal given by

$$x = \sum_{u=0}^{U-1} b^u x^u \tag{3.20}$$

In the PTS, the optimal PAPR can be found after an exhaustive search of computations. In other words, the search complexity also increases exponentially as the number of sub-sequences increases. This makes the technique complex to implement. Generally, the selection of the phase factors is limited to a set of elements to reduce the search complexity [108]. Another way to reduce

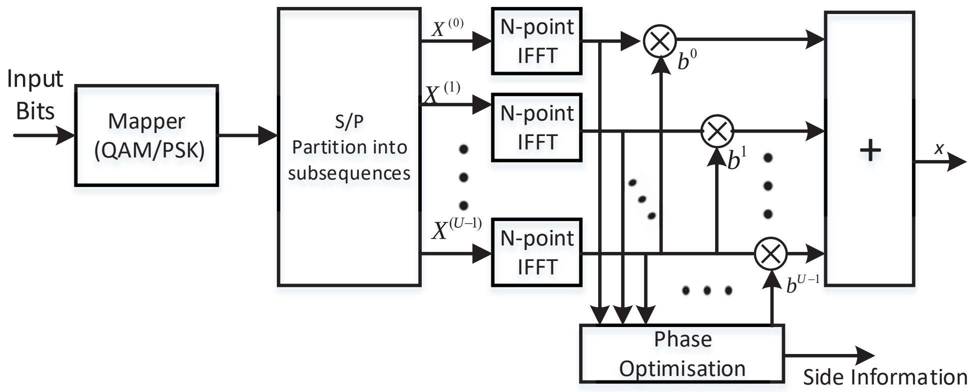

Figure 3.7: PTS technique block diagram

the computational complexity is to use a preset threshold PAPR [119]. Using this approach, the PAPR values are searched through the phase optimizer and the search will be stopped once the PAPR drops below the threshold. However, in situations where significantly low PAPR values are required, the search complexity will still be high. In the PTS technique, U IFFT operations are required for each data block and $\lfloor \log_2 W^u \rfloor$ bits of SI is required, where W represents the number of allowed phase factors. This makes the PTS technique less bandwidth efficient since it requires the transmission of a huge amount of SI.

Coding Techniques

Some error detection and correction codes have been considered for PAPR reduction by taking advantage of some of the properties of these codes. These codes have attracted much attention because they can be used to provide dual functions: error detection and correction, as well as PAPR reduction.

Linear Block codes

Wilkinson and Jones [20] proposed a $3/4$ rate block code for both error detection and PAPR reduction by simply transforming 3 bits to 4 bits by adding the odd parity bit. In doing so, the minimum PAPR of 2.48 dB can be obtained for a system using Quadrature Phase Shift Keying (QPSK) modulation. The major shortcoming of this approach, is that it can only be used for PAPR reduction for only 4-bit code words. This is because when sequences with long bit streams are used, the code words with high PAPR values cannot be eliminated.

In a related approach, a block code rate of $1/2$ is proposed for an OFDM system using QPSK modulation with 4 subcarriers [21]. In this scheme, a block of 4 bits, $b = [b_0\ b_1\ b_2\ b_3]$ is encoded by a 4×8 generator matrix, G and this is followed by a phase rotation vector, p to obtain the encoded output as

$$x = b.G + p(\bmod 2) \tag{3.21}$$

After considering all the possible M^N possibilities ($N = 4$ subcarriers and $M = 4$ number of bits per subcarrier in QPSK modulation), the generator matrix and the phase rotation vector that gives a minimum PAPR of 2.48 dB are given by [120]

$$G = \begin{bmatrix} 1 & 0 & 0 & 1 & 0 & 1 & 1 & 0 \\ 0 & 1 & 0 & 1 & 0 & 1 & 0 & 1 \\ 0 & 0 & 1 & 1 & 0 & 0 & 1 & 1 \\ 0 & 0 & 0 & 0 & 1 & 1 & 1 & 1 \end{bmatrix} \tag{3.22}$$

Ngajikin et al. [120] proposed a Modified Code Repetition (MCR) technique for PAPR reduction. Code repetition is a forward error correction technique where the idea is to repeat the input bits k times. For example, for $k = 4$, if the input bit is 0, then 0000 will be transmitted and if the input bit is 1, then 1111 will be transmitted. In the MCR technique [120], the last bit of the code word (LSB) is modified by toggling it up, i.e changing from 0 to 1 and vice versa. For example, if the bit to be transmitted is 1, the conventional code repetition will result into 1111 for $k = 4$ and this will have a maximum PAPR but when the MCR is used, the output will be 1110 and its PAPR will be less than that of the conventional code repetition [120].

Jiang and Zhu [121] proposed the Complement Block Coding (CBC) for PAPR reduction in OFDM systems. In this technique, complementary bits are added to the information bits. If the code length K is the number of subcarriers and k complement bits are used, the number of information bits in a block will therefore be $K - k$. The CBC technique can provide error detection capabilities as well as PAPR reduction since the possibility of generating a code with all 1s or all 0s does not arise in this code. In this technique, up to 3.0 dB PAPR reduction can be achieved when using coding rate $R > (N-2)/N$ for long size frames, where N is the number of subcarriers [121].

This technique can provide almost the same PAPR reduction performance compared to the techniques in [20, 21, 120] but with higher coding rate and less implementation complexity. Therefore, in the CBC, the bandwidth efficiency is improved which is an important consideration in wireless communication systems design.

Fountain Codes

Fountain codes are a class of erasure codes with a property that a potentially limitless sequence of coded symbols can be generated from a set of source symbols and these symbols can be recovered at the receiver from any subset of encoded symbols equal to or slightly higher than the source symbols [24]. They are rateless codes in a sense that they do not exhibit a fixed code rate. This packet coding property matches the N-dimensional property of OFDM systems and as a result, fountain codes have been used for PAPR reduction in addition to error detection and correction [25–27]. The simplest fountain codes are the random linear (RL) codes and the first practical realization of the fountain codes is the Luby Transform (LT) codes [28]. There are two fundamental principles underlying the LT codes: LT codes must generate new packets called symbols on the fly, and several of these symbols combined together may reconstruct the original data [28]. The encoding (symbol creation) consists in randomly taking the initial data blocks and combining them together. The XOR operation is used due to its ability to perform a reverse operation [28].

In [25], the authors proposed the SLM scheme for random linear (RL) codes and two LT coded PAPR reduction schemes, i.e. Symbol-wise SLM and Multi-symbol SLM based on SLM. In these schemes, for each encoded symbol, Q symbols are generated and the one with the least PAPR is considered for transmission. These methods are complex since they require a large number of IFFT operations proportional to the number of candidate encoded symbols. This complexity can be reduced by introducing a threshold PAPR and stopping the encoding process for a particular symbol when a candidate with a PAPR below the threshold is obtained [27].

The main advantage of using fountain codes for PAPR reduction is that there is no transmission of SI which makes these techniques more bandwidth efficient, a critical factor in the design of wireless communication systems.

Convolutional Codes

Convolutional codes are very useful and currently widely deployed in systems that require error correction in real time such as Digital Video Broadcasting-Terrestrial (DVB-T), Digital Video Broadcasting-Satellite (DVB-S) and tactical communication systems such as Wideband Network Waveform (WNW) [22]. Lower code rate results in better BER performance. However, the BER increases as the code rate and the constraint length decrease [23]. It was found out through computer simulations in [22] that a code rate of $1/2$ gives almost the same PAPR reduction performance as the uncoded OFDM signal but the PAPR performance degrades significantly as the code rate is decreased from $1/2$ to $1/4$ and $1/8$. Therefore, the convolutional code parameters such as the code rate and the constraint length need to be appropriately selected to avoid an increase in PAPR.

3.4.3 Hybrid Techniques

Hybrid techniques are methods for PAPR reduction that combine two or more techniques. These techniques have recently attracted a lot of attention from researchers because they take advantage of each of the techniques used [15]. Moreover, no single PAPR reduction technique can satisfy all the requirements of the OFDM communication system such as low PAPR, no BER degradation, low complexity, etc. Therefore, the best strategy is to employ hybrid techniques. Examples of hybrid techniques are methods that combine coding based and probabilistic techniques, coding based and signal distortion techniques, probabilistic based and signal distortion techniques. Probabilistic techniques such as SLM and PTS achieve significant PAPR reduction performance but at the expense of increased complexity, mainly as a result of an increased number of IFFT operations required to generate candidate signals and data rate loss due to the SI that has to be transmitted for information recovery. Signal distortion techniques such as clipping and filtering and use of companding transforms are simple to implement and can achieve significant PAPR reduction but at the expense of increased signal distortion leading to BER degradation. On the other hand, coding based techniques such as use of forward error correction codes, although complex can present good error control properties.

4 Low Complexity Hybrid SLM for PAPR Mitigation for ACO-OFDM

This chapter presents our results which were published in [42].

The high Peak-to-Average Power Ratio (PAPR) is the main challenge facing Asymmetrically Clipped Optical-OFDM (ACO-OFDM). We propose a new hybrid technique that incorporates a modified Selected Mapping (SLM) and companding called Low Complexity Hybrid Selected Mapping (LCHSLM) for PAPR mitigation in ACO-OFDM systems. It is demonstrated through computer simulations that our proposed system significantly reduces the PAPR compared to the conventional SLM or companding alone. In addition, LCHSLM achieves a significant reduction in complexity compared to conventional SLM without Bit Error Rate (BER) degradation.

4.1 Introduction

Asymmetrically Clipped Optical-OFDM (ACO-OFDM) is an attractive modulation technique in Visible Light Communication (VLC) systems due to its high power efficiency compared to the Direct Current biased Optical-OFDM (DCO-OFDM) [4, 9]. In addition, as an Orthogonal Frequency Division Multiplexing (OFDM) scheme, ACO-OFDM also has the ability to combat Inter-Symbol Interference (ISI) caused by a dispersive optical channel, high spectral efficiency and the ability to offer higher data rates without the need for complex equalizers at the receiver [7]. In spite of these advantages, the high Peak-to-Average Power Ratio (PAPR) caused by the possibility of the ACO-OFDM signals adding coherently in the time domain resulting in high signal peaks remains a major challenge. The high PAPR implies that the various components that make up the optical transmitter have to operate outside their limited linear dynamic range leading to major inefficiencies.

Accordingly, various PAPR mitigation techniques have been proposed for OFDM. These include clipping and filtering [34], pre-coding [122, 123], non-linear companding [124] and multiple signal representations such Selected Mapping (SLM) [32] and Partial Transmit Sequence (PTS) [33, 125].

Non-linear companding techniques such as μ-law and A-law achieve PAPR reduction through increasing the small amplitude peaks and decreasing the large amplitude peaks. Consequently, the small amplitude peaks are made more resilient to channel noise.

In SLM, multiple candidate signals representing the same information are generated and the candidate signal with the lowest PAPR is selected for transmission. This results into high complexity caused by the large number of Inverse Fast Fourier Transform (IFFT) blocks required to generate these candidate signals. Recent research in SLM has been focused on reducing its complexity [32, 126, 127]. A low complexity SLM is proposed in [126], whereby certain conversion matrices are used to lower the complexity. However due to the use of one conversion, the computational complexity will be about one half of the conventional SLM. To further reduce the complexity, more conversion matrices are used which leads to Bit Error Rate (BER) degradation. In [127], a low complexity SLM based on the Fast Hartley Transform (FHT) is proposed. Since this uses the FHT, hardware adaptation and modification may need to first be implemented before it can be fully adapted for ACO-OFDM that currently uses IFFT/Fast Fourier Transform (FFT). In [32] a low complexity SLM system for PAPR mitigation for Optical-OFDM is proposed. Specifically, the system uses partitioning and recombination to generate $2V^2$ candidate sequences from V IFFTs. However, since SLM is a probabilistic technique, the extent of PAPR reduction is limited. Moreover, the large number of partial candidate sequences increases the overall complexity.

A single PAPR mitigation technique cannot generally meet all the demands of ACO-OFDM systems such as significant PAPR reduction, no or less signal distortion and low complexity simultaneously. Therefore, hybrid schemes for PAPR reduction have been proposed and have shown better performance compared to the conventional methods. For example, in [128], a hybrid technique comprising PTS and μ-law companding shows better PAPR and BER performance at higher values of Signal-to-Noise Ratio (SNR). This scheme suffers from high complexity of the PTS section.

Motivated by the need to reduce the complexity of SLM and achieve a significant PAPR reduction, in this chapter, we propose a hybrid approach called Low Complexity Hybrid Selected Mapping (LCHSLM) for PAPR mitigation for ACO-OFDM. We utilize the properties of IFFT and Hermitian symmetry to reduce the complexity of the conventional SLM. The μ-law companding technique is then used to further reduce the PAPR.

The rest of the chapter is organized as follows: Section 4.2 presents the proposed scheme for PAPR mitigation. Section 4.3 gives the results along with a detailed analysis and discussion and finally the concluding remarks are given in Section 4.4.

4.2 Proposed Scheme (LCHSLM)

Figure 4.1 illustrates LCHSLM. Compared to the Conventional Selected Mapping (CSLM), LCH-SLM scheme is a hybrid of modified CSLM and μ-law companding techniques.

In our scheme, instead of reducing the number of candidate sequences, we can reduce the number of IFFTs as follows. Consider two candidate sequences $\tilde{X}^0(k)$ and $\tilde{X}^1(k)$ that are constrained to Hermitian symmetry according to Equation (2.35), then

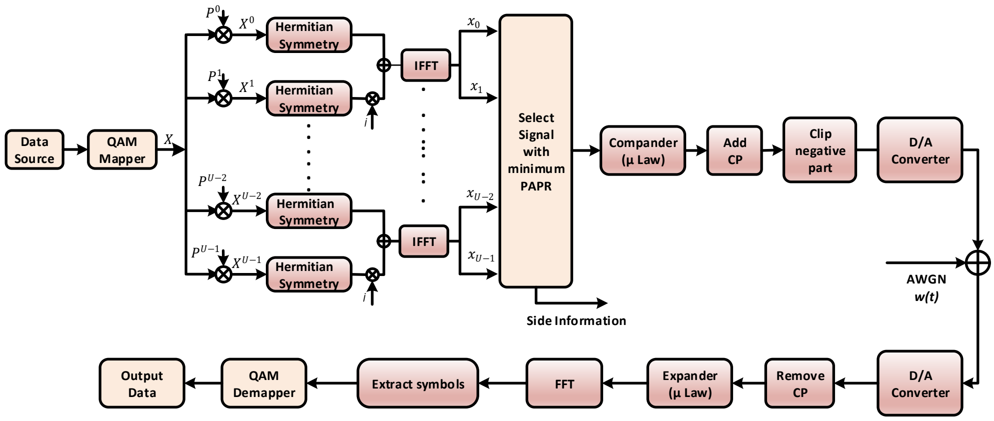

Figure 4.1: Proposed Method-LCHSLM for ACO-OFDM

$$IFFT\{\tilde{X}^0(k) + j\tilde{X}^1(k)\} = IFFT\{\tilde{X}^0(k)\} + jIFFT\{\tilde{X}^1(k)\} = x^0 + jx^1 \tag{4.1}$$

Therefore, the two time domain signals x^0 and x^1 can be recovered from the real and imaginary components of the IFFT operation at the receiver [32]. Hence, instead of using V IFFTs for V candidate sequences, we use $V/2$ IFFTs. This results into a significant reduction in complexity.

Similar to CSLM, after the IFFT operation, the candidate signal with the lowest PAPR will be selected. The next step is to further reduce the PAPR of the selected candidate signal using μ-law companding.

The μ-law companding is a compression technique that has been used to reduce PAPR in OFDM systems. It works by expanding small signal amplitudes making them more resilient to channel noise and decreasing the large amplitudes [124].

The μ-law expression for compressing the signal at the transmitter is given by

$$x_c(m) = \frac{A\ln\left[1+\mu\frac{|x(m)|}{A}\right]}{\ln(1+\mu)}\mathrm{sgn}[x(m)] \tag{4.2}$$

where $\mathrm{sgn}[x(m)]$ is the signum function and A is the normalization constant such that $0 \leq |x(m)/A| \leq 1$.

In our LCHSLM, at the receiver side before the FFT operation, a reverse process (expansion of the signal) will be carried out using the expression given by the inverse of Equation (4.2) given by

$$y_e(m) = \frac{A}{\mu}\left[\exp\left[\frac{|y(m)|\ln(1+\mu)}{A}\right] - 1\right]\mathrm{sgn}[y(m)] \tag{4.3}$$

After the FFT operation, the frequency domain symbols are extracted before demodulation to obtain the estimate of the original data.

4.2.1 Complexity Analysis

In this section we analyze the complexity of LCHSLM as compared to CSLM. We first analyze the complexity without the $\mu-$law companding technique and then discuss the time complexity introduced by this technique. The complexity of CSLM method considering no oversampling can be given in terms of complex additions and complex multiplications. In order to generate V candidate signals, V $4N$-point IFFT operations are required in ACO-OFDM. Therefore, the complexity in terms of complex multiplications and complex additions are given by [32]

$$\text{Complex multiplications} = 2VN\log_2 4N \tag{4.4}$$

$$\text{Complex additions} = 4VN\log_2 4N \tag{4.5}$$

where N is the total number of subcarriers. In LCHSLM, for V candidate signals, we require $V/2$ $4N$-point IFFT operations. Therefore, the complexity of our proposed scheme in terms of complex multiplications and complex additions is given by Equations (4.6) and (4.7)

$$\text{Complex multiplications} = VN\log_2 4N \tag{4.6}$$

$$\text{Complex additions} = 2VN\log_2 4N + VN/2 \tag{4.7}$$

The Computational Complexity Reduction Ratio (CCRR) of our LCHSLM over CSLM is given by [32]

$$CCRR = 1 - \frac{\text{Complexity of LCHSLM}}{\text{Complexity of CSLM}} \times 100\% \tag{4.8}$$

For example, consider $V = 16$ candidate signals and $N = 64$ subcarriers. For CSLM, the number of complex multiplications calculated by Equation (4.4) is 16,384 while for LCHSLM, the equivalent number of complex multiplications calculated by Equation (4.4) is 8,192 giving a CCRR of 50%. Considering the same example, for CSLM, the number of complex additions calculated by Equation (4.5) is 32,762 while for LCHSLM, the equivalent number of complex additions is 16,896 given by Equation (4.7) resulting in a CCRR of 48.4%. Therefore using, LCHSLM for ACO-OFDM results into significant complexity reduction.

The complexity introduced by the μ-law companding can be analyzed in terms of the time complexity introduced by this technique. Consequently, Equation (4.2) can be simplified as

$$x_c(m) = k_1 \ln\left(1 + k_2\,|x(m)|\right) \mathrm{sign}[x(m)], \quad \text{for } m = 1, 2, \cdots, n \tag{4.9}$$

where $n = 4N$, $k_1 = \frac{A}{\ln(1+\mu)}\mathrm{sign}[x(m)]$ and $k_2 = \mu/A$.

From Equation (4.9), considering one time domain sample, it can be observed that the number of real additions and real multiplications is fixed, therefore, the time complexity is $\mathscr{O}(1)$. Considering all the time domain samples, the time complexity becomes $n \times \mathscr{O}(1) = \mathscr{O}(n)$.

The time complexity introduced by μ-law companding increases linearly as n increases but is considerably small for low values of n.

4.3 Results and Discussions

The PAPR reduction performance of the proposed LCHSLM was compared to the CSLM, μ-law companding and CSLM combined with μ-law companding techniques using computer simulations. Table 4.1 shows the simulation parameters. 10^4 data blocks were generated randomly and each block was oversampled by an oversampling factor of $L = 4$ in order to approximate the true value of PAPR. The channel considered was an Additive White Gaussian Noise (AWGN) channel which is appropriate for VLC.

Table 4.1: Simulation Parameters

Simulation Parameter	**Value**
Number of subcarriers	$N = 128$
Oversampling factor	$L = 4$
Number of candidate signals	$V = 8$ for CSLM, 16 for LCHSLM
Modulation scheme	16 QAM
Type of companding	μ-law
Companding parameter	μ=2,4
Number of data blocks	10^4

Figures 4.2 and 4.3 show the PAPR reduction performance of LCHSLM compared to CSLM, μ-law companding and CSLM combined with μ-law companding techniques for PAPR reduction in ACO-OFDM systems. Table 4.2 shows the PAPR comparison for the above techniques at a Complementary Cumulative Distribution Function (CCDF) of 10^{-2}.

As shown in Figures 4.2, 4.3 and Table 4.2, for a given threshold, the LCHSLM performs better than CSLM, μ-law companding and CSLM combined with μ-law companding techniques. For comparison purposes, the same number of IFFTs were considered. As illustrated in Section 4.2.1, LCHSLM produces twice as many candidate signals compared to CSLM for the same number of IFFTs. In our case, we consider 16 candidate signals for LCHSLM and 8 candidate signals for CSLM. Note that in the two scenarios, these candidate signals are produced by the same number

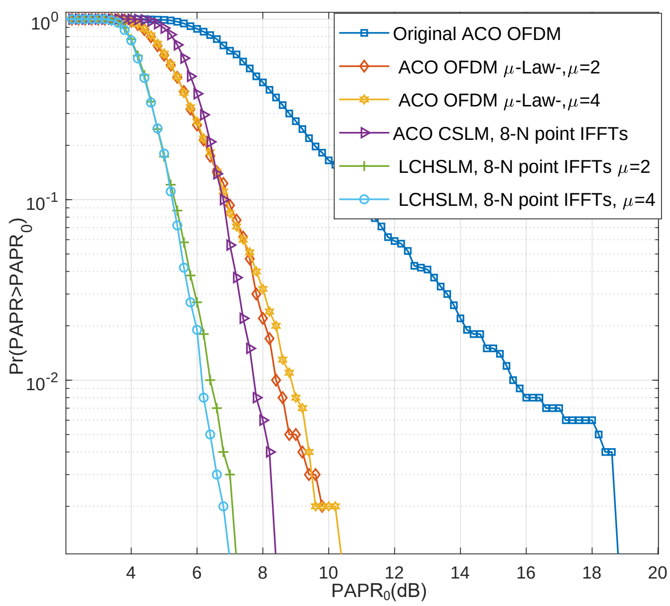

Figure 4.2: PAPR reduction performance of LCHSLM compared to CSLM and μ-law companding techniques

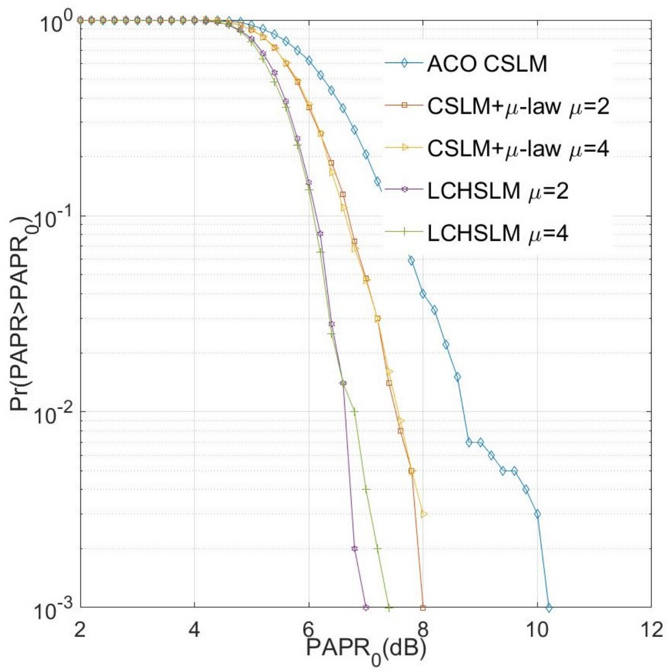

Figure 4.3: PAPR reduction performance of CSLM with μ-law companding and LCHSLM

Table 4.2: PAPR reduction comparison for CSLM, μ-law companding, CSLM combined with μ-law companding and the proposed LCHSLM

PAPR reduction method	**PAPR (dB)**
Original ACO-OFDM	15.8
CSLM	8.8
μ-law companding (μ=2)	8.4
CSLM with μ-law companding (μ=2)	7.5
Proposed LCHSLM (μ=2)	6.1

of IFFTs. From Figures 4.2, 4.3 and Table 4.2, we note that our proposed LCHSLM ($\mu = 2$) achieves significant PAPR reduction gains of 9.7 dB, 2.7 dB, 2.3 dB and 1.4 dB respectively for original ACO-OFDM without any PAPR mitigation, CSLM, μ-law companding ($\mu = 2$) and CSLM combined with μ-law companding (μ=2) companding techniques at a CCDF of 10^{-2}. This is attributed to the fact that LCHSLM is a combined scheme that takes advantage of both CSLM and μ-law companding techniques. In other words, in addition to reducing the complexity of the CSLM by almost 50% as illustrated in Section 4.2.1, the proposed scheme performs better also in terms of PAPR reduction for the same number of IFFTs. Therefore, given the same level of complexity which is determined by the number of required IFFT blocks to generate the candidate signals, LCHSLM performs better than the CSLM in terms of PAPR reduction because of the fact that twice the number of candidate signals will be generated. In addition, further PAPR reduction is achieved by appropriately applying μ-law companding. Even though μ-law companding introduces additional time complexity described in Section 4.2.1, the additional PAPR reduction as a result of this combination is advantageous in most practical applications requiring low PAPR.

The effect of μ-law companding on BER performance is an aspect that should be carefully investigated. This is because μ-law companding is a distortion based PAPR reduction technique and can lead to BER degradation if the companding parameters are not carefully selected.

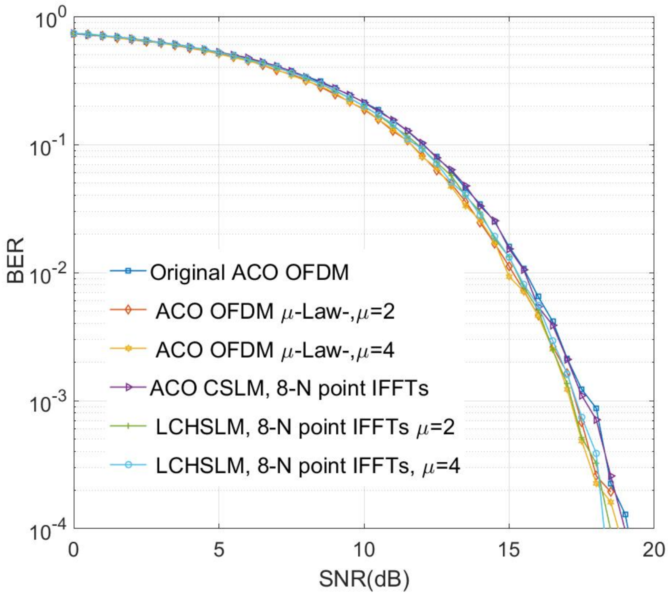

Figure 4.4: Comparison of BER of LCHSLM, CSLM and μ-law companding techniques.

Figure 4.4 shows the comparison of BER of the proposed LCHSLM, CSLM, μ-law companding and ACO-OFDM without any PAPR mitigation technique applied. Although the BER performance is almost the same, it is shown that LCHSLM and μ-law companding performs better than CSLM and ACO-OFDM without any PAPR reduction technique applied. This is because in μ-law companding, the small signal amplitudes are amplified making them more resilient to the channel noise. In addition, the average power of the signal is increased through companding leading to better BER performance. Furthermore, the higher the value of μ, the better the PAPR reduction at the cost of BER degradation. Therefore, an appropriate choice of μ needs to be considered for LCHSLM and in this case, a value of $\mu = 2$ was considered as appropriate.

4.4 Conclusion

We have proposed and verified the performance of a new hybrid PAPR reduction scheme for ACO-OFDM called LCHSLM. The proposed scheme achieved a better PAPR reduction as compared to CSLM and μ-law companding techniques in addition to achieving almost 50% reduction in complexity for the CSLM. Moreover, due to the companding technique, with an appropriate choice of the companding parameter, μ, there is a gain in BER performance, attributed to the fact that the small amplitude signals are amplified making them more resilient to the channel noise.

5 PAPR Reduction in Optical-OFDM using Lexicographical Permutations with Low Complexity

This chapter presents our results which were published in [46].

Efficient utilization of the spectrum, increased resilience to Inter-Symbol Interference (ISI) and simpler channel equalization are becoming important considerations in the design of wireless communication systems including Visible Light Communication (VLC) systems. In this regard, Orthogonal Frequency Division Multiplexing (OFDM) has become a preferred modulation technique in wireless communication systems design. However, one of its major challenges is the high Peak-to-Average Power Ratio (PAPR) that leads to major inefficiencies. Symbol Position Permutation (SPP) is a distortion-less technique that achieves substantial PAPR reduction without Bit Error Rate (BER) degradation. However, the existing works focus on PAPR reduction using SPP for the Radio Frequency (RF) OFDM and the use of this technique in optical-OFDM is not properly investigated. Therefore, in this chapter, we present a new PAPR reduction technique based on lexicographical permutations called Lexicographical Symbol Position Permutation (LSPP) for PAPR reduction in Direct Current biased Optical-OFDM (DCO-OFDM). The proposed scheme is less complex than the Conventional Selected Mapping (CSLM) scheme since there is no multiplication of the phase sequences with the DCO-OFDM symbol to generate the candidate signals. We further introduce a new way of reducing the complexity by introducing a threshold PAPR and demonstrate that the complexity in terms of Inverse Fast Fourier Transform (IFFT) operations can be reduced substantially depending on the selected threshold and the number of candidate signals.

5.1 Introduction

Visible Light Communication (VLC) has lately attracted consideration from researchers in academia, industry and governments around the globe due to its tremendous advantages such as interference-free communication, high levels of security, low cost due to the utilization of the license-free spectrum and availability of Light Emitting Diodes (LEDs) used for communication [1–3].

To attain the higher data rates required nowadays, multi-carrier modulation techniques such as Orthogonal Frequency Division Multiplexing (OFDM) have been considered for practical implementation in VLC systems [4, 5]. In addition to the higher data rates, OFDM also can combat Inter-Symbol Interference (ISI) in a diffuse optical channel without the need for complex equalization filters at the receiver [7].

Most of the practical VLC systems currently deployed use Intensity Modulation with Direct Detection (IM/DD) and therefore the optical carrier used for modulating the light intensity must be real and unipolar. In a VLC based OFDM system, the real signal is obtained by subjecting the frequency domain symbol to Hermitian symmetry and to obtain the unipolar signal, two well-known techniques have been extensively researched and considered in VLC systems, these are, Direct Current biased Optical-OFDM (DCO-OFDM) [8] and Asymmetrically Clipped Optical-OFDM (ACO-OFDM) [9]. In a DCO-OFDM system, the unipolar signal is obtained through the addition of an appropriate Direct Current (DC) bias after the Inverse Fast Fourier Transform (IFFT) operation and clipping the remaining negative peaks. All the subcarriers are used to carry data symbols unlike in an ACO-OFDM system where only the odd subcarriers are used and the unipolar signal obtained by clipping the entire negative signal excursions. Consequently, the DCO-OFDM system is more spectrally efficient and is preferred in VLC systems.

Regrettably, despite the advantages of OFDM, the multi-carrier nature of OFDM means that there will be constructive addition at certain instants of the subcarriers after the IFFT operation leading to a higher peak value [14]. Consequently, this will result in a high Peak-to-Average Power Ratio (PAPR). It is important to keep the devices at the transmitter such as the Light Emitting Diode (LED), the Digital-to-Analog Converter (DAC) and the power amplifier in the linear region of operation for reliable transmission. However, this is difficult to achieve in practice due to the high PAPR and as a consequence, the high peaks are often clipped leading to signal distortion and an increase in Bit Error Rate (BER).

Therefore, a lot of attention has been put on PAPR reduction and several techniques have been proposed in the traditional OFDM for wireless communication. However, since the transmitted signal in VLC must be real and positive due to the use IM/DD, most of these techniques cannot be directly applied in VLC systems.

Only a few techniques have been proposed for PAPR reduction in VLC systems. One of these techniques is clipping and filtering [113] that can be easily implemented, although it results in significant in-band distortion and out-of-band radiation which leads to performance degradation in terms of both the spectrum efficiency and the BER. On the other hand, companding transforms [129–131] such as μ-law and A-law offer better PAPR reduction performance with less distortion but at the cost of increased average power which is unacceptable in VLC systems.

Selected Mapping (SLM) [29–32] based techniques have been observed as the most popular techniques for PAPR reduction in VLC systems. This is because they are distortion-less and offer significant PAPR reduction without an observable BER degradation. In SLM, multiple candidate signals are generated by multiplying the OFDM symbol in the frequency domain with random phase sequences. The candidate signal after the IFFT operation with the least PAPR is selected for transmission and the Side Information (SI) associated with this candidate signal is transmitted for efficient recovery at the receiver.

Although the methods in [29–32] result in significant PAPR reduction, they result in complex systems because of two reasons. Firstly, their PAPR reduction performance capability is proportional to the number of candidate signals that are generated, the higher the number, the better the PAPR reduction performance. The large number of IFFT operations that have to be carried out to generate the candidate signals leads to an increase in complexity. Secondly, the complexity is exacerbated by the generation and multiplication of random phase sequences with the OFDM symbol.

Related to the SLM technique, the symbol or bit interleaving technique [43] and the Data Position Permutation (DPP) technique [44] also involve generation of multiple candidate signals for PAPR reduction. In the DPP technique, the OFDM symbol is divided into S sub-blocks which are then permutated to generate the candidate permutation sequences. Just like in SLM, the candidate permutation sequence with the least PAPR is selected for transmission and the SI associated with this candidate permutation sequence is transmitted for efficient recovery at the receiver. However, in the DPP technique, the number of candidate permutation sequences that can be generated is limited since it is given by $S!$ and therefore as the number of sub-blocks increases, the number of permutation sequences increases at a factorial rate of growth leading to a more complex transmitter system as a result of the large number of IFFT operations that have to be performed.

In this chapter, we focus our attention on PAPR reduction in DCO-OFDM systems using DPP based on lexicographical permutations. We call our scheme the Lexicographical Symbol Position Permutation (LSPP) method. We concentrate on DCO-OFDM because it is more spectrally efficient as compared to ACO-OFDM. Unlike in DPP, in our proposed LSPP, the m-th permutation sequence can be generated efficiently without generating the previous $m-1$ permutations. From the possible $S!$ sequences, where S is the number of sub-blocks, we determine U random permutation candidate sequences lexicographically using the factorial number system. Just like in DPP, the candidate sequence with the least PAPR is selected for transmission and the SI associated with this candidate sequence is transmitted for efficient recovery at the receiver. Further, we introduce an algorithm for complexity reduction using LSPP by setting a threshold PAPR value and generating the permutation candidate sequences one by one until a candidate sequence with PAPR below the threshold is reached. In this way, if the m-th $(m \leq U)$ permutation sequence satisfies the threshold condition, then $U-m$ candidate sequences are not generated and consequently, $U-m$ IFFT operations are not performed. This new method does not only reduce the PAPR but also results in a significant reduction in computational complexity.

This chapter is laid out into four sections together with this introductory part. The proposed scheme for PAPR reduction is described in Section 5.2. In Section 5.3, we present the results together with a detailed analysis and discussion and finally, the concluding remarks are presented in Section 5.4.

5.2 Proposed System for PAPR Mitigation

5.2.1 Lexicographical Symbol Position Permutation

The proposed system for PAPR reduction in DCO-OFDM systems using lexicographical permutations is given in Figure 5.1.

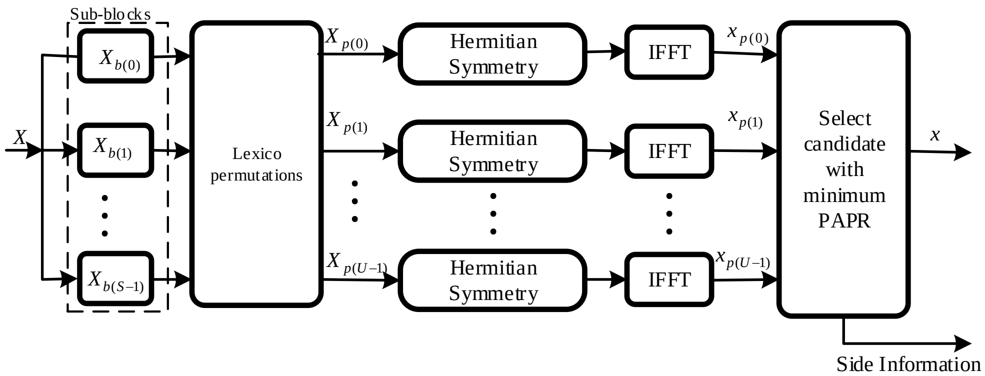

Figure 5.1: Proposed Scheme for PAPR mitigation

Let $X = X(k)_{k=0}^{N/2-1}$ denote the input data symbol sequence in the frequency domain, where $X(k) \sim \mathcal{N}(0, \sigma^2)$ is the k-th M-ary Quadrature Amplitude Modulation (QAM) symbol modulated on the k-th subcarrier with zero mean and variance σ^2. The input data block is divided into S permutation sub-blocks, $X_{b(s)}$ according to

$$X_{b(s)} = X_{S\times 0+s}, X_{S\times 1+s}, X_{S\times 2+s}, \cdots, X_{S\times (S-1)+s}, \tag{5.1}$$

where $0 \leq s \leq (S-1)$ and $N/2S$ is an integer so that the S permutation sub-blocks have the same size. For example, if the size of the input data sequence, $N/2 = 16$, i.e. $X = [X_0, X_1, \cdots, X_{15}]$ and the number of permutation sub-blocks, $S = 4$, then the permutation sub-blocks are given by

$$\begin{aligned} X_{b(0)} &= [X_0, X_4, X_8, X_{12}], \\ X_{b(1)} &= [X_1, X_5, X_9, X_{13}], \\ X_{b(2)} &= [X_2, X_6, X_{10}, X_{14}], \\ X_{b(3)} &= [X_3, X_7, X_{11}, X_{15}]. \end{aligned} \tag{5.2}$$

The S permutation sub-blocks are then used to generate U random lexicographical permutations, $(U \leq S!)$, according to algorithm 5.1, below.

Algorithm 5.1 An algorithm to generate the lexicographical permutations

Input: Permutation sub-blocks, $X_{b(s)}$, $0 \leq s \leq (S-1)$; Choose U, $(U \leq S!)$; set $i=1$;
Output: Permutation sequences $X_{p(0)}, X_{p(1)}, \cdots, X_{p(U-1)}$

for $i = 1 : U$ **do**
  Randomly generate the m-th permutation sequence index, β $(1 \leq \beta \leq S!)$
  Set $X_{p(u)} := []$
  while $X_{b(s)} \neq []$ **do**
    $d := \left(\left|X_{b(s)}\right| - 1\right)!$
    $j := \lfloor \beta / d \rfloor$
    $x := X_{b(j)}$
    $\beta := \beta \bmod d$
    Append x to $X_{p(u)}$
    Remove x from $X_{b(s)}$
    Return $X_{p(u)}$
  end while
end for

In order to obtain real-valued time domain signals after the IFFT operation, the permutation sequences are constrained to Hermitian symmetry according to

$$X_{p(u)}(k) = X^{*}{}_{p(u)}(N-k) \text{ for } 0 < k < \frac{N}{2}, \tag{5.3}$$

where $X_{p(u)}(0) = X^{*}{}_{p(u)}(N/2) = 0$ and X^{*} is the complex conjugate of X.

The time domain output candidate signals are generated by taking the N-point IFFT of the input frequency domain sequences

$$x_{p(u)}(n) = \frac{1}{\sqrt{N}} \sum_{k=0}^{N-1} X_{p(u)}(k) \exp\left(j \frac{2\pi kn}{N}\right), \tag{5.4}$$

where $0 \leq n \leq N-1$ and $X_{p(u)}(k)$ is obtained from algorithm 5.1. The PAPR values of the time domain candidate signals is calculated using Equation (3.1) and the candidate signal with the least PAPR is selected for transmission.

It is important to note that in our proposed LSPP just like in Conventional Selected Mapping (CSLM), the number of bits required for the SI is $\log_2(U)$ for each block of information that is transmitted. This SI is normally transmitted in a separate channel, or it can be embedded in the transmitted signal and is usually protected by error control codes to prevent erroneous detection at the receiver [44]. In this thesis, we assume that the SI is transmitted and received correctly.

5.2.2 Complexity Reduction

The PAPR reduction performance of LSPP is proportional to the number of candidate signals leading to high computational complexity as a result of a large number of IFFT operations to be performed. If the first permutation sequence has the least PAPR, then $U-1$ unnecessary permutations will be generated leading to $U-1$ unnecessary IFFT operations which makes the system complex. If the m-th $(m < U)$ permutation sequence has the least PAPR, then $U-m$ unnecessary permutation sequences are generated and ultimately $U-m$ unnecessary IFFT operations are generated.

In order to reduce the computational complexity of LSPP, we set a threshold PAPR, γ and then generate the candidate permutation sequences one by one while computing the PAPR of the corresponding candidate signal until we obtain a candidate signal whose PAPR is less than or equal to γ. That candidate signal is considered for transmission. If all the U permutation sequences have a PAPR that is more than the threshold, γ then the one with the smallest PAPR among them will be considered for transmission. Algorithm 5.2 describes our complexity reduction method.

Algorithm 5.2 The proposed algorithm for complexity reduction

Input: Choose S and $U(U \leq S!)$; select a predetermined PAPR, γ; set $i = 1$;
Output: Transmitted candidate signal, X_p
1: **while** $i \leq U$ **do**
2: Randomly generate a permutation sequence, $X_{p(i)}$ using algorithm 5.1
3: Calculate the PAPR of $X_{p(i)}$, PAPR_i
4: **if** $\text{PAPR}_i \leq \gamma$ **then**
5: Set $X_{p(i)}$ as X_p and consider it for transmission
6: **else**
7: $i++$ and go to step 2
8: **end if**
9: **if** $i = U$ **then**
10: Select X_p from $X_{p(1)}, X_{p(2)}, \ldots, X_{p(U)}$ whose PAPR is the smallest and consider it for transmission
11: **end if**
12: **end while**

5.2.3 Complexity Reduction Analysis

The generation of candidate permutation sequences can be modelled as a Bernoulli distribution with only two possible outcomes, i.e. PAPR below the threshold or PAPR above the threshold [27]. If the maximum number of permutation sequences U approaches infinity, the number of tries Y whose PAPR is less than the threshold can be modelled as a Geometric distribution.

Let p be the probability that the PAPR is less than or equal to the threshold PAPR γ, Then $p = \Pr(\text{PAPR} \leq \gamma) = (1-e^{-\gamma})^{\alpha N}$. According to Geometric distribution, the probability of exactly generating m sequences using algorithm 5.2 is

$$\Pr(Y=m)=(1-p)^{(m-1)}p. \tag{5.5}$$

Equation (5.5) is applicable when $m<U$. Therefore, the probability distribution of the random variable Y can be given as follows

$$\Pr(Y=m)=\begin{cases}(1-p)^{(m-1)}p, & 1\leq m\leq (U-1)\\ 1-\sum\limits_{k=1}^{U-1}(1-p)^{(m-1)}p=(1-p)^{(U-1)}, & m=U.\end{cases} \tag{5.6}$$

The average number of tried candidates (trials before a success is obtained) is

$$\langle Y\rangle=\sum_{m=1}^{U}\Pr(Y=m)m=\frac{1}{p}-\frac{1-p}{p}(1-p)^{U-1}. \tag{5.7}$$

In order to generate a candidate sequence, $2N$-point IFFT operations are required in DCO-OFDM, where N is the number of data subcarriers. Therefore, the total number of IFFT operations is

$$\mathrm{IFFT}_{\mathrm{Proposed}}=2N[\frac{1}{p}-\frac{1-p}{p}(1-p)^{U-1}]. \tag{5.8}$$

5.3 Results and Discussions

In this section, the PAPR reduction performance of our proposed LSPP for DCO-OFDM communication system is evaluated through conducting simulation experiments using MATLAB®. In our simulations, we consider a 16-QAM DCO-OFDM communication system with $N=512$ subcarriers and 1,000,000 data blocks were generated with each data block oversampled by $L=4$ which is sufficient to approximate the true value of the PAPR [109]. For comparison purposes, we obtained simulation results for the original DCO-OFDM without PAPR reduction, the CSLM and our proposed LSPP for the same number of candidate signals. The simulation parameters are given in Table 5.1.

Table 5.1: Simulation Parameters

Simulation Parameter	**Value**
Number of subcarriers	$N = 512$
Number of data blocks	10^6
Oversampling factor	$L = 4$
Modulation scheme	16-QAM
Number of sub-blocks for LSPP	$S = 8, 16$
Number of candidate signals	$U = 4, 8, 16, 32$

Figure 5.2 shows the PAPR reduction performance of the original DCO-OFDM system, the CSLM and the proposed LSPP using Complementary Cumulative Distribution Function (CCDF) defined by Equation (3.4). It can be seen that at a CCDF $= 10^{-3}$, the PAPR reduction achieved by our proposed LSPP is quite significant with values of 1.6, 2.4, 2.7 and 3 dB respectively for $U = 4, 8, 16$ and 32 candidate signals compared to the original DCO-OFDM.

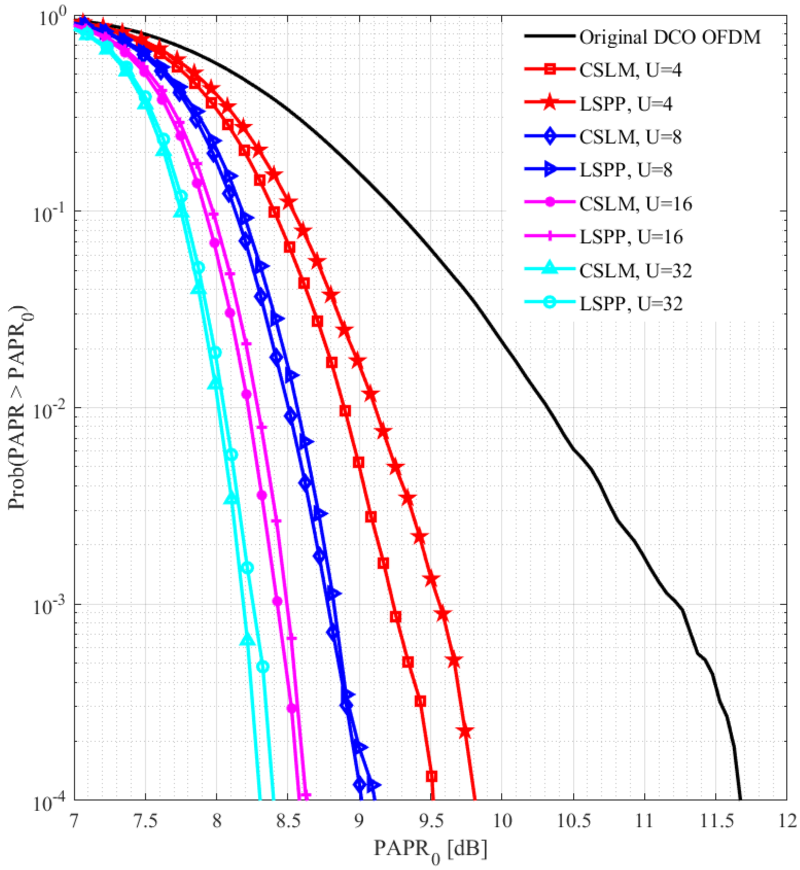

Figure 5.2: PAPR performance comparison between the original DCO OFDM, LSPP and CSLM for $S = 8$ sub-blocks.

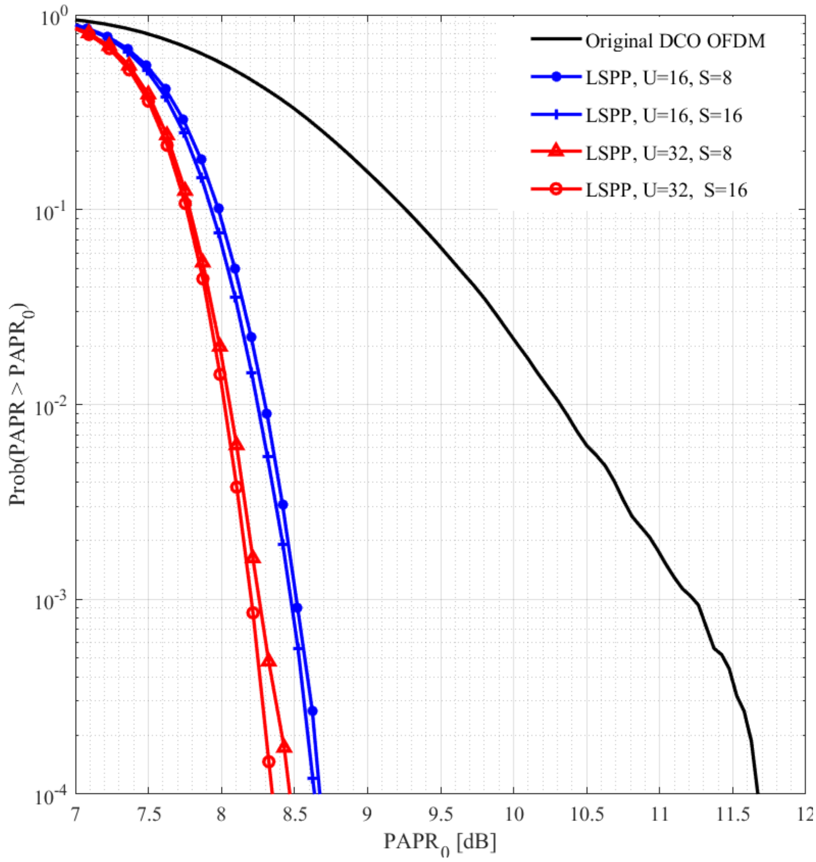

Figure 5.3: PAPR comparison for LSPP with $U = 16$ and 32 candidate signals for $S = 8$ and 16 sub-blocks. For the same number of candidate signals, increasing the number of sub-blocks improves the PAPR reduction performance.

As compared to the CSLM, our proposed LSPP achieves almost the same PAPR reduction performance with our scheme slightly inferior by 0.36, 0.01, 0.1, 0.05 dB for $U = 4,\ 8,\ 16,\ 32$ candidate signals respectively at a CCDF $=\ 10^{-3}$ for $S = 8$ sub-blocks. However, as the number of sub-blocks is increased from 8 to 16, it can be observed from Figure 5.3 that the PAPR reduction performance of our proposed LSPP almost approaches that of CSLM. This is because, as the number of sub-blocks, S increases, the candidate permutation sequences become more uncorrelated leading to low PAPR values.

Figure 5.4 compares the BER performance of the proposed technique to that of CSLM and the original DCO-OFDM signal over an Additive White Gaussian Noise (AWGN) channel. From Figure 5.4, it can be observed that our proposed LSPP and CSLM have almost the same BER performance with negligible BER degradation. It is quite clear from the results that the PAPR reduction performance of our proposed scheme is proportional to the number of candidate signals. However, when the number of candidate signals is increased, the complexity in terms of IFFT operations increases, hence there is a trade-off between PAPR reduction performance and system complexity.

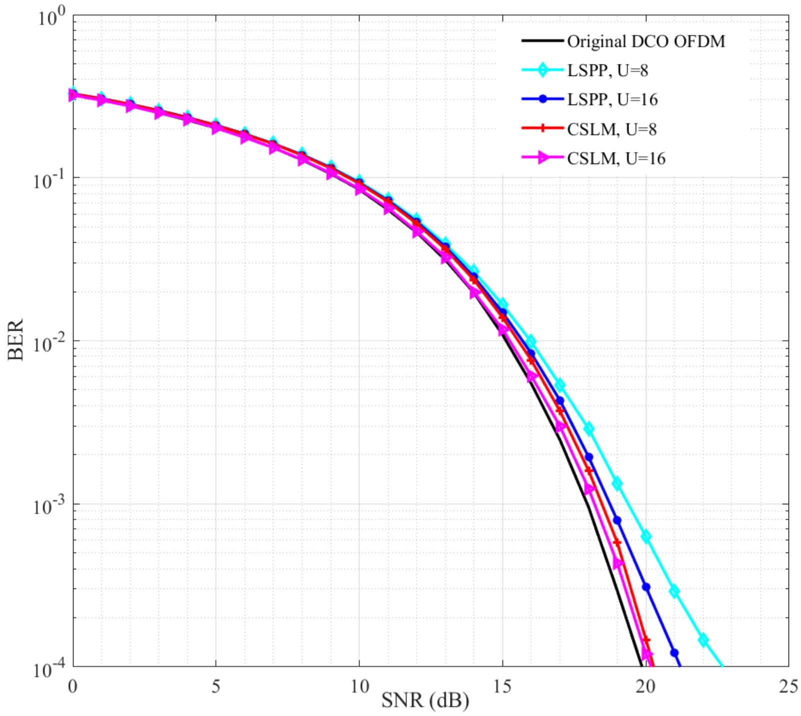

Figure 5.4: Comparison of BER performance of the original OFDM system, the CSLM and LSPP for $U = 8$ and 16 candidate signals

5.3.1 Complexity Reduction Analysis

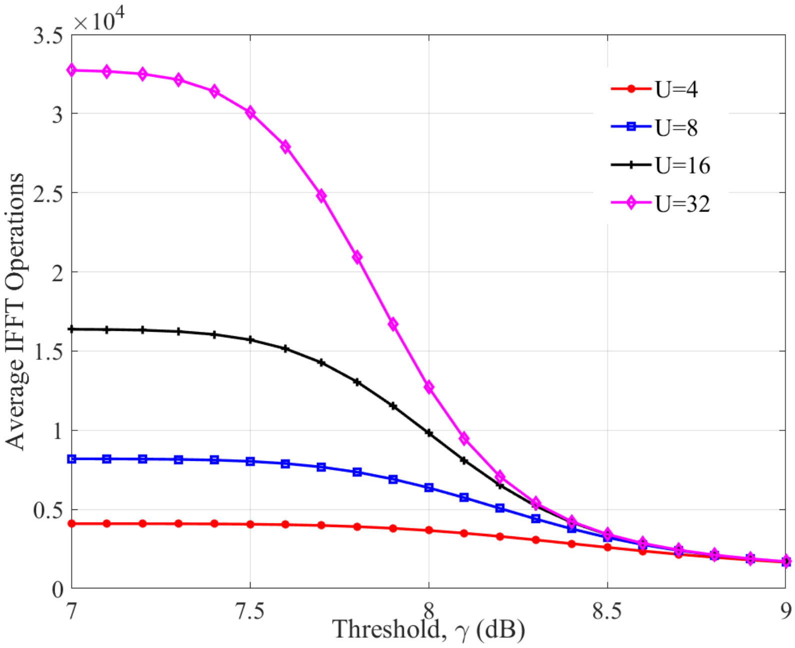

Figure 5.5: IFFT operations for different γ and U

In Figure 5.5, we plot the number of IFFT operations required to generate a candidate signal. The total number of IFFT operations is given by Equation (5.8). We can observe that the number of total IFFT operations reduces as the threshold, γ increases. This is because, as γ increases, the number of candidate signals with PAPR above γ will increase and hence will not be generated by algorithm 5.2 leading to a reduction in the number of IFFT operations. This reduction in IFFT operations can be analysed using the complexity reduction equation given by

$$\text{Complexity Reduction} = \frac{2NU - \text{IFFT}_{\text{Proposed}}}{2NU} \times 100\%, \tag{5.9}$$

where $\text{IFFT}_{\text{Proposed}}$ is given by Equation (5.8), N is the number of subcarriers and U is the number of candidate signals.

In Figure 5.6, we plot the complexity reduction performance for our proposed LSPP. The complexity reduction is calculated using Equation (5.9) and the results are summarised in Table 5.2. We can observe that the complexity reduction is proportional to γ when the number of candidate signals U is constant.

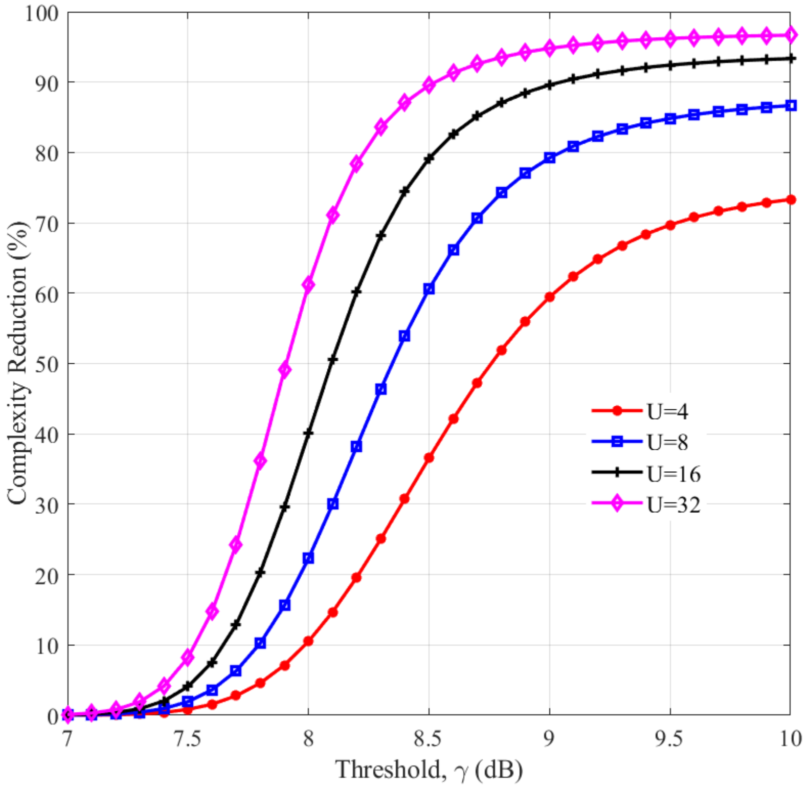

Figure 5.6: Complexity reduction performance for different γ and U

Table 5.2: Complexity Reduction

No. of candidate signals, U	Complexity Reduction %		
	8.0 dB	**8.5 dB**	**9.0 dB**
4	10.5	36.6	59.5
8	22.3	60.6	79.2
16	40.0	79.1	89.6
32	61.2	89.5	94.8

When γ is fixed, the number of candidate signals, U has an influence on complexity reduction. For instance, as given in Table 5.2 and Figure 5.6, when γ is 8 dB, the complexity reduction is 10.5, 22.3, 40.0 and 61.2% for $U = 4,\ 8,\ 16$ and 32 respectively. When $\gamma = 9$dB and $U = 16$, the complexity reduction that is achieved is 90% and when γ is increased to 10dB, the complexity reduction achieved increases to 96% for $U = 32$ candidate signals. The increase in complexity reduction as γ is increased corresponds to the reduction in the number of IFFT operations as γ increases given in Figure 5.5.

5.4 Conclusion

DCO-OFDM is an attractive modulation technique in VLC due to its high spectral efficiency compared to ACO-OFDM and its ability to combat ISI as a multi-carrier modulation technique. However, one of the major shortcomings of DCO-OFDM is the high PAPR of the transmitted signal which affects the system performance due to the presence of non-linear components like the DAC, power amplifier and LED whose performance is highly influenced by the PAPR.

In this chapter, we have proposed and experimentally demonstrated through computer simulations a new PAPR reduction technique called LSPP that effectively reduces the PAPR compared to the original DCO-OFDM with no PAPR mitigation. The proposed technique has almost the same PAPR reduction performance compared to the CSLM with less complexity since there is no multiplication of the phase sequences at the transmitter to generate the candidate signals as is done in CSLM.

Further, we also presented and analysed a new way to further reduce the complexity by introducing a threshold PAPR, since different applications require different PAPR performance. We show through our results that the complexity in terms of IFFT operations can be reduced substantially depending on the selected threshold γ and the number of candidate signals, U. For example, when $\gamma = 9$ dB and $U = 16$, the complexity reduction that is achieved is 90% and when $\gamma = 10$ dB, the complexity reduction achieved is 96% for $U = 32$ candidate signals.

6 Adaptive PAPR Reduction in Optical-OFDM Systems using Lexicographical Symbol Position Permutation

This Chapter presents our results in a paper recently submitted in [47].

It is clearly established that optical communication systems employing Direct Current biased Optical-OFDM (DCO-OFDM) as the modulation scheme experience high Peak-to-Average Power Ratio (PAPR). This negatively affects the system performance mainly at the transmitter due to the presence of non-linear devices and components such as the power amplifier, the Digital-to-Analog Converter (DAC) and the optical source, leading to bit error rate degradation and system inefficiency. In the previous chapter, Lexicographical Symbol Position Permutation (LSPP) technique was introduced as a technique for reducing the PAPR in DCO-OFDM systems. However, the existing works only focus on using random lexicographical permutation sequences. In this chapter, we look at the effectiveness of adjacent and interleaved lexicographical permutations in terms of PAPR reduction performance and compare the results with using random lexicographical permutation sequences. The results show that random lexicographical permutation sequences perform better than interleaved and adjacent lexicographical permutation sequences. Unfortunately, the generation of random lexicographical permutation sequences requires a constraint to avoid the generation of the repeated permutation sequences with the same PAPR values, which increases the time complexity. Adjacent and interleaved lexicographical permutation sequences can be preferred for a small number of sub-blocks especially for systems with a small number of subcarriers. All three categories achieve a negligible bit error rate degradation compared to the original DCO-OFDM system. Importantly, we introduce a new method of obtaining the most suitable number of candidate permutation sequences to achieve a reasonable PAPR reduction performance without increasing the computational complexity beyond the system requirements.

6.1 Introduction

6.2 Introduction

Multiple signaling and probabilistic techniques, such as Symbol Position Permutation (SPP) [132] and Selected Mapping (SLM) [30–32, 42], have gained popularity for mitigating the Peak-to-Average Power Ratio (PAPR) in optical-Orthogonal Frequency Division Multiplexing (OFDM) systems. These techniques effectively reduce PAPR without significantly degrading the Bit Error Rate (BER). SLM and SPP generate multiple candidate signals from the same optical-OFDM symbol and transmit the signal with the lowest PAPR, while transmitting the corresponding index to the receiver as side information.

SLM generates candidate signals by multiplying V random phase sequences with the optical-OFDM symbol in the frequency domain. On the other hand, SPP obtains V candidate sequences by permuting Q sub-blocks from the frequency domain optical-OFDM symbol. While SPP is less complex than SLM, it requires simultaneous generation of multiple candidate permutation sequences, increasing system complexity.

In Chapter 5, the Lexicographical Symbol Position Permutation (LSPP) method was presented for PAPR mitigation in Direct Current biased Optical-OFDM (DCO-OFDM) systems [46]. LSPP generates V random permutation candidate sequences lexicographically based on the factorial number system. Building upon this work, this chapter focuses on comparing the PAPR reduction performance of random [46], adjacent, and interleaved lexicographical permutations in DCO-OFDM systems using the Complementary Cumulative Distribution Function (CCDF).

Different application environments require varying complexity levels in terms of hardware and time. To address this, the global gain concept [45] is used to determine the suitable number of candidate permutation sequences for PAPR reduction in DCO-OFDM systems, avoiding unnecessary computational complexity. The DCO-OFDM system is chosen due to its higher spectral efficiency compared to Asymmetrically Clipped Optical-OFDM (ACO-OFDM), as it uses both odd and even subcarriers to carry data symbols [89].

The remaining sections of this chapter are structured as follows: Section 6.3 explains the global gain concept, while Section 6.4 presents the algorithm for generating adjacent and interleaved permutations, along with determining the optimal number of candidate sequences. Section 6.5 presents simulation results comparing LSPP with adjacent and interleaved lexicographical permutations against LSPP with random permutations from Chapter 5. Finally, Section 6.6 provides concluding remarks.

6.3 Background

6.3.1 Global Gain

For the purpose of determining the most suitable number of candidate permutation sequences to circumvent increasing the PAPR, it is worthwhile to consider the various factors taken into account when choosing a PAPR reduction technique or algorithm. In this thesis, two factors are considered, i.e. PAPR reduction performance and the resulting increase in computational complexity. We consider these two factors because in LSPP, the number of candidate permutation sequences is directly proportional to the PAPR reduction performance and this can lead to an increase in both hardware and time complexity as a result of a large number of Inverse Fast Fourier Transform (IFFT) operations required to generate the candidate signals.

For a given scenario and set of requirements, we propose to use the global gain (net gain) for the system which we define as a particular case of the fitness/objective function-based approach [45], where the two factors of interest under consideration are the PAPRreduction performance and the computational complexity.

Therefore, under given Visible Light Communication (VLC) link configurations, such as diffuse, directed line of sight, non-directed line of sight and tracked, the PAPR reduction performance can be expressed in relative terms as follows

$$Z_1 = -10\log_{10}\left(\frac{\text{PAPR}_{\text{after}}}{\text{PAPR}_{\text{before}}}\right). \tag{6.1}$$

Similarly, the relative increase in computational complexity is given by

$$Z_2 = -10\log_{10}\left(\frac{\text{Complexity}_{\text{after}}}{\text{Complexity}_{\text{before}}}\right). \tag{6.2}$$

Accordingly, if σ_a represents the weights of factors related to the significance level of PAPR reduction $a = 1$ and increase in computational complexity $a = 2$ in the system, the aggregate fitness value is [15]

$$\Omega = \sum_{a=1}^{2} \sigma_a.Z_u, \tag{6.3}$$

where

$$\sum_{a=1}^{2} \sigma_a = 1. \tag{6.4}$$

Based on aggregate fitness values, the appropriate number of candidate permutation sequences can be chosen in order to achieve the desirable PAPR reduction performance as well as satisfy the computational complexity requirements of the system.

6.4 Adjacent and Interleaved Lexicographical Permutation Sequences

The V lexicographical permutation sequences from the possible $Q!$ permutation sequences generated from Equation (5.2) can be random, interleaved or adjacent. The adjacent and interleaved lexicographical permutation sequences are given by

$$X_l^{(v)} = X^{(0)}_{\varsigma+0\times\Delta}, X^{(1)}_{\varsigma+1\times\Delta}, X^{(2)}_{\varsigma+2\Delta}, \cdots, X^{(V-1)}_{\varsigma+V\Delta-1} \tag{6.5}$$

where $\Delta = 1$ for adjacent lexicographical permutations and $\Delta = 2$ for interleaved lexicographical permutations. $\varsigma, 0 \leq \varsigma \leq (Q! - \Delta V)$ is the index of the first permutation in the lexicographical order and $0 \leq v \leq (V-1)$.

The adjacent and interleaved lexicographical permutations can be generated from algorithm 6.1.

Algorithm 6.1 An algorithm to generate interleaved and adjacent lexicographical permutations

Input: Input: Permutation sub-blocks, $X_p^{(q)}$, $0 \leq q \leq (Q-1)$; Select V, $V \in \{0, 1, \cdots, Q!\}$; Set the index of the first permutation sequence, $\varsigma, 0 \leq \varsigma \leq (Q! - \Delta V)$; Select either, $\Delta = 1$ for adjacent or $\Delta = 2$ for interleaved permutations; Set $i = 1$;

Output: Either adjacent or interleaved lexicographical permutation sequences, $X_l^{(0)}, X_l^{(1)}, \cdots, X_l^{(V-1)}$

1: Set $\Delta = 1$ or $\Delta = 2$
2: **for** $i = 1 : V$ **do**
3:     Set $X_l^{(v)} := []$
4:     **while** $X_p^{(q)} \neq []$ **do**
5:         $\omega := \left(\left|X_p^{(q)}\right| - 1\right)!$
6:         $j := \lfloor \varsigma / \omega \rfloor$
7:         $\vartheta := X_p^{(j)}$
8:         $\varsigma := \varsigma \bmod \omega$
9:         ϑ is appended to $X_l^{(v)}$
10:         ϑ is removed from $X_p^{(q)}$
11:     **end while**
12:     $X_l^{(v)}$ is returned
13:     $\varsigma = \varsigma + \Delta$ and go to step 3.
14: **end for**

6.4.1 Most Suitable Number of Candidate Permutation Sequences

In order to determine the most suitable number of candidate permutation sequences, we use the global gain defined in Section 6.3.1.

Figure 6.1 illustrates the procedure for obtaining the most suitable number of candidate permutation sequences where Ω_{sys} is the global gain required for a particular system, σ_1 and σ_2 are the levels of

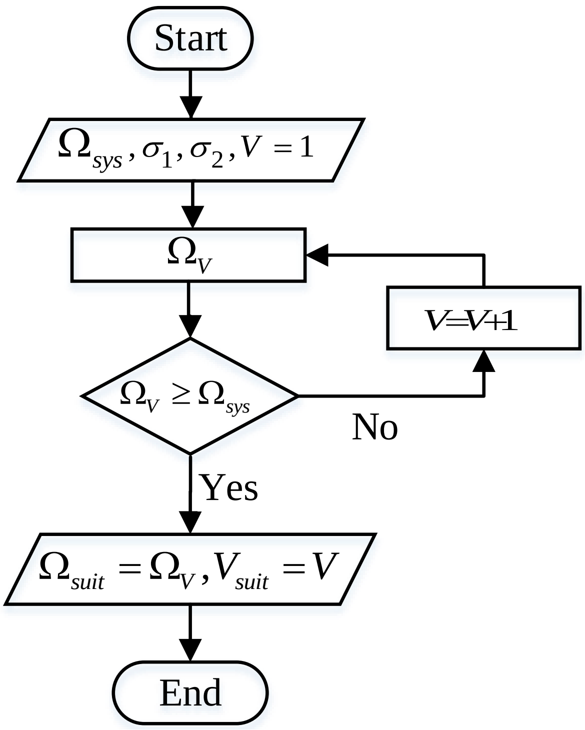

Figure 6.1: Algorithm for obtaining the most suitable number of candidate permutation sequences based on global gain.

importance attached to PAPR reduction performance and the computational complexity respectively and V_{suit} is the most suitable number of candidate permutation sequences for a particular scenario.

Furthermore, we need to specify the value of the CCDF of the PAPR in order to compare the global gains. The typical values of CCDF of the PAPR used in the available literature are between 10^{-2} and 10^{-4} [15] and therefore in this thesis, we use 10^{-3} as a reference for global gain calculations.

In order to generate V lexicographical candidate permutation sequences, V $2N$-point IFFT operations are required. Therefore the complexity is given by

$$\text{Complexity} = 2VN \tag{6.6}$$

6.5 Results and Discussions

In this section, computer simulation was used to compare the performance of the different categories of lexicographical permutation sequences particularly random [46], interleaved and adjacent described in Section 6.4 in terms of PAPR reduction performance and BER degradation performance. We did this by considering a DCO-OFDM communication system with a 16-Quadrature Amplitude Modulation (QAM) constellation and the total number of subcarriers, $N = 256$. We generated approximately 10^6 data blocks and each block was oversampled by an oversampling factor of $L = 4$ which is commensurable to correctly provide the true value of the PAPR [109]. In addition, we obtained the results for the DCO-OFDM communication system using the same constellation without any PAPR reduction technique applied. In Table 6.1 we list all the parameters that we used during our simulation.

Table 6.1: Simulation Parameters

Simulation Parameter	**Value**
Modulation scheme	16-QAM
Number of subcarriers	$N = 256$
Number of data blocks	10^6
Number of candidate sequences	V = 8, 16, 32
Number of sub-blocks	$Q = 16$
Oversampling factor	$L = 4$
$\mathrm{DC_{offset}}$	13 dB

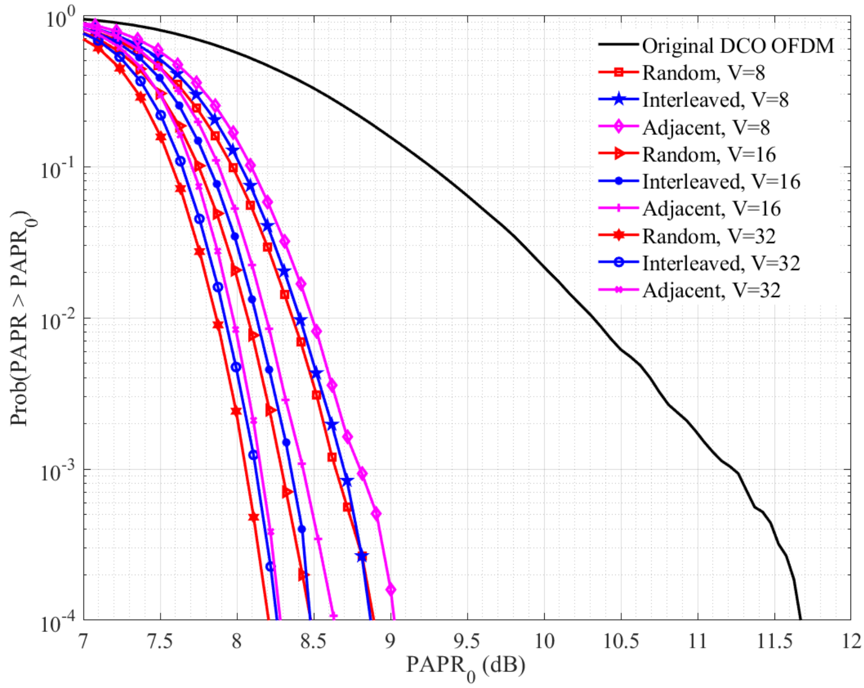

Figure 6.2: Comparing the PAPR performance of DCO-OFDM versus the three types of lexicographical permutations: random, interleaved, and adjacent for $Q = 16$ sub-blocks and the number of candidate signals, $V = 8, 16$ and 32.

6.5.1 Performance of Lexicographical Symbol Position Permutation Categories

Figure 6.2 illustrates the performance of the three categories of lexicographical symbol position permutation sequences i.e. random [46], interleaved and adjacent in terms of PAPR reduction performance using the CCDF defined by Equation (3.4). The results of the original DCO-OFDM system are also included for reference purposes. In Figure 6.2, the PAPR threshold values, $\mathrm{PAPR_0}$ and the CCDF of the PAPR are plotted on the abscissa and ordinate respectively. It can be noted that the PAPR reduction performance achieved by LSPP using random lexicographical permutations [46] is slightly better when compared to LSPP using interleaved and adjacent lexicographical permutations. For example, at a CCDF of 10^{-3}, the PAPR values are respectively 11.26 dB, 8.62 dB, 8.70 dB, and 8.80 dB for the original DCO-OFDM system, LSPP using random permutations, LSPP using interleaved permutations and LSPP using adjacent permutations when the number of candidate permutation sequences, $V = 8$ and the number of subblocks used to generate the candidate permutation sequences being $Q = 16$. This represents a difference of 0.08 dB and 0.18 dB respectively for LSPP using interleaved and LSPP using adjacent permutation sequences respectively when compared to LSPP using random permutations. When the number of candidate permutation sequences is increased from $V = 8$ to $V = 16$ and $V = 32$, the performance of LSPP using random permutation sequences remains slightly better as compared to LSPP using interleaved and adjacent permutation sequences. This better performance of LSPP using random permutation sequences can be attributed to the fact that the permutation sequences are more uncorrelated compared to interleaved and adjacent lexicographical permutations. Furthermore, from Figure 6.2, it should also be observed that LSPP using interleaved permutation sequences performs better in terms of PAPR reduction as compared to LSPP using adjacent permutation sequences. There is a difference of about 0.1 dB and this can also be attributed to the fact that the interleaved lexicographical permutation sequences are more uncorrelated as compared to adjacent lexicographical permutation sequences.

It should be noted that in order to generate the random lexicographical permutation sequences, the number of sub-blocks, Q should be sufficiently large so that the possibility of generating repeated permutation sequences with the same PAPR is minimized. This situation of generating repeated random lexicographical permutation sequences can be avoided by setting up a constraint in algorithm 5.1 that might increase the time complexity. Therefore, the adjacent and interleaved lexicographical permutation sequences can be preferred for low values of Q.

Figure 6.3 shows the BER performance comparison of a 16-QAM DCO-OFDM communication system using LSPP for PAPR reduction employing random, interleaved and adjacent lexicographical permutation sequences. Further, the results of the original DCO-OFDM communication system are also included for comparison purposes. From Figure 6.3, it can be noted that three categories of LSPP can achieve almost the same BER performance and the BER degradation is negligible when compared to the original DCO-OFDM communication system without any PAPR mitigation applied. The results are not surprising since LSPP, regardless of the category of lexicographical permutation sequences, is a distortionless technique, and therefore no BER degradation is expected except in cases where the SI is received in error.

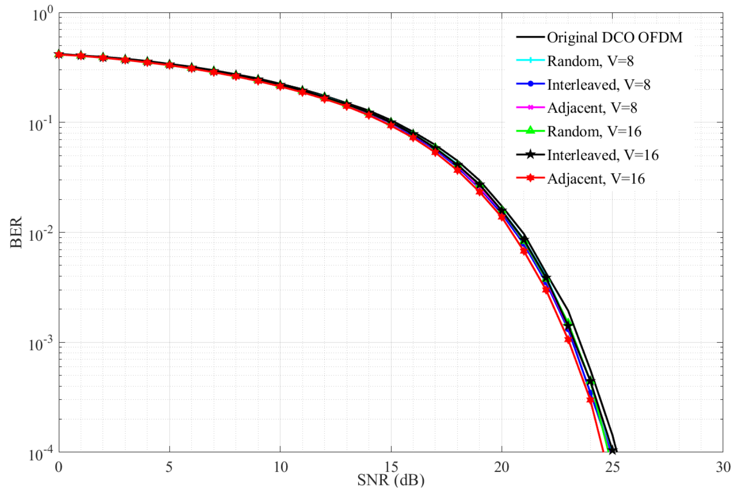

Figure 6.3: Comparing the BER performance of DCO-OFDM versus the three types of lexicographical permutations: random, interleaved, and adjacent for $Q = 16$ sub-blocks and the number of candidate signals, $V = 8, 16$ and 32

6.5.2 Analyzing suitable permutation sequence candidates to minimize computational complexity

In determining the most suitable number of candidate permutation sequences to avoid an increase in computational complexity beyond the system requirements, we considered LSPP using random lexicographical permutations since it gives better PAPR reduction performance compared to using adjacent and interleaved lexicographical permutations.

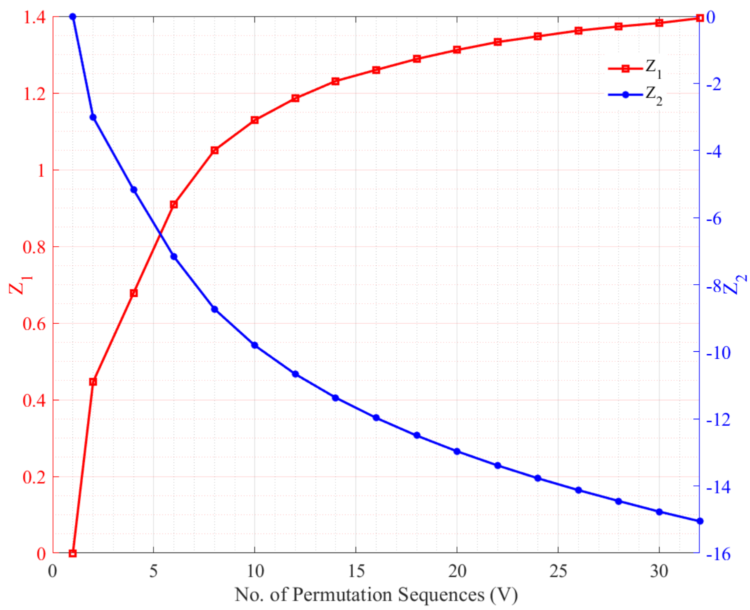

Figure 6.4: Z_1 and Z_2 for different candidate sequences

In Figure 6.4, we plot Z_1 from Equation (6.1) and Z_2 from Equation (6.2) on the left vertical axis and right vertical axis respectively for different numbers of candidate permutation sequences, V. As V increases, the absolute values of both Z_1 and Z_2 increase but the rate of increase decreases as V

is increased beyond about 8 candidate sequences. For example, from $V = 2$ up to $V = 8$, Z_1 and Z_2 increase respectively by 135% and 190% while for V from 8 to 16 Z_1 and Z_2 increase respectively by 19% and 37%. This rate of increase decreases further as V is increased. The implication here is that as V is increased, the benefit achieved in terms of PAPR reduction performance increases rapidly up to a certain V and then the rate of this increase decreases significantly as V is increased.

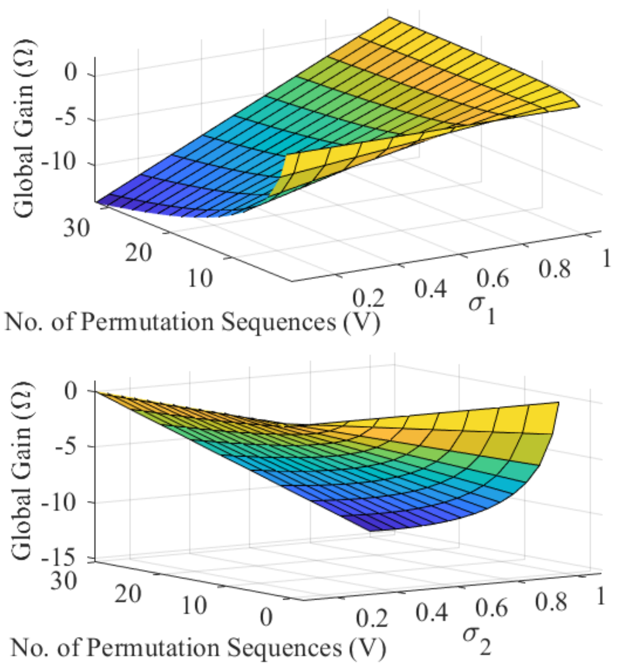

Figure 6.5: Global gain for different numbers of candidate sequences at different levels of importance attached to PAPR reduction performance (σ_1) and computational complexity (σ_2)

In Figure 6.5, we present the results for the global gain (Ω) for different numbers of candidate permutation sequences under different levels of importance attached to PAPR reduction performance (σ_1) and the resulting increase in computational complexity (σ_2). It is clear that the values of (σ_1) and (σ_2) affect the resultant Ω.

Table 6.2: Global gain, Ω values for different numbers of random lexicographical permutation sequences at a $CCDF = 10^{-3}$ and number of subcarriers, $N = 256$ for three different cases i.e. Case 1 $(\sigma_1 = 0.8, \sigma_2 = 0.2)$, Case 2 $(\sigma_1 = 0.2, \sigma_2 = 0.8)$ and Case 3 $(\sigma_1 = \sigma_2 = 0.5)$

V	**PAPR (dB)**	**Complexity**	**Global Gain, Ω**		
			Case 1	**Case 2**	**Case 3**
2	9.90	1024	−0.205	−2.309	−1.257
4	9.14	2048	−0.529	−4.648	−2.589
8	8.67	4096	−0.948	−7.010	−3.979
16	8.30	8192	−1.399	−9.381	−5.390
32	8.05	16384	−1.894	−11.762	−6.828

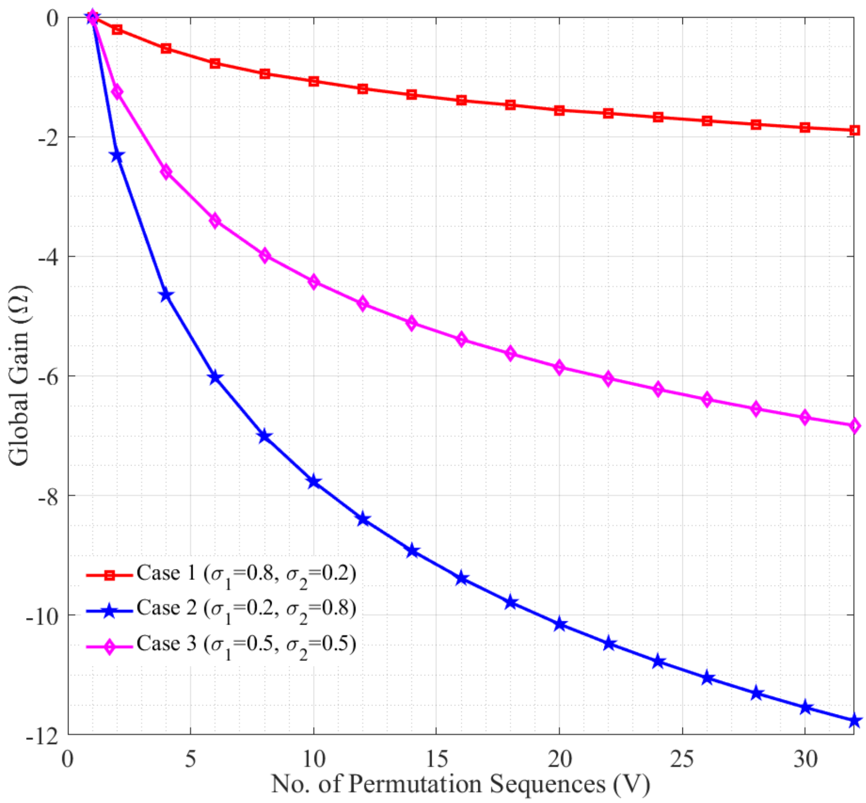

Figure 6.6: Global gain for different numbers of random lexicographical permutation sequences, V at a $CCDF = 10^{-3}$, number of subcarriers, $N = 256$.

In Figure 6.6 and Table 6.2, the global gain values for three different cases are presented: 1) when $\sigma_1 = \sigma_2 = 0.5$ implying that equal significance is attached to both the PAPR reduction performance and increase in computational complexity; 2) when $\sigma_1 = 0.8$ and $\sigma_2 = 0.2$, i.e. PAPR reduction performance is more significant compared to increase in computational complexity; and 3) $\sigma_1 = 0.2$ and $\sigma_2 = 0.8$, i.e. increase in computational complexity is more significant.

From Equations (6.1) and (6.2), a higher value of Z_1 is desirable since it represents a lower PAPR value and similarly a higher value of Z_2 is desirable since it represents a lower complexity. Therefore, from Equation (6.4), a higher value of the global gain, Ω is desirable. However as shown in Figure 6.6, it is necessary to select the most suitable value of the global gain based on the significance that is attached to computational complexity and the PAPR reduction performance.

As the PAPR reduction performance becomes more significant, the global gain reduces due to the increase in the computational complexity generated by the number of IFFT operations required to generate the candidate signals. Therefore, the most suitable number of permutation candidate sequences should be selected to achieve an acceptable PAPR reduction performance without going above the computational complexity that the system can tolerate.

6.6 Conclusion

DCO-OFDM is a modulation technique for VLC systems that is attractive due to its ability to deal with Intercarrier Interference (ICI) and Inter-Symbol Interference (ISI) that are frequently present in dispersive optical channels. Additionally, the DCO-OFDM communication system can achieve very high data rates which are required in today's applications such as, indoor localization, virtual reality, telemedicine and sensing. However, one the challenges that affects the practical implementation of DCO-OFDM is its resulting high PAPR that results in the signal when the subcarriers are summed constructively. This consequently negatively affects the system performance mainly at the transmitter due to the presence of non-linear devices and components such as the power amplifier, the Digital-to-Analog Converter (DAC) and the Light Emitting Diode (LED) leading to BER degradation and system inefficiency.

Therefore, several techniques have been proposed by researchers to deal with the problem of high PAPR. Among the techniques is LSPP which is a distortionless technique that yields significant reductions in PAPR with negligible BER degradation.

In this chapter, we perform a comparative study in terms of PAPR reduction performance of the different categories of lexicographical permutation sequences, i.e. random, interleaved and adjacent.

By using computer simulations, we have shown that using random lexicographical permutation sequences provides better PAPR reduction results compared to using interleaved and adjacent lexicographical permutation sequences. For a small number of sub-blocks, the adjacent and interleaved lexicographical permutation sequences are preferred since there is no possibility of generating the same permutation sequence unlike in random lexicographical permutations. Although this can be minimized by setting up a constraint that stops the generation of the same permutation sequences in random lexicographical permutation sequences, there will be an increase in time complexity.

Our results also show that the three categories of lexicographical permutation sequences provide almost the same BER performance compared to the original DCO-OFDM without any PAPR reduction technique applied.

Furthermore, we propose a new method based on global gain for determining the most suitable number of candidate permutation sequences to achieve a reasonable PAPR reduction performance without leading to unacceptable levels of computational complexity for the system.

7 Conclusion

This research was motivated by the challenges that affect the practical implementation of probabilistic-based techniques for Peak-to-Average Power Ratio (PAPR) reduction in optical-Orthogonal Frequency Division Multiplexing (OFDM), which is the most widely used modulation technique in Visible Light Communication (VLC) systems due to a number of advantages such as ability to combat Inter-Symbol Interference (ISI), high data rates and ease of practical implementation using Inverse Fast Fourier Transform (IFFT) and Fast Fourier Transform (FFT) operations. This research has made significant contributions to the field, which are summarized in Section 7.1. Additionally, Section 7.2 provides insightful recommendations for future work that can build upon this research and further advance the field.

7.1 Contributions

This thesis proposed a Low Complexity Hybrid Selected Mapping (LCHSLM) technique for PAPR reduction for Asymmetrically Clipped Optical-OFDM (ACO-OFDM) systems. This was motivated by the literature findings, where it is established that no single PAPR reduction technique can meet all the demands of optical-OFDM systems such as significant PAPR reduction, no or less signal distortion and low complexity simultaneously. The research therefore, proposed a hybrid scheme composed of a modified Selected Mapping (SLM) and μ-law companding techniques. From the mathematical analysis and simulation results, the proposed scheme achieves better PAPR reduction performance when compared to Conventional Selected Mapping (CSLM) and μ-law companding techniques when used individually in addition to achieving almost 50% reduction in complexity.

The thesis also introduced a novel technique based on lexicographical permutations called Lexicographical Symbol Position Permutation (LSPP). To this end, the three different ways of selecting the U permutation candidate sequences, that is, adjacent, interleaved, and random were compared in terms of PAPR reduction performance by computer simulation using Complementary Cumulative Distribution Function (CCDF) diagrams. Although the simulation results show that random lexicographical permutation sequences give a slightly better PAPR reduction performance compared to adjacent and interleaved lexicographical permutations, they require a large number of sub-blocks to avoid generating repeated permutation sequences that will have the same PAPR values leading to an increase in complexity. Therefore, the interleaved and adjacent permutations can be preferred for a smaller number of sub-blocks especially in systems where the number of subcarriers is small. Furthermore, the thesis introduced an algorithm for complexity reduction using LSPP by setting a threshold PAPR value and generating the permutation candidate sequences one by one until a candidate sequence with PAPR below the threshold is reached. In this way, if the m-th, $(m \leq U)$ permutation sequence satisfies the threshold condition, then $U - m$ candidate sequences are not generated and consequently, $U - m$ IFFT operations are not performed. This new method does not only reduce the PAPR but also results in a significant reduction in computational complexity.

Motivated by the fact that different scenarios and application environments require different degrees of complexity reduction and complexity, to further reduce the complexity in the proposed LSPP, the thesis proposed two solutions. In the first solution, an algorithm where a threshold PAPR value is introduced and the candidate signals are generated one at a time until a candidate with PAPR value less or equal to the threshold is obtained. The results show that the complexity in terms of IFFT operations can be reduced substantially depending on the selected threshold, γ and the number of candidate signals, U. For example, when $\gamma = 9$ dB and $U = 16$, the complexity reduction that is achieved is 90% and when $\gamma = 10$ dB, the complexity reduction achieved is 96% for $U = 32$ candidate signals. The second solution is the introduction of a new algorithm based on the global gain (net gain) to determine the most suitable number of permutation candidate sequences to achieve a reasonable PAPR reduction performance without increasing the time and hardware complexity to levels that the systems cannot tolerate.

7.2 Recommendations for Future Work

The work presented in this thesis provides fascinating methods and results for PAPR mitigation in optical-OFDM systems. However, it can also be extended in the following suggested research directions:

The hybrid PAPR reduction technique proposed for ACO-OFDM communication systems considers a combination of μ-law companding and modified SLM techniques. New studies could consider a combination of other PAPR reduction techniques such as Partial Transmit Sequence (PTS), Symbol Position Permutation (SPP) and coding techniques. Additionally, the research can be extended by hardware implementation of the hybrid techniques to verify their performance in terms of PAPR reduction performance, hardware and time complexity, and other performance parameters such as Bit Error Rate (BER) degradation and bandwidth utilization.

While determining the global gain to determine the most suitable number of candidate permutation sequences, two performance parameters were considered, namely, PAPR reduction and the resulting increase in computational complexity in terms of IFFT operations. In addition to these, new studies could take into consideration other performance parameters such as BER performance degradation, increase in bandwidth, cost savings, etc.

In the proposed techniques, the Side Information (SI) was transmitted using a separate channel and we assumed that it was received without error. Even though the VLC technology is considered to have infinite bandwidth, the practical bandwidth is limited by the modulation bandwidth of the

Light Emitting Diode (LED). Therefore, instead of transmitting the SI in a separate channel which decreases the bandwidth efficiency, new studies could consider introducing blind SI detection techniques so as to improve the bandwidth utilization efficiency.

Finally, this thesis has proposed PAPR reduction using lexicographical symbol position permutation for Direct Current biased Optical-OFDM (DCO-OFDM) systems. This can be extended to cover other modulation schemes for optical-OFDM including Multiple Input-Multiple Output (MIMO)-OFDM, which has been identified as a key technology for Fifth Generation (5G) communication systems. Moreover, since in VLC, the LED is utilized for both data communication and lighting, it would be interesting to see how dimming control schemes can be implemented in our proposed techniques.

References

[1] Shintaro Arai, Masayuki Kinoshita, and Takaya Yamazato. “Optical wireless communication: A candidate 6G technology?” In: *IEICE Transactions on Fundamentals of Electronics, Communications and Computer Sciences* 104.1 (2021), pp. 227–234.

[2] Luiz Eduardo Mendes Matheus, Alex Borges Vieira, Luiz FM Vieira, Marcos AM Vieira, and Omprakash Gnawali. “Visible light communication: concepts, applications and challenges”. In: *IEEE Communications Surveys & Tutorials* 21.4 (2019), pp. 3204–3237.

[3] Ahmed Al-Kinani, Cheng-Xiang Wang, Li Zhou, and Wensheng Zhang. “Optical wireless communication channel measurements and models”. In: *IEEE Communications Surveys & Tutorials* 20.3 (2018), pp. 1939–1962.

[4] Yaqi Sun, Fang Yang, and Ling Cheng. “An overview of OFDM-based visible light communication systems from the perspective of energy efficiency versus spectral efficiency”. In: *IEEE Access* 6 (2018), pp. 60824–60833.

[5] Xiaoyu Zhang, Zunaira Babar, Periklis Petropoulos, Harald Haas, and Lajos Hanzo. “The Evolution of Optical OFDM”. In: *IEEE Communications Surveys & Tutorials* 23.3 (2021), pp. 1430–1457. DOI: 10.1109/COMST.2021.3065907.

[6] Omer Narmanlioglu and Murat Uysal. “Multi-User Massive MIMO Visible Light Communications With Limited Pilot Transmission”. In: *IEEE Transactions on Wireless Communications* 21.6 (2022), pp. 4197–4211. DOI: 10.1109/TWC.2021.3127719.

[7] Zabih Ghassemlooy, Wasiu Popoola, and Sujan Rajbhandari. *Optical wireless communications: system and channel modelling with Matlab®*. CRC Press, 2019.

[8] Joseph M Kahn and John R Barry. “Wireless infrared communications”. In: *Proceedings of the IEEE* 85.2 (1997), pp. 265–298.

[9] Jean Armstrong and Arthur J Lowery. “Power efficient optical OFDM”. In: *Electronics letters* 42.6 (2006), pp. 370–372.

[10] Sian C Jeffrey Lee, Sebastian Randel, Florian Breyer, and Antonius MJ Koonen. “PAM-DMT for intensity-modulated and direct-detection optical communication systems”. In: *IEEE Photonics Technology Letters* 21.23 (2009), pp. 1749–1751.

[11] Sarangi D. Dissanayake, Kusha Panta, and Jean Armstrong. “A novel technique to simultaneously transmit ACO-OFDM and DCO-OFDM in IM/DD systems”. In: *2011 IEEE GLOBECOM Workshops (GC Wkshps)*. 2011, pp. 782–786. DOI: 10.1109/GLOCOMW.2011.6162561.

[12] Nirmal Fernando, Yi Hong, and Emanuele Viterbo. “Flip-OFDM for unipolar communication systems”. In: *IEEE Transactions on Communications* 60.12 (2012), pp. 3726–3733.

[13] Qi Wang, Chen Qian, Xuhan Guo, Zhaocheng Wang, David G Cunningham, and Ian H White. “Layered ACO-OFDM for intensity-modulated direct-detection optical wireless transmission”. In: *Optics Express* 23.9 (2015), pp. 12382–12393.

[14] Tao Jiang and Yiyan Wu. "An overview: Peak-to-average power ratio reduction techniques for OFDM signals". In: *IEEE Transactions on broadcasting* 54.2 (2008), pp. 257–268.

[15] Francisco Sandoval, Gwenael Poitau, and François Gagnon. "Hybrid peak-to-average power ratio reduction techniques: Review and performance comparison". In: *IEEE Access* 5 (2017), pp. 27145–27161.

[16] Seung Hee Han and Jae Hong Lee. "An overview of peak-to-average power ratio reduction techniques for multicarrier transmission". In: *IEEE Wireless Communications* 12.2 (2005), pp. 56–65.

[17] Luqing Wang and Chmtha Tellambura. "An Overview of Peak-to-Average Power Ratio Reduction Techniques for OFDM Systems". In: *2006 IEEE International Symposium on Signal Processing and Information Technology*. 2006, pp. 840–845. DOI: `10.1109/ISSPIT.2006.270915`.

[18] Yasir Amer Jawhar, Lukman Audah, Montadar Abas Taher, Khairun Nidzam Ramli, Nor Shahida Mohd Shah, Mustafa Musa, and Mustafa Sami Ahmed. "A review of partial transmit sequence for PAPR reduction in the OFDM systems". In: *IEEE Access* 7 (2019), pp. 18021–18041.

[19] Dae-Woon Lim, Seok-Joong Heo, and Jong-Seon No. "An overview of peak-to-average power ratio reduction schemes for OFDM signals". In: *Journal of Communications and Networks* 11.3 (2009), pp. 229–239.

[20] T.A. Wilkinson and A.E. Jones. "Minimisation of the peak to mean envelope power ratio of multicarrier transmission schemes by block coding". In: *1995 IEEE 45th Vehicular Technology Conference. Countdown to the Wireless Twenty-First Century*. Vol. 2. 1995, 825–829 vol.2. DOI: `10.1109/VETEC.1995.504983`.

[21] Hyo-Joo Ahn, Yoan Shin, and Sungbin Im. "A block coding scheme for peak-to-average power ratio reduction in an orthogonal frequency division multiplexing system". In: *VTC2000-Spring. 2000 IEEE 51st Vehicular Technology Conference Proceedings (Cat. No.00CH37026)*. Vol. 1. 2000, 56–60 vol.1. DOI: `10.1109/VETECS.2000.851417`.

[22] Francisco Sandoval, Gwenael Poitau, and François Gagnon. "Optimizing forward error correction codes for COFDM with reduced PAPR". In: *IEEE Transactions on Communications* 67.7 (2019), pp. 4605–4619.

[23] Emma Frontana and Ivan Fair. "Avoiding PAPR degradation in Convolutional Coded OFDM Signals". In: *2007 IEEE Pacific Rim Conference on Communications, Computers and Signal Processing*. 2007, pp. 312–315. DOI: `10.1109/PACRIM.2007.4313237`.

[24] David JC MacKay. "Fountain codes". In: *IEE Proceedings-Communications* 152.6 (2005), pp. 1062–1068.

[25] Shih-Kai Lee, Yen-Ching Liu, Hsin-Liang Chiu, and Yung-Chih Tsai. "Fountain codes with PAPR constraint for multicast communications". In: *IEEE transactions on broadcasting* 57.2 (2011), pp. 319–325.

[26] Tao Jiang and Xiangming Li. "Using fountain codes to control the peak-to-average power ratio of OFDM signals". In: *IEEE Transactions on Vehicular Technology* 59.8 (2010), pp. 3779–3785.

[27] Dadi Bi, Peng Ren, and Zheng Xiang. "A novel joint PAPR reduction algorithm with low complexity using LT codes". In: *IEEE Wireless Communications Letters* 7.2 (2017), pp. 166–169.

[28] John W Byers, Michael Luby, Michael Mitzenmacher, and Ashutosh Rege. “A digital fountain approach to reliable distribution of bulk data”. In: *ACM SIGCOMM Computer Communication Review* 28.4 (1998), pp. 56–67.

[29] Wei-Wen Hu and Da-Huei Lee. “PAPR reduction for visible light communication systems without side information”. In: *IEEE Photonics Journal* 9.3 (2017), pp. 1–11.

[30] Siva Prasad Valluri, Vejandla Kishore, and Venkata Mani Vakamulla. “A new selective mapping scheme for visible light systems”. In: *IEEE Access* 8 (2020), pp. 18087–18096.

[31] Stéphane Y Le Goff, Samer S Al-Samahi, Boon Kien Khoo, Charalampos C Tsimenidis, and Bayan S Sharif. “Selected mapping without side information for PAPR reduction in OFDM”. In: *IEEE Transactions on Wireless Communications* 8.7 (2009), pp. 3320–3325.

[32] Yating Wu, Congcong He, Qianwu Zhang, Yanzan Sun, and Tao Wang. “Low-complexity recombined SLM scheme for PAPR reduction in IM/DD optical OFDM systems”. In: *Optics Express* 26.24 (2018), pp. 32237–32247.

[33] Stefan H Muller and Johannes B Huber. “OFDM with reduced peak-to-average power ratio by optimum combination of partial transmit sequences”. In: *Electronics letters* 33.5 (1997), pp. 368–369.

[34] Jean Armstrong. “Peak-to-average power reduction for OFDM by repeated clipping and frequency domain filtering”. In: *Electronics letters* 38.5 (2002), pp. 246–247.

[35] Dapeng Hao and Peter Adam Hoeher. “Iterative Estimation and Cancellation of Clipping Noise for Multi-Layer IDMA Systems”. In: *7th International ITG Conference on Source and Channel Coding*. 2008, pp. 1–6.

[36] R. van Nee and A. de Wild. “Reducing the peak-to-average power ratio of OFDM”. In: *VTC ’98. 48th IEEE Vehicular Technology Conference. Pathway to Global Wireless Revolution (Cat. No.98CH36151)*. Vol. 3. 1998, 2072–2076 vol.3. DOI: 10.1109/VETEC.1998.686121.

[37] Yasir Rahmatallah and Seshadri Mohan. “Peak-to-average power ratio reduction in OFDM systems: A survey and taxonomy”. In: *IEEE communications surveys & tutorials* 15.4 (2013), pp. 1567–1592.

[38] Xianbin Wang, Tjeng Thiang Tjhung, and Chun Sum Ng. “Reduction of peak-to-average power ratio of OFDM system using a companding technique”. In: *IEEE transactions on broadcasting* 45.3 (1999), pp. 303–307.

[39] Darryn Lowe and Xiaojing Huang. “Optimal Adaptive Hyperbolic Companding for OFDM”. In: *The 2nd International Conference on Wireless Broadband and Ultra Wideband Communications (AusWireless 2007)*. 2007, pp. 24–24. DOI: 10.1109/AUSWIRELESS.2007.52.

[40] Yasir Rahmatallah, Nidhal Bouaynaya, and Seshadri Mohan. “On the performance of linear and nonlinear companding transforms in OFDM systems”. In: *2011 Wireless Telecommunications Symposium (WTS)*. 2011, pp. 1–5. DOI: 10.1109/WTS.2011.5960877.

[41] Tao Jiang, Yang Yang, and Yong-Hua Song. “Companding technique for PAPR reduction in OFDM systems based on an exponential function”. In: *GLOBECOM ’05. IEEE Global Telecommunications Conference, 2005.* Vol. 5. 2005, 4 pp.–2801. DOI: 10.1109/GLOCOM.2005.1578269.

[42] Roland Niwareeba, Mitchell A Cox, and Ling Cheng. “Low complexity hybrid SLM for PAPR mitigation for ACO OFDM”. In: *ICT Express* 8.1 (2022), pp. 72–76.

[43] Anagiyaddage DS Jayalath and Chintha Tellambura. “Reducing the peak-to-average power ratio of orthogonal frequency division multiplexing signal through bit or symbol interleaving”. In: *Electronics Letters* 36.13 (2000), pp. 1161–1163.

[44] Jyh-Horng Wen, Shu-Hong Lee, and Chih-Chung Kung. “SLM-based data position permutation method for PAPR reduction in OFDM systems”. In: *Wireless Communications and Mobile Computing* 13.11 (2013), pp. 985–997.

[45] Rakesh Rajbanshi. “OFDM-based cognitive radio for DSA networks”. PhD thesis. University of Kansas, 2007.

[46] Roland Niwareeba, Mitchell A Cox, and Ling Cheng. “PAPR Reduction in Optical OFDM Using Lexicographical Permutations With Low Complexity”. In: *IEEE Access* 10 (2021), pp. 1706–1713.

[47] Roland Niwareeba, Mitchell A Cox, and Ling Cheng. “Adaptive PAPR Reduction in Optical OFDM Systems using Lexicographical Symbol Position Permutation”. In: *(Submitted to MDPI-Electronics-Under Review)* ().

[48] Tezcan Cogalan and Harald Haas. “Why would 5G need optical wireless communications?” In: *IEEE Int. Symp. Pers. Indoor Mob. Radio Commun. PIMRC* 2017-October (2018), pp. 1–6. DOI: 10.1109/PIMRC.2017.8292749.

[49] Cisco. “Annual internet report. 2020”. In: *Cisco annual internet report (2018–2023) white paper* ().

[50] Theodore S. Rappaport et al. “Millimeter wave mobile communications for 5G cellular: It will work!” In: *IEEE Access* 1 (2013), pp. 335–349. ISSN: 21693536. DOI: 10.1109/ACCESS.2013.2260813.

[51] Toshihiko Komine and Masao Nakagawa. “Fundamental analysis for visible-light communication system using LED lights”. In: *IEEE transactions on Consumer Electronics* 50.1 (2004), pp. 100–107.

[52] Peng Zou, Yiheng Zhao, Fangchen Hu, and Nan Chi. “Underwater visible light communication at 324 Gb/s using novel two-dimensional bit allocation”. In: *Opt. Express* 28.8 (2020), p. 11319. ISSN: 10944087. DOI: 10.1364/oe.390718.

[53] Jia Wang, Ahmed Al-Kinani, Wensheng Zhang, Cheng-Xiang Wang, and Li Zhou. “A general channel model for visible light communications in underground mines”. In: *China Communications* 15.9 (2018), pp. 95–105.

[54] Nicholas A.A. Howarth and Jan Rosenow. “Banning the bulb: Institutional evolution and the phased ban of incandescent lighting in Germany”. In: *Energy Policy* 67.April (2014), pp. 737–746. ISSN: 03014215. DOI: 10.1016/j.enpol.2013.11.060.

[55] Gheorghe Brezeanu. “Silicon Carbide (SiC): A short history. An analytical aproach for SiC power device design”. In: *Proc. Int. Semicond. Conf. CAS* 2 (2005), pp. 345–348. DOI: 10.1109/SMICND.2005.1558796.

[56] Georges Destriau. “Research on zinc sulfide scintillations at α rays”. In: *Physical Chemistry Journal* 33 (1936), pp. 587–625.

[57] Rubin Braunstein. “Radiative transitions in semiconductors”. In: *Physical Review* 99.6 (1955), p. 1892.

[58] Herbert Kroemer. “The double-heterostructure concept: How it got started”. In: *Proceedings of the IEEE* 101.10 (2013), pp. 2183–2187.

[59] J W Allen and Hermann G Grimmeiss. “Visible Light-Emitting Diodes - The Formative Years”. In: *Mater. Sci. Forum* 590 (2008), pp. 1–16. DOI: 10.4028/www.scientific.net/MSF.590.1.

[60] Shuji Nakamura, Masayuki Senoh, Naruhito Iwasa, and Shin-ichi Nagahama. "High-Brightness {InGaN} Blue, Green and Yellow Light-Emitting Diodes with Quantum Well Structures". In: *Jpn. J. Appl. Phys.* 34.Part 2, No. 7A (1995), pp. L797–L799. DOI: 10.1143/jjap.34.l797. URL: https://doi.org/10.1143/jjap.34.l797.

[61] Govind P Agrawal. "Optical Communication: Its History and Recent Progress". In: *Opt. Our Time*. Ed. by Mohammad D Al-Amri, Mohamed El-Gomati, and M Suhail Zubairy. Cham: Springer International Publishing, 2016, pp. 177–199. ISBN: 978-3-319-31903-2. DOI: 10.1007/978-3-319-31903-2_8. URL: https://doi.org/10.1007/978-3-319-31903-2{_}8.

[62] Harald Haas, Liang Yin, Yunlu Wang, and Cheng Chen. "What is LiFi?" In: *J. Light. Technol.* 34.6 (2016), pp. 1533–1544. ISSN: 07338724. DOI: 10.1109/JLT.2015.2510021.

[63] Chien-Hung Yeh, Yen-Liang Liu, and Chi-Wai Chow. "Real-time white-light phosphor-LED visible light communication (VLC) with compact size". In: *Optics express* 21.22 (2013), pp. 26192–26197.

[64] Xicong Li, Zabih Ghassemlooy, Stanislav Zvanovec, and Paul Anthony Haigh. "Experimental Demonstration of a 40 Mb/s VLC System Using a Large Off-the-Shelf LED Panel". In: *2020 12th International Symposium on Communication Systems, Networks and Digital Signal Processing (CSNDSP)*. 2020, pp. 1–5. DOI: 10.1109/CSNDSP49049.2020.9249608.

[65] Xicong Li, Zabih Ghassemlooy, Stanislav Zvánovec, and Paul Anthony Haigh. "A 40 Mb/s VLC system reusing an existing large LED panel in an indoor office environment". In: *Sensors* 21.5 (2021), p. 1697.

[66] Rui Bian, Iman Tavakkolnia, and Harald Haas. "15.73 Gb/s visible light communication with off-the-shelf LEDs". In: *Journal of Lightwave Technology* 37.10 (2019), pp. 2418–2424.

[67] Reham W Zaki, Heba A Fayed, Ahmed Abd El Aziz, and Moustafa H Aly. "Outdoor Visible Light Communication in Intelligent Transportation Systems: Impact of Snow and Rain". In: *Applied Sciences* 9.24 (2019), p. 5453.

[68] Elizabeth Eso, Zabih Ghassemlooy, Stanislav Zvanovec, Juna Sathian, and Asghar Gholami. "Fundamental analysis of vehicular light communications and the mitigation of sunlight noise". In: *IEEE Trans. Veh. Technol.* 70.6 (2021), pp. 5932–5943. ISSN: 19399359. DOI: 10.1109/TVT.2021.3078576.

[69] K. Siddiqi, A. D. Raza, and S. Sheikh Muhammad. "Visible light communication for V2V intelligent transport system". In: *2016 International Conference on Broadband Communications for Next Generation Networks and Multimedia Applications (CoBCom)*. 2016, pp. 1–4. DOI: 10.1109/COBCOM.2016.7593510.

[70] Whitney Bolton. "Technical review". In: *Comput. Hum.* 28.3 (1994), pp. 191–198. ISSN: 15728412. DOI: 10.1007/BF01830739.

[71] Toha Ardi Nugraha and Yudhi Ardiyanto. "Li-Fi Technology for Transmitting Data in Hospital Environments". In: *Proceeding - 1st Int. Conf. Inf. Technol. Adv. Mech. Electr. Eng. ICITAMEE 2020* 0 (2020), pp. 81–84. DOI: 10.1109/ICITAMEE50454.2020.9398406.

[72] Ryosuke Murai, Tatsuo Sakai, Hajime Kawano, Yoshihiko Matsukawa, Yukihiko Kitano, Yukio Honda, and Kenneth C. Campbell. "A novel visible light communication system for enhanced control of autonomous delivery robots in a hospital". In: *2012 IEEE/SICE Int. Symp. Syst. Integr. SII 2012* (2012), pp. 510–516. DOI: 10.1109/SII.2012.6427311.

[73] Obaid Ur-Rehman and Natasa Zivic. "Wireless communications". In: *Signals Commun. Technol.* 19.1 (2018), pp. 7–21. ISSN: 18604870. DOI: 10.1007/978-3-319-78942-2_2.

[74] Mohammad Vahid Jamali, Pooya Nabavi, and Jawad A. Salehi. "MIMO underwater visible light communications: Comprehensive channel study, performance analysis, and multiple-symbol detection". In: *IEEE Trans. Veh. Technol.* 67.9 (2018), pp. 8223–8237. ISSN: 00189545. DOI: 10.1109/TVT.2018.2840505. arXiv: 1704.00909.

[75] Mohammad Furqan Ali, Dushantha Nalin K Jayakody, and Yonghui Li. "Recent trends in underwater visible light communication (UVLC) systems". In: *IEEE Access* 10 (2022), pp. 22169–22225.

[76] Galefang Allycan Mapunda, Reuben Ramogomana, Leatile Marata, Bokamoso Basutli, Amjad Saeed Khan, and Joseph Monamati Chuma. "Indoor Visible Light Communication: A Tutorial and Survey". In: *Wirel. Commun. Mob. Comput.* 2020 (2020). ISSN: 15308677. DOI: 10.1155/2020/8881305.

[77] Dario. Tagliaferri and C. Capsoni. "Enabling on-aircraft visible-light communications in low-light conditions". In: *Electron. Lett.* 55.5 (2019), pp. 274–276. ISSN: 00135194. DOI: 10.1049/el.2018.7637.

[78] Yousef Almadani, David Plets, Sander Bastiaens, Wout Joseph, Muhammad Ijaz, Zabih Ghassemlooy, and Sujan Rajbhandari. "Visible light communications for industrial applications—Challenges and potentials". In: *Electronics* 9.12 (2020), p. 2157.

[79] Jian Chen, Tian Liu, and Tao Shu. "A Survey on Visible Light Communication Standards". In: *GetMobile: Mobile Computing and Communications* 25.1 (2021), pp. 9–15.

[80] Arthur Astrin. "IEEE Standard for Local and metropolitan area networks part 15.6: Wireless Body Area Networks". In: *IE EE Std 802.15. 6* (2012).

[81] A. C. Boucouvalas, Periklis Chatzimisios, Zabih Ghassemlooy, Murat Uysal, and Konstantinos Yiannopoulos. "Standards for indoor Optical Wireless Communications". In: *IEEE Communications Magazine* 53.3 (2015), pp. 24–31. DOI: 10.1109/MCOM.2015.7060515.

[82] Richard D. Roberts, Sridhar Rajagopal, and Sang Kyu Lim. "IEEE 802.15.7 physical layer summary". In: *2011 IEEE GLOBECOM Work. GC Workshops 2011* (2011), pp. 772–776. DOI: 10.1109/GLOCOMW.2011.6162558.

[83] ITU. *High-speed indoor visible light communication transceiver – System architecture, physical layer and data link layer specification*. 2019. URL: https://www.itu.int/ITU-T/recommendations/rec.aspx?rec=13781\&lang=en.

[84] Hao Li. "Principle of OFDM and Multi-carrier Modulations". In: *Encyclopedia of Wireless Networks*. Springer, 2020, pp. 1093–1097.

[85] Jean Armstrong. "OFDM for optical communications". In: *Journal of lightwave technology* 27.3 (2009), pp. 189–204.

[86] Erik Dahlman, Gunnar Mildh, Stefan Parkvall, Janne Peisa, Joachim Sachs, Yngve Selén, and Johan Sköld. "5G wireless access: requirements and realization". In: *IEEE Communications Magazine* 52.12 (2014), pp. 42–47.

[87] Ping Yang, Yue Xiao, Ming Xiao, and Shaoqian Li. "6G wireless communications: Vision and potential techniques". In: *IEEE network* 33.4 (2019), pp. 70–75.

[88] Jeffrey B. Carruthers and Joseph M. Kahn. “Multiple-subcarrier modulation for nondirected wireless infrared communication”. In: *IEEE journal on selected areas in communications* 14.3 (1996), pp. 538–546.

[89] Sarangi Devasmitha Dissanayake and Jean Armstrong. “Comparison of ACO-OFDM, DCO-OFDM and ADO-OFDM in IM/DD Systems”. In: *Journal of Lightwave Technology* 31.7 (2013), pp. 1063–1072. DOI: 10.1109/JLT.2013.2241731.

[90] Stephen B Weinstein. “The history of orthogonal frequency-division multiplexing [History of Communications]”. In: *IEEE Communications Magazine* 47.11 (2009), pp. 26–35.

[91] Robert W Chang. *Orthogonal frequency multiplex data transmission system*. US Patent 3,488,445. 1970.

[92] Stephen Weinstein and Paul Ebert. “Data transmission by frequency-division multiplexing using the discrete Fourier transform”. In: *IEEE transactions on Communication Technology* 19.5 (1971), pp. 628–634.

[93] A. Peled and A. Ruiz. “Frequency domain data transmission using reduced computational complexity algorithms”. In: *ICASSP ’80. IEEE International Conference on Acoustics, Speech, and Signal Processing*. Vol. 5. 1980, pp. 964–967. DOI: 10.1109/ICASSP.1980.1171076.

[94] Leonard Cimini. “Analysis and simulation of a digital mobile channel using orthogonal frequency division multiplexing”. In: *IEEE transactions on communications* 33.7 (1985), pp. 665–675.

[95] Jacky S. Chow, Jerry C. Tu, and John M. Cioffi. “A discrete multitone transceiver system for HDSL applications”. In: *IEEE journal on selected areas in communications* 9.6 (1991), pp. 895–908.

[96] William Shieh, Xingwen Yi, Yiran Ma, and Qi Yang. “Coherent optical OFDM: has its time come?” In: *Journal of Optical Networking* 7.3 (2008), pp. 234–255.

[97] Dayou Qian, Junqiang Hu, Philip Nan Ji, Ting Wang, and Milorad Cvijetic. “10-Gb/s OFDMA-PON for delivery of heterogeneous services”. In: *Optical Fiber Communication Conference*. Optical Society of America. 2008, OWH4.

[98] Fan Wang, Amitava Ghosh, Chandy Sankaran, Philip J Fleming, Frank Hsieh, and Stanley J Benes. “Mobile WiMAX systems: performance and evolution”. In: *IEEE Communications Magazine* 46.10 (2008), pp. 41–49.

[99] IEEE Computer Society LAN/MAN Standards Committee et al. “IEEE Standard for Information technology-Telecommunications and information exchange between systems-Local and metropolitan area networks-Specific requirements Part 11: Wireless LAN Medium Access Control (MAC) and Physical Layer (PHY) Specifications”. In: *IEEE Std 802.11^* (2007).

[100] Liang Chen, Brian Krongold, and Jamie Evans. “Theoretical characterization of nonlinear clipping effects in IM/DD optical OFDM systems”. In: *IEEE Transactions on Communications* 60.8 (2012), pp. 2304–2312.

[101] Xiaowen Wang and KJ Ray Liu. “Performance analysis for adaptive channel estimation exploiting cyclic prefix in multicarrier modulation systems”. In: *IEEE Transactions on Communications* 51.1 (2003), pp. 94–105.

[102] Xiaowen Wang and K.J. Ray Liu. “Adaptive channel estimation using cyclic prefix in multicarrier modulation system”. In: *IEEE Communications Letters* 3.10 (1999), pp. 291–293. DOI: 10.1109/4234.798021.

[103] Ali Zaidi, Fredrik Athley, Jonas Medbo, Ulf Gustavsson, Giuseppe Durisi, and Xiaoming Chen. "Chapter 5 - Multicarrier Waveforms". In: *5G Physical Layer*. Ed. by Ali Zaidi, Fredrik Athley, Jonas Medbo, Ulf Gustavsson, Giuseppe Durisi, and Xiaoming Chen. Academic Press, 2018, pp. 119–158. ISBN: 978-0-12-814578-4. DOI: `https://doi.org/10.1016/B978-0-12-814578-4.00010-2`. URL: `https://www.sciencedirect.com/science/article/pii/B9780128145784000102`.

[104] Bilal Ranjha and Mohsen Kavehrad. "Hybrid asymmetrically clipped OFDM-based IM/DD optical wireless system". In: *Journal of Optical Communications and Networking* 6.4 (2014), pp. 387–396.

[105] Hany Elgala, Raed Mesleh, and Harald Haas. "Indoor optical wireless communication: potential and state-of-the-art". In: *IEEE Communications Magazine* 49.9 (2011), pp. 56–62.

[106] T Lueftner, C Kroepl, M Huemer, J Hausner, R Hagelauer, and R Weigel. "Edge-position modulation for high-speed wireless infrared communications". In: *IEE Proceedings-Optoelectronics* 150.5 (2003), pp. 427–437.

[107] Richard van Nee and Ramjee Prasad. *OFDM for wireless multimedia communications*. Artech House, Inc., 2000.

[108] Yong Soo Cho, Jaekwon Kim, Won Y Yang, and Chung G Kang. *MIMO-OFDM wireless communications with MATLAB*. John Wiley & Sons, 2010.

[109] Jose Tellado-Mourelo. "Peak to average power reduction for multicarrier modulation". PhD thesis. stanford university, 1999.

[110] V Vijayarangan and R Sukanesh. "An overview of techniques for reducing peak to average power ratio and its selection criteria for orthogonal frequency division multiplexing radio systems." In: *Journal of Theoretical & Applied Information Technology* 5.1 (2009).

[111] UB Mahadevaswamy and MN Geetha. "A comparative survey on PAPR reduction in OFDM signal". In: *2016 International Conference on Electrical, Electronics, Communication, Computer and Optimization Techniques (ICEECCOT)*. IEEE. 2016, pp. 123–126.

[112] Rorie O'Neill and Luis B Lopes. "Envelope variations and spectral splatter in clipped multicarrier signals". In: *Proceedings of 6th International Symposium on Personal, Indoor and Mobile Radio Communications*. Vol. 1. 1995, pp. 71–75. DOI: `10.1109/PIMRC.1995.476406`.

[113] Zheng-rong Tong, Ya-nong Hu, and Wei-hua Zhang. "PAPR reduction in CO-OFDM systems using IPTS and modified clipping and filtering". In: *Optoelectronics Letters* 14.3 (2018), pp. 209–211.

[114] Per Ola Börjesson, Hans G Feichtinger, Niklas Grip, Mikael Isaksson, Norbert Kaiblinger, Per Ödling, and Lars-Erik Persson. "A low-complexity PAR-reduction method for DMT-VDSL". In: *International Symposium on Digital Signal Processing for Communication Systems: 17/02/1999*. 1999, pp. 164–169.

[115] Per Ola Börjesson, Hans G Feichtinger, Niklas Grip, Mikael Isaksson, Norbert Kaiblinger, Per Odling, and Lars-Erik Persson. "DMT PAR-reduction by weighted cancellation waveforms". In: *Proc. Radiovetenskaplig Konferens* (1999), pp. 303–307.

[116] Hyun-Bae Jeon, Jong-Seon No, and Dong-Joon Shin. "A new PAPR reduction scheme using efficient peak cancellation for OFDM systems". In: *IEEE Transactions on Broadcasting* 58.4 (2012), pp. 619–628.

[117] Xiao Huang, Jianhua Lu, Junli Zheng, K.B. Letaief, and Jun Gu. "Companding transform for reduction in peak-to-average power ratio of OFDM signals". In: *IEEE Transactions on Wireless Communications* 3.6 (2004), pp. 2030–2039. DOI: `10.1109/TWC.2004.837619`.

[118] Stefan H Muller and Johannes B Huber. “A novel peak power reduction scheme for OFDM”. In: *Proceedings of 8th International Symposium on Personal, Indoor and Mobile Radio Communications-PIMRC’97*. Vol. 3. IEEE. 1997, pp. 1090–1094.

[119] Lin Yang, Ru-Shan Chen, Yun-Ming Siu, and Kwok-Kai Soo. “PAPR reduction of an OFDM signal by use of PTS with low computational complexity”. In: *IEEE Transactions on broadcasting* 52.1 (2006), pp. 83–86.

[120] N Ngajikin, Norsheila Fisal, and SK Yusof. “PAPR reduction in WLAN-OFDM system using code repetition technique”. In: *Proceedings. Student Conference on Research and Development, 2003. SCORED 2003.* IEEE. 2003, pp. 85–89.

[121] Tao Jiang and Guangxi Zhu. “Complement block coding for reduction in peak-to-average power ratio of OFDM signals”. In: *IEEE Communications Magazine* 43.9 (2005), S17–S22.

[122] Abbas Ali Sharifi. “Discrete Hartley matrix transform precoding-based OFDM system to reduce the high PAPR”. In: *ICT Express* 5.2 (2019), pp. 100–103.

[123] Abbas Ali Sharifi. “PAPR reduction of optical OFDM signals in visible light communications”. In: *ICT Express* 5.3 (2019), pp. 202–205.

[124] Imad A Shaheen, Abdelhalim Zekry, Fatma Newagy, and Reem Ibrahim. “Performance evaluation of PAPR reduction in FBMC system using nonlinear companding transform”. In: *ICT Express* 5.1 (2019), pp. 41–46.

[125] Mehdi Hosseinzadeh Aghdam and Abbas Ali Sharifi. “PAPR reduction in OFDM systems: An efficient PTS approach based on particle swarm optimization”. In: *ICT Express* 5.3 (2019), pp. 178–181.

[126] Chin-Liang Wang, Ming-Yen Hsu, and Yuan Ouyang. “A low-complexity peak-to-average power ratio reduction technique for OFDM systems”. In: *GLOBECOM’03. IEEE Global Telecommunications Conference (IEEE Cat. No. 03CH37489)*. Vol. 4. IEEE. 2003, pp. 2375–2379.

[127] Laia Nadal, Michela Svaluto Moreolo, Josep M Fàbrega, and Gabriel Junyent. “Low complexity PAPR reduction techniques for clipping and quantization noise mitigation in direct-detection O-OFDM systems”. In: *Optical Fiber Technology* 20.3 (2014), pp. 208–216.

[128] Chidurala Anjaiah et al. “Mu-law companded PTS for PAPR reduction in OFDM systems”. In: *2015 IEEE International Conference on Electrical, Computer and Communication Technologies (ICECCT)*. IEEE. 2015, pp. 1–4.

[129] Mohamed Mounir and Mohamed Bakry El_Mashade. “On the selection of the best companding technique for PAPR reduction in OFDM systems”. In: *Journal of Information and Telecommunication* 3.3 (2019), pp. 400–411.

[130] Nazar Ali, Rola Almahainy, Abdullah Al-Shabili, Nawaf Almoosa, and Raed Abd-Alhameed. “Analysis of improved μ-law companding technique for OFDM systems”. In: *IEEE Transactions on Consumer Electronics* 63.2 (2017), pp. 126–134.

[131] Jaewoon Kim and Yoan Shin. “An effective clipped companding scheme for PAPR reduction of OFDM signals”. In: *2008 IEEE International Conference on Communications*. IEEE. 2008, pp. 668–672.

[132] Roland Niwareeba. “Mitigation of the high PAPR in Optical OFDM systems using Symbol Position Permutation”. In: *2021 IEEE International Mediterranean Conference on Communications and Networking (MeditCom)*. IEEE. 2021, pp. 372–377.